Studying the Factors Affecting the Drag Coefficient in Free Settling in Non-Newtonian Fluid

A Thesis
Submitted to the College of Engineering
of Nahrain University in Partial Fulfillment of the
Requirements for the Degree of
Master of Science
in
Chemical Engineering

by

DINA ADIL ELIA HALAGY
(B.Sc. in Chemical Engineering 2003)

Jamada II 1427
June 2006

Certification

I certify that this thesis entitled **"Studying the Factors Affecting the Drag Coefficient in Free Settling in Non-Newtonian Fluid"** was prepared by **Dina Adil Elia Halagy,** under my supervision at Nahrain University/ College of Engineering in partial fulfillment of the requirements for the degree of Master of Science in Chemical Engineering.

Signature: M.A.R.

Name: **Dr.Muhanned A.RMohammed**

(Supervisor)

Date :24/7/2006

Signature:

Name: **Prof. Dr. Qasim J. Slaiman**

(Head of Department)

Date: 7/8/2006

Certificate

We certify, as an examining committee, that we have read this thesis entitled **"Studying the Factors Affecting the Drag Coefficient in Free Settling in Non-Newtonian Fluid"**, examined the student **Dina Adil Elia Halagy** in its content and found it meets the standard of thesis for the degree of Master of Science in Chemical Engineering.

Signature: M.A.R.
Name: **Dr.Muhanned A.RMohammed**
(Supervisor)
Date : 24/7/2006

Signature: Latif
Name: **Dr. Mohammed.N.Latif**
(Member)
Date : 18/7/2006

Signature:
Name: **Dr. Malek M. Mohammed**
(Member)
Date : 17/7/2006

Signature: Nada
Name: **Prof. Dr. Nada B. Nakkash**
(Chairman)
Date : 31/7/2006

Approval of the College of Engineering.

Signature: M. J. Jweeg
Name: Prof. Dr. Muhsin J. Jweeg
(Acting Dean)
Data: 14/8/2006

ABSTRACT

The aim of this research is to study the effect of rheological properties ,concentrations of non-Newtonian fluids, particle shape, size and the density difference between particle and fluid on drag coefficient (C_d) and settling velocity (V_S), also this study show the effect drag coefficient (C_d) and Reynolds' number (Re_P) relationship and the effect of rheological properties on this relationship.

An experimental apparatus was designed and built, which consists of Perspex pipe of length of 160 cm. and inside diameter of 7.8 cm. to calculate the settling velocity, also electronic circuit was designed to calculate the falling time of particles through fluid.

Two types of solid particles were used; glass spheres with diameters of (0.22, 0.33, 0.4, 0.6, 0.8, 1, 1.43, 2) cm. and crushed rocks as irregularly shaped particles with different diameters (0.984, 1.102, 1.152, 1.198, 1.241, 1.388, 1.420, 1.563, 1.789, 1.823, 1.847, 2.121) cm and compared with each other. The concept of equivalent spherical diameter (D_S) was used to calculate the diameters of irregularly shaped particles.

The settling velocity was calculated for Non-Newtonian fluids which represented by Power-Law fluid. Two types polymers were used, Carboxy Methyl Cellulose with concentrations of (3.71, 5, 15, 17.5) g/l and polyacrylamide with concentrations of (2, 4, 6) g/l and compared with Newtonian fluid which represented by water.

The results showed that the drag coefficient decreased with increasing settling velocity and particle diameters and sizes; and increased as fluid become far from Newtonian behavior and concentrations and the density difference between particle and fluid.

The results showed that the rheological properties of Non-Newtonian fluids have a great effect on the drag coefficient and Reynolds number relationship, especially in laminar-slip regime and decreases or vanishes at transition and turbulent-slip regimes.

CONTENTS

NOMECLATURE

A_P	Projected area of the particle in a planeperpendicular to the direction of the flow.	cm^2
A_R	Archimedes number.	cm^2
C_d	Particle drag coefficient.	dimensionless
D	Inside pipe diameter.	cm
D_P	Particle diameter.	cm
D_S	Diameter of particle having the same volume as a spherer.	cm
d_*	Dimensionless diameter.	dimensionless
F	Force.	dyne
F_B	Bouncy force.	dyne
F_D	Drag force.	dyne
F_G	Gravity force.	dyne
F_W	Settling velocity correction factor for wall.	
g	Acceleration due to gravity	cm/s^2
k	Power-Law consistency index, Shape factor.	$g.s^n/100cm^2$
k	Constant volume.	
L	Length.	cm
n	Power-Law flow behavior index.	dimensionless
Re_P	Particle Reynolds' number.	
u_*	Dimensionless velocity.	dimensionless
V_P	Solid particle volume.	cm^3
V	velocity.	cm/s
V_S	Settling velocity.	cm/s

GREEK SYMBOLS

γ	Shear rate	s^{-1}
θ_{300},	Dial reading of Fann-VG meter at 300 rpm and 600 rpm,	degrees
θ_{600}	respectively	
μ	Newtonian fluid viscosity.	cp
μ_a	Apparent viscosity.	cp
μ_e	Effective viscosity.	cp
μ_{eq}	Equivalent viscosity.	cp
ρ	Density.	g/cm^3
ρ_F	Density of fluid.	g/cm^3
ρ_P	Density of particle.	g/cm^3
τ	Shear stress.	$g.s/100cm^2$
Φ	Speed.	rpm
Ψ	Sphericity.	dimensionless

ABBEREVIATIONS

HEC	Hydroxy Ethyl Cellulose.
CMC	Carboxy Meyhyl Cellulose.
cp	Centipoise.
ppg	Pound per gallon.

CHAPTER ONE
Introduction

Knowledge of the terminal velocity of solid in liquid is required in many industrial applications. Typical examples include hydraulic transport slurry system for coal transportation, thickeners, mineral processing, solid-liquid mixing, water waste processing, cement industries, fluidized bed equipment, drilling for oil and gas, geothermal drilling [1].

The theory of settling finds an extensive application in a number of industrially important processes, the shape of the particle is an important factor in these processes. The extremes of interest are given by the examples of the paint industry, which is concerned with colloidally sized particle settling in highly viscous polymer fluids, also oil industry which interested in particles of millimeter or centimeter size, settling in polymers or clay based fluids which can be easily and efficiently pumped [2,3].

It has been shown theoretically and experimentally that the resisting force acting on a body moving in a fluid depends on particle's shape, size and projected area, the relative velocity of the body, and on the density and viscosity of the fluid [4].

The influence of shape on the terminal velocity and drag coefficient of some regular geometric shapes has been studied such as sphere, disk, cylinder or isometric particles due to their advantages in the studies. Few studies have been done on irregularly shapes particles especially for settling these particles in non-Newtonian fluids.

Some studies had been used a shape factor to classify irregularly shapes particles, which can be expressed as a sphericity (Ψ), which is the ratio of the surface area of sphere having same volume of particle to surface area of the particle. The sphericity of sphere is equal to one, while for irregular shaped particles are less than one [5].

Previous works studied the factors affected on the drag coefficient by knowing the relationship between the drag coefficient and particle Reynolds' number, but in this study a new graphs have been plotted to show the effect of difference factors on drag coefficient in Newtonian and non-Newtonian fluids by using Power-Law fluid as a model.

Aim of this work:

1. To Calculate drag coefficient of spherical and non-spherical particles from calculating the terminal settling velocity for Newtonian and non-Newtonian fluids.

2. To study the factors that affect drag coefficient, such as settling velocity, size of the particle, density difference between the particle and the fluid concentrations, and rheological properties of the fluid.

3. To give the relationship between drag coefficient and particle Reynolds' number.

CHAPTER TWO
LITERATURE SURVEY

2.1. Stockes Flow past a Sphere

The problem of sphere moving very slowly through a stationary fluid was first solved by Stockes in 1851. There is a whole class of problems dealing with very slow motion of fluids past bodies of various shapes. Stockes'law is commonly encountered and is by far the most important of these. Most practical applications of Stockes flow involve determination of the settling velocity of small solid or liquid particles fall through a fluid such as air or water or two phase flows with very low relative motion between fluid and particle.

Solution of Stokes problem solved by application of Navier-Stokes equation for steady flow, by assuming the inertial term is negligible and the fluid is incompressible. So, Stockes' law relates the force resisting motion on sphere which is exerted by fluid, generally referred to as drag force F_D, to the diameter of particle, its velocity V and physical properties of the surrounding fluid as density ρ and viscosity μ [6]:

$$F_D = 3\pi D_P \mu V \qquad \text{... (2.1)}$$

This study was dealt with single particle fall in a stagnant fluid. Generally, there is two type of falling velocity, which are as following;

2.2. Terminal Settling Velocity:

The terminal settling velocity is the most important factor, which affecting relationship between the drag coefficient and particle Reynolds' number, since it is involving in the evaluation of these two quantities. Therefore, all the variables which affect terminal settling velocity can be correlated and clearly shown in drag coefficient-particle Reynolds' number relationship [7].

Consider a solid particle falling from a rest in a stationary fluid under the action of gravity. At first, the particle will accelerate as it does in a vacuum, but unlike in a vacuum, its acceleration will be retarded due to friction with the surrounding fluid. As frictional force increases with the velocity, this force will eventually reach a value equal to that of the gravitational force. From this point on, the two forces balanced and the particle continue to fall with constant velocity. Since this velocity is attained at the end of the acceleration period, it is called terminal settling velocity [3].

In practice, the acceleration period is of a very short duration, often of the order of a small fraction of a second. It is therefore customary to ignore this period in all practical problems concerned with settling processes, and the terminal settling velocity then becomes the only important factor in this kind of problem. Its magnitude is closely related to the physical properties of the fluid and the particle [3].

When the particle is at sufficient distance from the boundaries of the container and from other particles, so that the falling of a single particle is not affected by them, the process is called free settling [8].

The settling behavior at low Reynolds' number is known as laminar-slip and that of high Reynolds' number as the turbulent-slip between these two regimes is the transitional-slip regime. In laminar-slip regime, the settling velocity is affected by viscosity and rheology of fluid. While in the turbulent-slip regime, the settling velocity is affected mainly by the density of the fluid and the surface characteristics of particle [9].

It is clear that settling velocity depends mainly on various factors; such as density; an increase in density of fluid will increase the bouncy force thus the settling velocity will reduce, also on rheological properties as the fluid becomes more viscous the settling velocity for given particle will decrease because of the increase of the drag force exerted by fluid. Also, settling velocity depends on projected area of particle that facing the direction of relative motion between the fluid and the solid particle.

The irregularly shaped particles settle at lower velocity than does the spherical particles because the lacked of the symmetrical and geometrical shaped, in other words; decrease in spherecity and increase in projected area will increase the drag so they tend to orient and take different trajectories in a preferred direction during their fall, this preferred orientation is not generally predictable, depending on the position of their center of gravity relative to the center of force since these two centers must fall on the same line of direction of motion, also increase roughness of particle surface increase drag [10, 11].

For non-spherical particles; of ($Re_P > 10$), the particles settle flat wise with no tilt of the particle plane. For ($2 < Re_P < 10$), the particles settle predominantly flat wise; however, the largest projected area is tilted between 0° and 45°.

For ($Re_P < 2$), the orientation stability was dependent on the relationship of the center of mass to the geometric center of the particle [12].

Isometric particles follow vertical path, just like sphere, when their particle Reynolds' number have values under 300. For flows with Reynolds' numbers between 300 and 150000, they rotate, oscillate and follow helicoidal trajectories. The disk have always flat fall when $Re_P < 13$, and have edge fall when $Re_P < 3.5$. Unstable fall is occurred when particle Reynolds' number range from 2.5 to 10.0 [13, 14].

Chien developed the following settling velocity equation which is depended on the type of the non-Newtonian fluid for irregular particle. It covers all slips regimes:

$$V_S = 120.0\left(\frac{\mu_e}{D_P \rho_F}\right)\left[\sqrt{1 + 0.0727 D_P\left(\frac{\rho_P}{\rho_F} - 1\right)\left(\frac{D_P \rho_F}{\mu_e}\right)^2} - 1\right] \quad \text{... (2.2)}$$

μ_e = effective viscosity of Non-Newtonian fluid.

Chien suggested different effective viscosity values for each type of non-Newtonian fluids. The different values of effective viscosity of non-Newtonian fluids are due to the shear stress-shear rate relationship. Chien's correlation considers size, surface condition, and density of the particle and density and viscosity of the fluid [9].

Kelessidis proposed generalized explicit equation to find directly the settling velocity for non-Newtonian (Pseudo-plastic) fluid by using dimensionless diameter d_* and dimensionless velocity u_* [15].

$$U_* = \left\{ \frac{1}{\left(\frac{18}{d_*^{1+n}}\right)^{0.824/n}} + \left(\frac{0.321}{d_*}\right)^{0.412} \right\}^{1.214} \qquad \text{... (2.3)}$$

Where

$$d_* = d \left\{ \left(\frac{g(\rho_P - \rho_F)}{\rho_F} \right)^{2-n/2+n} \left(\frac{\rho_F}{k}\right)^{2/2+n} \right\} \qquad \text{... (2.4)}$$

n= flow behavior index.

k= consistency index of fluid.

2.3. Hindered Settling Velocity:

The theory relating to free settling is not directly applicable to suspensions, in which the particles affected by the presence of nearby particles and they interfered with each other. The settling rates of the hindered velocity lower than that of terminal settling velocity because hindered velocity is occurred when there is an increase in the concentration and interaction or collision between the particles, so the correlations of normal drag do not apply. This reduction may be expressed in term of the free space available between the particles, as defined by the viodage fraction, and numbers of attempts have been made to correlate experimental data on this basis. If the particles are very small about 2 to 3 μm, Brownian movement appears whereby collisions between the particles and fluid molecules result in the particles following random path, so there is no settling by gravity [3, 6, 8].

2.4. Previous Works:

In 1948 Heywood [11] concluded from his own experiments with irregular particles, which covered wide range of Reynolds' number values (0.01 to 1000) that the fall velocity of a given shape is a function of its projected area. Thus for every shape he introduced a volume constant k such that $k=\frac{\text{volumeofparticle}}{D^3}$, where D^3 is the diameter of a circle of an area equal to the projected area of the particle in its most stable settling position. He plotted drag coefficient with Reynolds' number for different values of k as a significant shape factors also computed value of k for several regular geometric shaped and suggested using C_d-Re_P diagram to solve settling velocity for any irregular particles .

In same year Pettyjhon and Chritiansen [4] conducted experimental work on falling particles freely in a fluid under the effect of gravity, using isometric particles and different Newtonian fluids having different densities. They concluded that the sphericity is a satisfactory criterion for the effect of particle shape on the resistance to motion of particles. As sphericity decreased, the drag coefficient was increased they stated also that for viscous flow ($Re_P < 0.05$) stock's law can be applied, while for highly turbulent flow (Re_P=200 to 20, 000) Newton's law can be applied, and for intermediate range (Re_P=0.05 to 200) the plot of C_d=f (Re_P, Ψ) can be used.

In 1959, Becker [16] stated that the drag on oriented bodies (or particles) in motion through an infinite fluid is composed of a viscous drag and an inertial drag, in which a quadratic drag formula was adopted. This drag is related to the fluid velocity and to properties of the fluid and the particle. According to that drag is related to particle Reynolds' number. Application of drag formulation showed that inertial drag deceases with minimum dependence on shape and Reynolds' number.

The first attempt is made by Slattery and Bird in 1961 [17], to understand the behavior of non-Newtonian fluid around particles. They used Ellis rheological model in their study, and they measured the drag coefficient of spheres moving through CMC solutions. Two dimensionless correlations for drag coefficient in terms of a modified particle Reynolds' number based on Ellis parameters, have been adopted.

Wasserman and Slattery [18] in 1964 used a variational method to obtain upper and lower bounds of the drag coefficient for a sphere moving through a power law fluid. However, the agreement between this method and available experimental data was poor.

The first study on a modified C_d-Re_P relationship for sphere in Bingham Plastic non-Newtonian fluid is conducted by Valentick and Whitmore [19] in 1965. They used a flocculated aqueous clay suspension of six densities with different flow parameters. These suspensions follow Bingham Plastic model. Spheres of different diameters and densities were dropped into these suspensions in order to measure their settling velocities. Reynolds' number was modified to take into account the flow parameters of Bingham Plastic model. They stated that the drag forces of a particle moving in a Bingham fluid are composed of force of falling in Newtonian fluid and a force to overcome the yield stress of Bingham Plastic.

Plessis and Ansely in 1967 [20] studied experimentally the settling characteristics of solid particles settling in clay suspensions of different concentrations, which followed Bingham plastic models. According to that, sand and glass particles with different sizes were used; in which diameters were determined using sieving analysis. They compared the C_d-Re_P relationship for these clay suspensions with that for water. They concluded that the settling characteristics of particles in clay-water slurries is different from those in water, and that the drag coefficient for particles is functional of a plasticity number in terms of the rheological properties.

Issacs and Thodos [21] presented drag coefficients from settling velocity measurements of cylinder particles which have a ratio of length to diameter 1/10 and Reynolds' numbers between 200 and 600,000. They made all the measurements using two large cylindrical settling tanks containing quiescent water at room temperature. They found separate analytical correlations for cylinders of L/D>1 and for L/D<1 independent of Reynolds' number. They described the motion generated by the particle during settling for cylinder of L/D less than, equal to, and greater than one.

Hottovy and Sylvestor in 1979 [22], used different irregularly shaped particles of different diameters with density of 0.88 g/cm^3. These particles were dropped through a column of liquid of 0.5 g/cm^3 density. They concluded from a plot of C_d-Re_P curve that for Re_P<100, the drag force acting on the irregularly shaped particles is similar to that acting on a sphere of comparable size, while for Re_P>100, the C_d-Re_P curve was deviated from standard trend. This deviation was due to the drag force on these particles is higher than drag force on sphere of comparable size. They repeated their runs for three different temperatures, and concluded that the settling rate increased with increasing temperature. They stated that this increasing was due to the fact that the temperature reduced the viscosity of liquid and increased density difference between liquid and solid.

Torrest in 1983 [23], studied the settling behavior of different sizes of solid particles in non-Newtonian polymer solutions. He concluded that as polymer concentrations increased, velocity will decrease. Also, as particle size increases, settling velocity will increase, and this confirm Stock' law.

Flemmer and Banks in 1986 [24] presented a mathematical approximation to experimental data of the drag coefficient and particle Reynolds' number of a sphere in Newtonian fluids. A Newton-Raphson technique was used, in order to determine settling velocity from the know ledge of C_d-Re_P^2 and of particle diameter from knowledge of Re_P/C_d.

Meyer [25] presented a modified correlation for particle Reynolds' number and drag coefficient for Laminar, transition, and Turbulent flow. He stated that the wall and concentrations effects have a large impact on hindering particle settling.

Concha and Barrientos [13] developed empirical equations for describing settling velocity and drag coefficient of isometric particles. These equations were developed by using corrections to the available equations of sphere. They consider different assumptions, base pressure, thickness, and the angle of separation of the boundary layer, depend on the shape of the particle and on the densities of the particle and the fluid.

In 1987 Dedegil [26] stated that the forces due to yield stress must be considered in calculating drag force on particles settled in non-Newtonian fluids, which obey Bingham- plastic flow model. He stated that the Reynold's number must be calculated by means of the fully representive shear stress including the yield stress which can be traced back to that of Newtonian fluids.

Reynolds and Jones in 1989 [2] studied the settling behavior of spherical and of irregularly shaped particles of different diameters in non-Newtonian polymer fluids. These follow not correctly a power law model, but depended on its concentration. They concluded that particles through the polymer fluids generate a localized shear rate in the fluid surrounding it. It is difficult to obtain a polymer fluid which behaved as a polymer power law fluid at shear rates generated by the falling spheres for Reynolds' number below 0.1. The other conclusion they made that settling velocities of particles of irregularly shaped could be approximated by that of a sphere of equivalent volume and density.

Chien in 1994 [9] studied the settling velocity of irregularly shaped particles in non-Newtonian and Newtonian fluids for all types of slip regimes. He derived new settling velocity correlations for irregularly shaped particles. Also, these correlations consider size, surface condition, and velocity of the fluid and cover all types of fluids and slip regimes with particle Reynolds' numbers from 0.001 to 10,000. He used an effective viscosity in determining the settling velocity, which is based on settling shear rate for Bingham plastic, power law, Casson, and divided by particle size. He concluded that a trial-and-error or a numerical iteration method, such as the Newton-Raphson method, can be used to solve for settling velocity. He also concluded that the fluid rheology plays a minor role in Turbulent-slip regime and the settling velocity is essentially determined by the fluid density and particle density and surface characteristics.

In 1999 Ataid, Pereira and Barrazo [27] studied the wall effects on terminal velocity. They used 30 spherical particles of several sizes ranging from 6.92 to 35.00 mm and made of materials of such as Teflon, glass, PVC, brass, steel, ceramics and porcelain and dropped each of them in five vertical different diameters cylindrical tubes in Newtonian and non-Newtonian liquids. They presented a correlation for estimating Reynolds' number as a function of drag coefficient and particle diameter to tube diameter ratio (β). Also, they presented a correlation for estimating the wall factor in Newtonian liquid and expression for prediction the characteristics shear rate associated with the physical situation of falling spheres in non-Newtonian liquids, which accounted for not only the particle and tube diameters, but also particle and fluid density.

Lessano and Esson [28] measured experimentally terminal velocity of irregular particles in a free–falling stream by using Particle Image Velocimetry (PIV) to asses the influence of particle shape on the particle dynamics. They used particle diameters ranged from 150 μm to 180 μm. They found that the velocity of irregular particles in developing region showed a distinct peak in the centerline of the flow, whilst the spherical particles exhibits a nearly flat radial profile in the self-similar region.

In 2003, Kelessidis [1] measured the terminal velocity of solid spheres through stagnant Newtonian and shear thinning non-Newtonian fluids. They proposed an equation for predicting the terminal velocity in both types of fluids.

In 2004, Klessidis [15] established an explicit equation which predicting the terminal velocity of solid spheres falling through stagnant Pseudo-plastic fluid from knowledge of the physical properties of spheres surrounding fluid. The equation is a generalized of the equation proposed for Newtonian liquids. He derived dimensionless velocity U_* as a function of Reynolds' number and a dimensionless diameter D_* as a function of Archimedes number, Ar.

CHAPTER THREE
THEORY OF OPERATION

3.1. Particle Dynamics

Particle dynamics is a branch of general mechanics dealing with relative motion between a particle (solid or liquid), and a surrounding fluid (liquid or gas).

The basic theory which follows relates to the motion of a single particle in a finitely large volume liquid. Under such an extraneous condition, the particle enjoys complete freedom in its motion, unlike a situation in a very limited space. If, the concentration of particle is reasonably low, their behavior may not be different from that of a single particle. We refer to this motion as to free motion or free settling when it is under gravity. Otherwise the motion said to be hindered [3].

The movement of a particle through a fluid requires external force acting on a particle. This force may come from a density difference between the particle and the fluid or may be the result of electric or magnetic fields.

Three forces act on a particle moving through a stagnant fluid : The gravitational (F_G), the buoyant force (F_B) which acts parallel with the external force but in opposite direction and the drag force (F_D) which appears whenever there is relative motion between the particle and the fluid. The drag force acts to oppose the motion and acts parallel with direction of movement but in opposite direction, as shown in figure 3-1[8, 3].

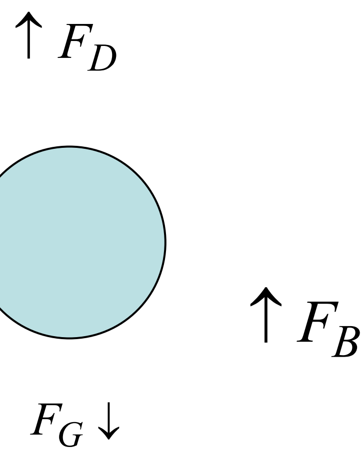

Figure 3-1 A free falling particle under the action of gravity and resistance of forces [3].

Consider a spherical solid particle of density ρ_P, falling in a stationary fluid of density ρ_F under the action of gravity. The gravitational force acts on the particle even when it is at rest, and remains constant during the whole period of fall. Let D_P be the diameter of the particle, then its volume is $V_P = \frac{4}{3}\pi r_P^3 = \frac{\pi D_P^3}{6}$ and $(\rho_P \frac{\pi D_P^3}{6})$ it's mass. From Newtonian's second law of motion, using the absolute system of units

$$F_G = \frac{\pi D_P^3 \rho_P}{6} g - \frac{\pi D_P^3 \rho_F}{6} g \qquad \text{... (3.1)}$$

where g is the gravitational acceleration.

The last term of this equation represents the buoyancy effect. This effect may be ignored if the density of fluid is negligibly small compared with the density of fluid of solid particle, as in the case when the fluid is a gas. Otherwise equation 3.1 becomes

$$F_G = \frac{\pi D_P^3}{6}(\rho_P - \rho_F)g \qquad \text{... (3.2)}$$

For a particle settling at its terminal velocity the two opposing forces are in a balance, so that by combining with Stokes'equation 2.1

$$F_D = F_G \qquad \text{... (3.3)}$$

Let V_S be the terminal settling velocity, then substituting in the above equation for F_D and F_G from the equations 2.1 and 3.2 so:

$$3\pi D_P \mu V_S = \frac{\pi D_P^3}{6}(\rho_P - \rho_F)g \qquad \text{... (3.4)}$$

From which

$$V_S = \frac{D_P^2(\rho_P - \rho_F)}{18\mu} g \qquad \text{... (3.5)}$$

This equation is restricted to the region where Stokes' law applies [3]. The assumptions made in the derivation of Stock's law of settling velocity are:

1. The particle must be spherical, smooth and rigid; there must be no slip between it and the liquid.
2. The particle must move as it would in a fluid of infinite extent.
3. The terminal velocity must have been reached.
4. The fluid must be homogeneous compared with size of particle.
5. The settling speed must be low so that only viscous forces are brought into play.

In any actual situation the assumptions listed above will not usually be valid and correction factors are sometimes necessary [29].

3.2. Drag Coefficient

Basically, the drag coefficient (C_d) represents the fraction of the kinetic energy of the settling velocity that is used to overcome the drag force on the particle [7].

$$C_d = \frac{F_D / A_P}{\rho_F V_S^2 / 2} \quad \text{... (3.6)}$$

Thus the drag force for spherical particle in terms of drag coefficient,

$$F_D = \frac{\pi}{8} \rho_F C_d D_S^2 \, V_S^2 \quad \text{... (3.7)}$$

After balance condition, the drag force equals to the force of gravity (F_D=F_G) by combining equations 3.6 and 3.2:

Thus,

$$C_d = \frac{4}{3} \frac{D_S(\rho_P - \rho_F)}{\rho_F V_S^2} g \quad \text{… (3.8)}$$

In field units equation 3.8 becomes:

$$C_d = 12880 \frac{D_S(\rho_P - \rho_F)}{V_S^2 \rho_F} \qquad \text{... (3.9)}$$

Where, D_S in inches, ρ_F in ppg, V_S ft/min and μ_{eq} in cp [6].

The drag coefficient (C_d) of a smooth solid in a fluid depends upon particle Reynolds number. It is (in field units) defined as

$$Re_P = 15.46 \frac{\rho_F V_S D_P}{\mu_{eq}} \qquad \text{… (3.10)}$$

At low $Re_P < 1.0$ implies a relatively high viscous force, and a major portion of the drag force is used to overcome the viscous resistance of the fluid. The experimental and the theoretical analysis shows that for very low Re_P drag coefficient is:

$$C_d = \frac{A}{Re_P} \qquad \text{... (3.11)}$$

While at high $Re_P > 200$ the inertial force becomes dominant the fluid density, particle shape and surface roughness affect the drag force. At Re_P (>500), the drag coefficient of a given particle approaches a constant value the drag coefficient is:

$$C_d = B \qquad \text{... (3.12)}$$

Where A, B are constants [7, 8]. For particles having shapes other than spherical, it is necessary to specify the size and geometrical form of the body and its orientation with respect to the direction of flow. One major dimension is chosen as the characteristic length, and other important dimensions are given as ratios to chosen one. Such ratios are called shape factor. Thus for short cylinders, the diameter is usually chosen as defining dimension, and the ratio of length to diameter (L/D) is a shape factor. A different C_d-Re_P relation exists for each shape and orientation. The relation must in general be determined experimentally, for particles having shapes other than spherical as in figure 3.2 [8].

Particle Reynolds' number and drag coefficient have a very unique relationship, it can be shown by a logarithmic plot of C_d vs. Re_P figure 3.3. For spherical particle settling in a liquid in which there are three zones. The laminar zone, also called the stream line or viscous zone, transition and turbulent zones. In general, as the Re_P increases, the drag coefficient will decrease and at very high Re_P, the drag coefficient will approach a small constant value. During this increases in Re_P, the settling velocity will be less dependent on the fluids' viscosity [3].

We can see from the figure;

For laminar zone; $C_d = \frac{24}{Re_p}$ $10^{-6} \leqslant Re_P < 0.2$ ... (3.13)

In which the settling velocity (Stock's equation) as in equation (2.1):

$$V_S = \frac{D_P^2(\rho_P - \rho_F)}{18\mu}$$

For transition zone; $C_d = \frac{18.5}{(Re_P)^{0.6}}$ $0.2 \leqslant Re_P < 500$ ... (3.14)

Allen's settling equation is used for settling velocity [6]:

$$V_S = 0.2\left[\frac{g(\rho_P - \rho_F)}{\rho_F}\right]^{0.72} \frac{D_P^{1.18}}{\left(\mu/\rho_F\right)^{0.45}} \quad \text{... (3.15)}$$

For turbulent zone; $C_d = 0.44$ $500 \leqslant Re_P < 2*10^5$ ... (3.16)

Newton's law is used for settling velocity:

$$V_S = 1.75\sqrt{\frac{gD_p(\rho_p - \rho_F)}{\rho_F}} \quad \text{… (3.17)}$$

As shown in equations 2.1, 3.17 the terminal velocity V_S varies with D_P^2 in Stock's law range, whereas in Newton's-law range it varies with $D_P^{0.5}$ [8, 3].

The flow behaviors of non-Newtonian fluids obey different reheological models, which represent the shear stress-shear rate flow curves. The effect of the reheological properties n, k of these non-Newtonian fluids on the drag coefficient- particle Reynolds' number relationship was studied this workl.

Zeidler [12] showed that drag coefficient is not a function of particle Reynolds' number only, but is a function of the degree of non-Newtonity (as behavior index n for Power-Law fluid).

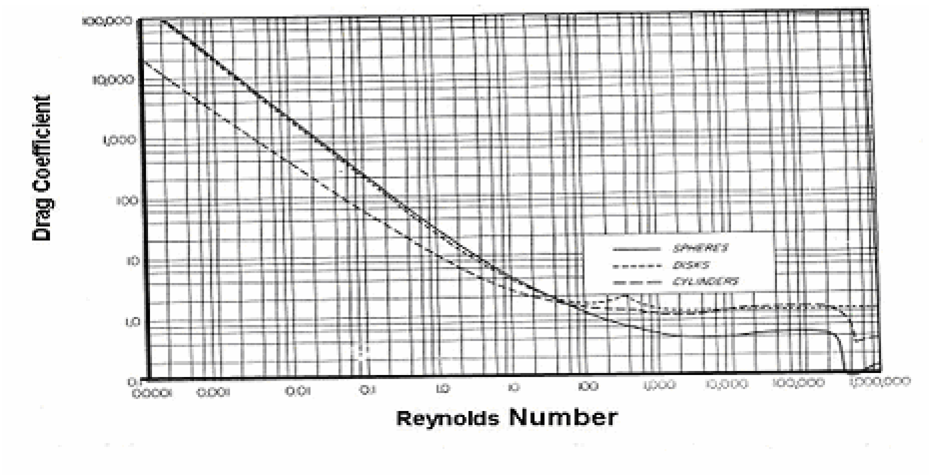

Figure 3-2 Drag coefficients for spheres, disks and cylinders [8].

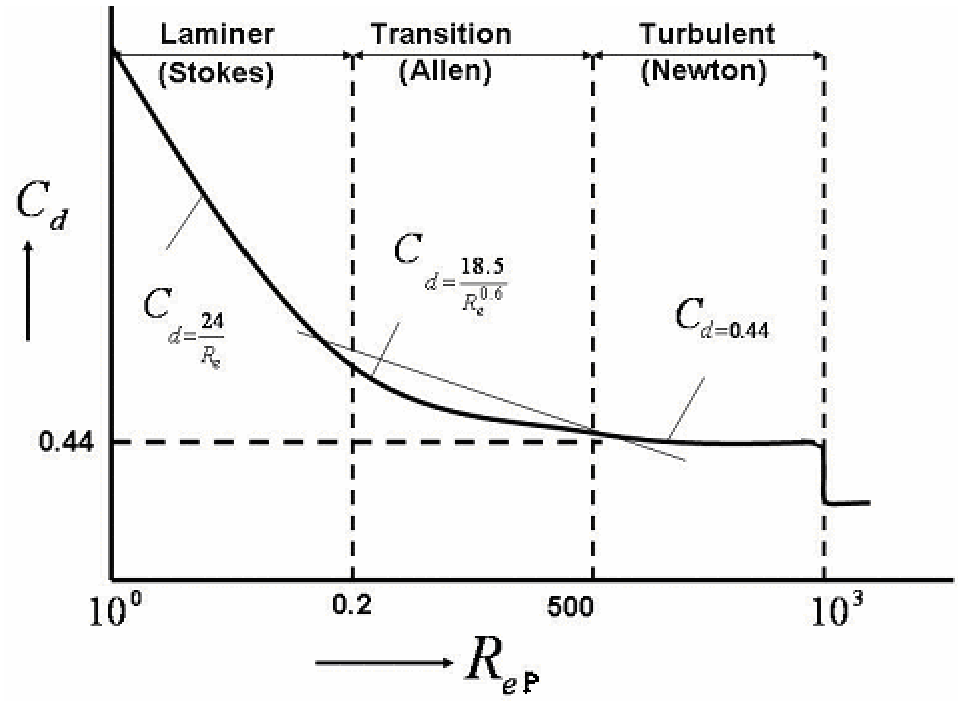

Figure 3-3 Drag coefficient vs. Rynolds' number relationship [8].

3.3. Particle Reynolds' Number, Re_p:

Particle Reynolds' number is used to indicate whether the boundary layer around a particle is turbulent or laminar, and the drag exerted will depended on this. It is a measure of the relative important of inertial to viscous forces of flow [10, 2], and is given by their ratio by following formula;

$$\mathrm{Re}_P = \frac{\rho_F V_S D_P}{\mu} \qquad \text{... (3.18)}$$

Thus when Re_P is small (laminar-slip regime) the viscous forces which results from fluid viscosity dominate the inertial force so the drag coefficient proportional to particle Reynolds' number, but as Re_P becomes larger the inertial forces, which result from the density of the fluid and the surface characteristics of particle, become of greater importance. At large values of particle Reynolds' number (turbulent-slip regime) the inertial forces completely dominate the viscous force, thus the viscosity of fluid has no effect on the drag coefficient. The drag coefficient in turbulent-slip regime is less dependent on Re_P, because of that the C_d will reach a small constant value. Between these two regions is the transition region, where the resistance to the particle settling in the liquid by both the viscous and inertial forces.

For Newtonian fluid, viscosity μ is constant independent of shear rate and the concept settling shear rate is not used [7].

For Non-Newtonian fluid the viscosity varies with the shear rate. Therefore, an expression of equivalent viscosity μeq can be used, which represent the viscosity of fluid around the particle during its movement. The equivalent viscosity is defined as the ratio of shear stress on particle surface to average shear rate of the particle [7].

$$\mu_{eq} = 478.8 \frac{\tau_P}{\gamma_P} \qquad \text{... (3.19)}$$

There are several equations that relate shear stress to shear rate for non-Newtonian fluids. According to that, there are several forms of equivalent viscosities, depending on the type of the non- Newtonian model. In this study Power-Law model's equation is only used and the equivalent viscosity of this model as follows [7]:

$$\mu_{eq} = 478.8k\left(0.6\frac{V_S}{D_P}\right)^{n-1} \qquad \text{… (3.20)}$$

3.4. General C_d-Re_P Formula:

There are many formulas for C_d-Re_P relationships in Newtonian fluids concerned with spherical and irregularly shaped particles in Newtonian fluids and very little available formulas that concerned with particles falling in non-Newtonian fluids. The following formulas are:

1. Oseen formulae for Newtonian fluids[24]:

a. $C_d = \frac{24}{Re_P}\left(1 + \frac{3}{16}Re_P\right)$, (Re_P<1.0) … (3.21)

2. Perry and Chilton formula for Newtonian fluids [24]:

a. $C_d = \frac{24}{Re_P}$, $(Re_P < 0.3)$ … (3.22)

b. $C_d = \frac{18.5}{Re_P^{0.6}}$, $(0.3 < Re_P < 1000)$ … (3.23)

c. $C_d = 0.44$, $(1000 < Re_p < 200000)$ … (3.24)

3. Massey formula [24]:

$$C_d = \frac{24}{Re_P}\left(1 + \frac{3}{16} Re_P\right)^{\frac{1}{2}} \quad , (Re_p \leqslant 1) \qquad \text{… (3.25)}$$

4. Schiller and Nauman formula for Newtonian fluids [24]:

$$C_d = \frac{24}{Re_P} + \frac{3.6}{Re_P^{0.313}} \quad , (0.1 < Re_p < 1000) \qquad \text{… (3.26)}$$

5. Fouda and Capes formula for Newtonian fluids [24]:

$$Y = \sum_{n=0}^{5} a_n X^n \quad , (10^{-1} < Re_p < 10^{-5}) \qquad \text{… (3.27)}$$

Where;

a. $Y = \log_{10}(P_d)$, $X = \log_{10}(V_s/Q)$

$P_d = \sqrt[3]{C_d \, Re_P^2}$, $V_s/Q = \sqrt{\frac{Re_P}{C_d}}$

$a_\circ = -1.37323$, $a_1 = 2.06962$, $a_2 = -0.453219$,

a_3=-0.334612×10 $^{-1}$, a_4=-0.745901×10^{-2}, a_5=0.249580×10^{-2}

b. $Y=\log_{10}(\frac{V_S}{Q})$, $X=\log_{10}(P_d)$

$a_\circ$=0.785724, a_1=.684342, a_2=0.168457,

a_3=0.103834, a_4= 0.20901×10 $^{-1}$, a_5= 0.57664×10 $^{-2}$

6. Al-Salim and Geldart formula for Newtonian fluids [24]:

$$\frac{567}{Re_P^2}=\frac{3.318\times10^5}{\left(C_d\ Re_P^2\right)^{2}}+\frac{2.954\times10^4}{\left(C_d\ Re_P^2\right)^{1.5928}}+$$

$$\left[\frac{9.479\times10^{11}}{\left(C_d\ Re_P^2\right)^{4.1949}}+\frac{8.440\times10^{10}}{\left(C_d\ Re_P^2\right)^{3.7877}}\right]^{0.313}, (0.1<Re_p<1000) \qquad \ldots (3.28)$$

7. Flemmer and Banks for Newtonian fluids [24]:

$$C_d=\frac{24}{Re_P}10^E \qquad ,(Re_P<3\times10^5) \qquad \ldots (3.29)$$

Where; $E=0.261Re_P^{0.369}-0.105Re_P^{0.431}-\frac{0.124}{1+\left(\log_{10}Re_P\right)^2}$

8. For spherical particles falling in a Bingham-Plastic:

8.1. Plessis formula [20]:

$$C_d=f\left(\frac{\frac{\mu_P V_S}{\rho_F}+\tau_y}{\rho_F V_S^2}\right) \qquad \ldots (3.30)$$

8.2. Dedegil formula [26]:

a. $C_d = \frac{24}{Re_P}$, $(Re_P < 8)$ … (3.31)

b. $C_d = \frac{22}{Re_P} + 0.25$, $(8 < Re_P > 150)$ … (3.32)

c. $C_d = 0.40$, $(Re_P > 150)$ … (3.33)

9. Haider and Levenspiel formulas for Newtonian fluids [28]:

9.1. For non-spherical particles:

$$C d = \frac{24}{Re_P}\left[1 + \left(8.171 exp(-4.0655\Psi)\right)\right] Re_P^{0.0964+0.5565\Psi} + \frac{73.69\, Re_p\, exp(-5.748\Psi)}{Re_p + 5.378\, exp(6.2122\Psi)} \quad \text{… (3.34)}$$

9.2. For spherical particles:

$$C_d = \frac{24}{Re_P}\left(1 + 0.1806\, Re_P^{0.6459}\right) + \frac{0.4251}{1 + \frac{6880.95}{Re_P}} \quad \text{... (3.35)}$$

10. Mpandelis and Kelessidis formula for Newtonian fluids and non-Newtonian [30]:

$$C_d = \frac{24}{Re_P}\left(1 + 0.1407\, Re_P{}^{0.6018}\right) + \frac{0.2118}{1 + \frac{0.4215}{Re_P}} \quad \text{... (3.36)}$$

3.5. Equivalent Particle Diameter

In the free motion of non-spherical particles through a fluid, the orientation is constantly changing. This change consumes energy, increasing the effective drag on the particle, and C_d is greater than for the motion of fluid past a stationary particle [8].

A major problem associated with study of drag coefficient of non-spherical bodies is finding a characteristic diameter. The knowledge of size and diameter and projected area of these bodies is not straight forward as spheres particles, because these particles have no regular geometric shapes.

To calculate the diameter of irregular shape in this study, this method is used by assuming that the diameter of particle having same volume of sphere which called equivalent spherical diameter D_s [29, 31, 32].

$$\text{Vol.} = \tfrac{\pi}{6} D_S^3 \qquad \text{... (3.37)}$$

$$D_S = \left(\tfrac{6}{\pi} vol.\right)^{\frac{1}{3}} \qquad \text{... (3.38)}$$

And the particle Reynolds' number becomes

$$\text{Re}_P = 15.46 \frac{\rho_F V_S D_S}{\mu_{eq}} \qquad \text{… (3.39)}$$

3.6. Effect of Pipe Wall

It's well known that the presence of wall finite boundaries exerts a retarding on terminal velocity of particles in a viscous medium. Knowledge of this effect is needed to deduce the net hydrodynamics drag on the particle due solely to the relative motion between the particle and the fluid medium. It is customary to introduce a wall factor, F_w to quantify the extent of wall effect on terminal velocity of a particle [27].

Effect of pipe wall on settling velocity of particle in vertical pipe is largely studied experimentally and theoretically such as:

3.6.1 Brown and Associates [29]:

They developed an empirical correction factors by which the terminal velocity must be multiplied to obtain the actual settling velocity.

For laminar-slip regime;

$$F_w = 1 - \left(\frac{D_P}{D}\right)^{2.25} \qquad \dots (3.40)$$

For turbulent-slip regime;

$$F_w = 1 - \left(\frac{D_P}{D}\right)^{1.5} \qquad \dots (3.41)$$

Where D is the diameter of the pipe, and F_w is the correction factor.

3.6.2 Valentik and whitmore[19] :

They used an experimental approach for correcting the terminal settling velocities due to the effect of pipe wall. Settling velocities of the particles should be measured using different pipe diameters, then extrapolation of plot of these measured settling velocities with the reciprocal of the pipe diameter, yields the corrected settling velocity. But these results were difficult to reproduce.

3.6.3 Reynold and Jones [2]:

They suggested that the ratio of particle radius to tube radius should be less than 0.1, in order to avoid the effect of tube wall.

3.6.4 Hopkin [33]:

They developed wall correction factor as follows;

$$F_w = 1 - \left(\frac{D_S}{D}\right)^2 \qquad \dots (3.42)$$

This is inadequate correction factor, because it gives unreasonable results at high particle Reynolds' number.

3.6.5 Walker and Mayes [14]:

They presented an empirical correction factor, which has the following formula;

$$F_w = \frac{D - 1.6 D_P}{D - D_P} \quad \dots (3.43)$$

3.6.6 Fidleris and whitmore [34]:

They suggested using $F_w = 1 - \left(\frac{D_P}{D}\right)^{1.5}$ at the low Reynolds' number (laminar regime), $F_w = \left(\frac{1 - \frac{D_P}{D}}{1 - 0.475\frac{D_P}{D}}\right)^4$ at high Reynolds' number (turbulent regime) and graphs for intermediate region.

3.6.7 Ataid, Pereira and Barrazo [27]:

They found an equation for Newtonian fluids to find, F_w, this equation is a function of Re_P and $\frac{D_P}{D}$ as follow;

$$F_w = \frac{1.092}{1 + A\, Re_P^B} \quad \dots (3.44)$$

Where, $A = 0.1\exp^{8.541\frac{D_p}{D}}$, $B = -0.042 - 0.939\frac{D_P}{D}$.

The range of the validity of the parameters for this equation are $0.38<Re_p<310.7$ and $0<\frac{D_P}{D}<0.61$.

3.6.8 Turian [35]:

He used extrapolation method by plotting terminal settling velocity vs. reciprocal of cylinder diameter (1/D).

3.7. Types of Fluids:

The plot of shear stress versus shear rate is called a “flow curve”. The fluids may be classified according to the observed flow curve into;

3.7.1 Newtonian Fluids:

Newtonian fluid is defined by a straight line relationship between shear stress τ and shear rate γ with slop equal to the viscosity of fluid:

$$\tau = \mu\gamma \qquad \dots (3.45)$$

In this type of fluid, viscosity is constant and is only influenced by changes in temperature and pressure, as shown in figure 3.4. Examples of Newtonian fluids are oil and water [6].

3.7.2 Non-Newtonian Fluids:

In these fluids, the shear stress-shear rate ratio is not constant, or the shear stress-shear rate relationship is non-linear. These fluids require two or more parameters to describe their flow behavior, thus the apparent viscosity μ_a of these fluids is defined by:

$$\mu_a = \frac{\tau}{\gamma} \qquad \text{... (3.46)}$$

In which, the apparent viscosity varies with shear rate at a constant temperature and pressure. Because, there is no direct proportionality between Shear stress and shear rate of these fluids, there are number of rheological equations which describe the flow behavior of these fluids [6].

As shown in figure 3.4 some liquids, for example, sewage sludge, do not flow at all until a minimum value of shear stress, denoted by $\tau_\circ$, is required and then flow linearly . Liquids acting this way are called Bingham-Plastic as shown in curve B. The curve C which represents Pseudo-plastic fluid is passed through the origin, concaves downward at low shear, and becomes linearly at high shear. Rubber Latex is an example of such fluid. Curve D represents a dilatant's fluid which is concaving upward at low shear and almost linear at high shear. Quick sand and some sand-filled emulsions show this behavior. Pseudo-plastics are said to be shear-thinning and dilatants fluids shear-thickening [8].

Dilatant's fluids are similar to Pseudo-plastics fluids, but the flow behavior index n is greater than unity for dilatant's fluids while for Pseudo-plastics fluids is less than unity. Equivalent viscosity of Pseudo-plastics fluids decreases with rate of shear but it increases with increasing of rate of shear for dilatant's fluids as shown in figure 3.5 [36].

All fluids mentioned above are time-independent fluids in which the shear stress of these fluids at constant temperature is solely dependent on the rate of shear at this temperature. Also, there are time-dependent fluids in which shear stress of these fluids at constant temperature is a function of both magnitude an duration of shear rate like Thixotropic fluids and Rheopectic fluids [36].

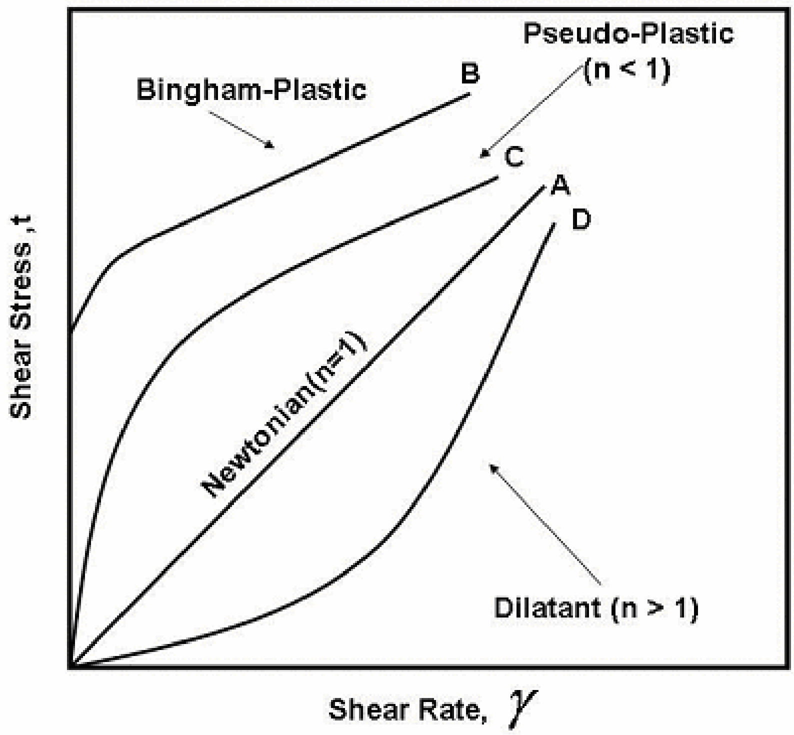

Figure 3-4 Shear stress vs. shear rate for Newtonian and non-Newtonian fluids [8].

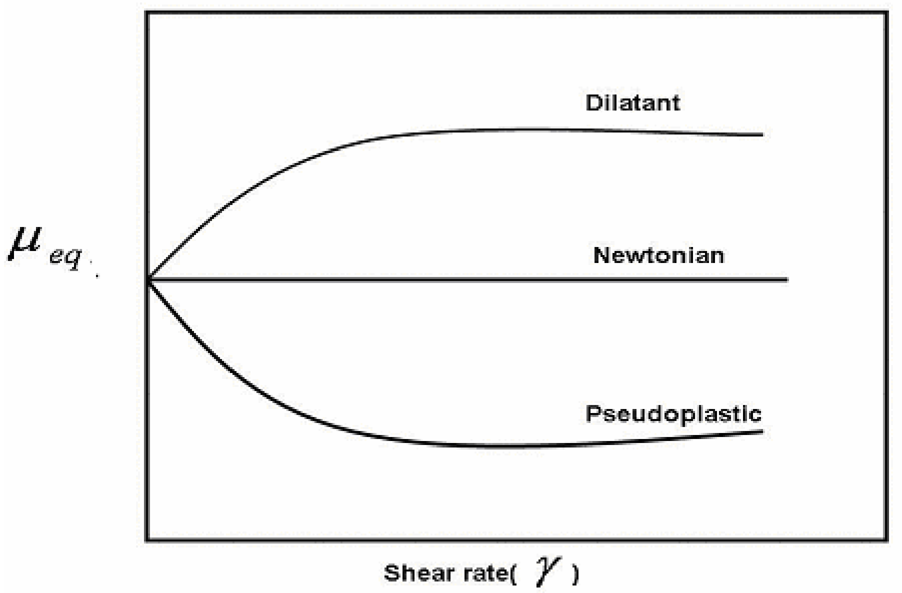

Figure 3-5 Effect of shear rate on equivalent viscosity for Newtonian and non-Newtonian fluids [36].

3.8. Rheological-Models for Non-Newtonian Fluids:

There are many rheological correlations which describe shear stress-shear rate relationship. All these relationships are empirical equations. Like Bingham-Plastic model, Power-Law model, Modified Power-Law model, Casson model, Robertson-Stiff model, Ellis equation, Reiner-Philippof equation, Modified Robertson-Stiff model and others.

The most common model which is used in this study is Power-law model. The Power-law model was chosen for determining the rheological properties of non-Newtonian fluids used in this study due to fact that this model is more applicable and most widely used.

The flow curve of Power-Law model can be described by an empirical equation which is:

$$\tau = k\gamma^n \qquad \dots (3.47)$$

A plot of τ vs. γ on log-log paper gives a straight line with a slop of n and intercept of k at γ=1.0, where n and k are rheological parameters of Power-Law fluid. The parameter n is the flow behavior index, which discuss the degree of non-Newtonian behavior. As n becomes far from unity, this means a greater non-Newtonian behavior. The parameter k is the consistency index, which is an indication of the thickness of the fluid. As k, increases this means thickness of fluid increases. The parameters n and k can be determined approximately using a Fann-VG reading as follow;

$$n = 3.32 \log\frac{\theta_{600}}{\theta_{300}} \qquad \dots (3.48)$$

$$k = \frac{\theta_{600}}{(1022)^{\ n}} \qquad \dots (3.49)$$

Where; θ_{600} =dial reading at 600 rpm, and

; θ_{300}= dial reading at 300 rpm.

Or they can be determined accurately using a linear regression technique:

$$n = \frac{\Sigma log\, \tau.\ \Sigma log\, \gamma - N.\ \Sigma(log\, \tau.log\, \gamma)}{\left(\Sigma log\, \gamma\ \right)^2 - N\ \Sigma(log\, \gamma)^{\ 2}} \qquad \dots (3.50)$$

$$\text{Log } k = \frac{\Sigma log\, \tau - n.\ \Sigma log\, \gamma}{N} \qquad \dots (3.51)$$

Where, N is the number of shear stress-shear rate test values [7].

3.8. Water Soluble Polymers:

Polymers are large molecules composed of seed extracts (guar, starch), modified cellulose (CMC, HEC), biosynthetic gums (xanthenes and welan gums), and synthetic Polymers. The simple molecules, from which Polymers are formed, are called monomer which is consisting primarily of compounds of carbon.

Viscosity is the most important property of polymer solution. In general, Polymer solutions showed non-Newtonian Pseudo plastic behavior, where viscosity decrease with shear rate.

Synthetic polymers behave in a similar manner, when they are in solid state. The hydrogen bonds of polymer are weak, because the molecules need crystalline. The water will penetrate the solid particle of the polymer and will hydrating the molecules. The process will continue until each solid will surrounded by water molecules and thus the polymer will be named as hydrophilic [37]. The polymers used in this study are:

3.9.1 Sodium Carboxy Methyl Cellulose (CMC):

It is prepared by the reaction of cellulose with chloroacetic acid in the presence of sodium hydroxide. It contains strong carboxyl groups which place it in the anionic polyelectrolyte category.

There are three grades available of CMC: low, medium, and high viscosity. CMC solutions have high apparent viscosities at very low shear rate, which decrease with temperature [37].

3.9.2 Synthetic Polymers:

Synthetic water dispersible polymers have been made from monomeric materials. The main kinds of these polymers are acryl amide and copolymers. They are extremely high molecular weight.

Generally, polymers attract water particles due to their high molecular weight and anionic groups [38].

CHAPTER FOUR
Experimental Work

4.1 Experimental Apparatus and Materials
4.1.1 Experimental Apparatus:

An experimental apparatus has been designed and built to measure the terminal settling velocity for solid particles. The test apparatus is consisting of vertical and transparent Perspex pipe, with length of 160 cm, outside diameter of 8 cm and inside diameter of 7.8 cm to avoid wall effects. The pipe was fixed on iron base plate that has an iron cylinder with height of 10 cm in which the pipe is fitted; at the end of this cylinder a tap for draining test fluid was connected. Another threaded cylinder had welded at the bottom of iron base in order to drain the particles, this cylinder had a plug to relieve the particles, and the diameter of this cylinder was designed such that largest particle size is enabled to pass through it and out. Figure 4-1 shows the schematic diagram for the settling velocity apparatus.

For careful determination of terminal settling velocity the pipe was divided into four sections as follows;

1. First section is inlet section L1. It is used for acceleration which defined as the distance that particle should travel before reaching an equilibrium of forces to get constant velocity (settling velocity). The first section must have sufficient settling length for accurate timing, so the inlet length used in this work was 85 cm.

2. Second section is test section L2. It is used for calculating the terminal settling velocity. The length was 50 cm, this section divided into two sections each of them 25 cm.
3. The third section is Drainage section L3. It is used for draining the fluid and avoids end effects.

The choice of these values was empirical for all sorts of fluid behaviors. Figure 4-2a shows the photograph of the settling column and the tests sections.

4.1.2 Electrical Circuit

The precision of measurement of the velocity is directly related to the time taken by the particle to travel a known distance (after travel L1). Aiming to assure the precision of the time measurement and to eliminate the human error, a digital electronic circuit was designed with three photo-sensor nets; as shown in figure 4-2b, these three nets are measured the time of particle falling in test section through fluid. These nets had connected to a digital board have nine 7-segments as shown in figure 4-2c; first three for giving the reading for first net and the second three for giving the reading for second net, all these equipments are connecting to power supply.

These nets were located at distances of 85 cm, 100 cm, and 125 cm from the top of the column. These nets consist of photo-sensor of one transmitter face to five receivers. The transmitter generates square wave signal with 20 KHz frequency, this signal suitable for reception by five receivers. The active transmission area 60°, so five receivers were facing the transmitter thus any of them could sense and receive the signal. Because the orientation of irregular shaped particles another transmitter and five receivers were fixed in three nets. They were located parallel to those, which means, the first transmitter parallel to the second transmitter and the first five receivers parallel to the second five receivers.

The transmitter transmits an Infera-Red ray to five receivers, when particle fell down through the column and reaches distance of 85 cm the ray will disconnect so the internal clock in first net starts to count and after the particle reaches distance of 100 cm the ray will disconnect also, the internal clock will stop counting and number of count will appear in first three 7-segments, at same time the second internal clock in second net starts to count and after the particle reaches distance of 125 cm the ray will disconnect again so internal clock in the third net will stop counting and number of count will appear in second three 7-segments. The designs of the counter's circuit, transmitters and receivers are shown in figures 4-3 a, b, c.

This number of counts will change to time by multiplying with a counters' factor. Because the viscosity of the test fluids were different the counter in the board which give the count in micro second could change manually so the counters' factor used for low concentration and water was taken 1024 micro second and for those with high concentration was taken 4096 micro second, because as concentration increased the number of counts must increased to get accurate results.

For sphere particles that have a diameters of (0.22, 0.3) cm, the photo-sensor nets were not sufficiently sensitive to record the passing of these particles. For these particles the time was taken manually by stop watch.

4.1.3 Test Fluids

In order to get different rheological properties two polymers were used, CMC and polyacrylamide with different concentrations as non-Newtonian fluids and water as Newtonian fluid. Seven different concentrations were prepared, four for CMC and three for polyacrylamide, these values are given in table 4.1.

The choice of these polymers was because; availability in a market, Infra-Red ray can pass through it, also to see the particles that falling time measured manually and these polymers are solved in water so they do not need certain solvent. Each polymer was obtained in the powdered form so the preparation was similar in each case.

7 liters of each fluid was prepared in batches by shaker or mixer adding the necessary amounts of polymer in water, added slowly, for long period because rapid addition of polymer in water will cause a rapid wetting of solid particles of the polymer so development of a barrier will prevent the water molecules from penetration the solid particles, thus slow addition of polymer will increase the surface area of polymer particles exposed to water with agitation to get complete solubility, after the batches collected, the mixture was letting for 24 hour to ensure; all the mixture was deareated to prevent air bubbles to form and then rheological properties of each samples were measured.

4.1.4 Density of Fluid

The densities of each test fluids used in this experimental work have been measured by pyknometer of volume 25 ml. By weighting of pyknometer when it is empty and full with certain test fluid and taking the difference between them, then divided by the volume of pyknometer, thus the density will be known at room temperature 27-28 C.

4.1.5 Fluid Rheology Determination

Power-Law model was used to represent the flow behavior of non-Newtonian fluids. The plots of shear stress τ versus shear rate γ of each test fluid on log-log paper gave a straight line with slop n and intercept k. These values are given in table 4.1.

The rheological properties (n, k) of each non-Newtonian fluid used for settling velocity determinations were measured by Fann VG meter model 35A rotational coaxial cylinder type. By preparing a 500 ml. of each fluid first, to determine the shear stress directly from the dial reading on the top of the instrument which has six rotational speeds 3, 6, 100, 200, 300, and 600 rpm. These speeds represent shear rates

The shear stress, τ, is given by;

$$\tau = 1.067\theta \qquad \text{... (4.1)}$$

where θ is the dial reading Fann viscometer and τ is in (lb/100 ft^2)

The shear rate, γ, is given by;

$$\gamma = 1.7034\varphi \qquad \text{... (4.2)}$$

where φ is the speed in rpm and γ is the shear rate in 1/sec.

4.1.6 Particle diameter's Measurements

Two groups of solid particles have been used in this study;

a. Sphere Particles

Spherical particles are made of glass with different diameters; the diameters were measured by a vernier with an accuracy of 0.01mm. The weight of particles was measured by a digital balance and the volume was calculated using

$$\text{Vol.} = \frac{\pi}{6} D_s^3 \text{ , while the area } = \frac{\pi}{4} D_s^2$$

Then, the density of the particle is the ratio of its weight to its volume; the physical characteristics of spherical particles are given in table 4.2.

b. Irregular Shaped Particles

The irregular shaped particles are formed from crushed rocks. The problem with these particles that they do not have standard diameters, so the concept of the equivalent spherical diameter D_s was used, which represented the diameter has a volume of sphere as discussed in Chapter Three.

The volume of irregular shaped particles had been measured by displacement method using Kerosene. The volume of displaced Kerosene in a graduated cylinder is equal to the particle volume. The mass of these particles had been measured by digital balance. Density of each particle is calculated by taking the ratio of its mass and volume. The area was calculated in same way as in sphere, the physical characteristics of irregular shaped particles are given in table 4.3.

4.2 Procedure of Experimental Work

In order to get accurate results, great attention must be paid to each of the followings:

1. Firstly, all the used particles were washed in water and dried in oven, in order to avoid the error reading from dirty particles.

2. The temperature of the fluid was recorded of each run by a thermometer. The temperature remained at 27-28°C; therefore the fluid properties remained constant throughout the experiment.

3. The pipe was set exactly vertical by using a balance with a bubble, when the bubble in the center of the balance, that means, the pipe is in a vertical position.

4. After the test fluid prepared and the pipe was filled with a test fluid, a single particle was introduced into the top of the pipe. The particle should place in the center of the pipe just below the surface of the test fluid and leave it to settle freely.

5. The first inlet section L1 was neglected in order to ensure that the acceleration of particle is ended. When the particle crossed the test sections of L2, L3 the variation in signal will produce in each photo-sensor net as explained previously and the number of counts will appear in 7-segments displays in the board for each net, then the number of counts changed to time by multiplying with counters' factor, so the time required for falling particle in each sections L2, L3 will be known.

6. All particles dropped in same way and number of counts recorded. The falling times for each particle in test section (L2 and L3) were measured.

7. The terminal settling velocity of the particle is the measure of the total times along L2 and L3 that the particle required to settle through a known distance of 50 cm, which represented the total test section.

$$V_s = 50 / t$$

8. The time of falling of small spherical particles (0.2, 0.3) cm. was recorded manually by digital stop watch with accuracy of 0.01 sec. along test section of 50 cm.

9. The orientation of each falling particles were observed, to show the difference between the falling of spherical particles and irregular shaped particles.

10. Then the test fluid was drained by the valve in iron base and particles were released by the second valve at the end of cone.

11. To minimize the error, each experiment repeated 3-4 times. An average time was used, thus average settling velocity was taken.

12. The effect of pipe wall on settling velocity was avoided by taking the ratio of particle diameter to pipe diameter less than or equals to 0.25. If the particle was attached the wall of pipe the settling velocity was corrected according to the particle diameter by using equation 3.42, since it is more general and applicable in many literatures.

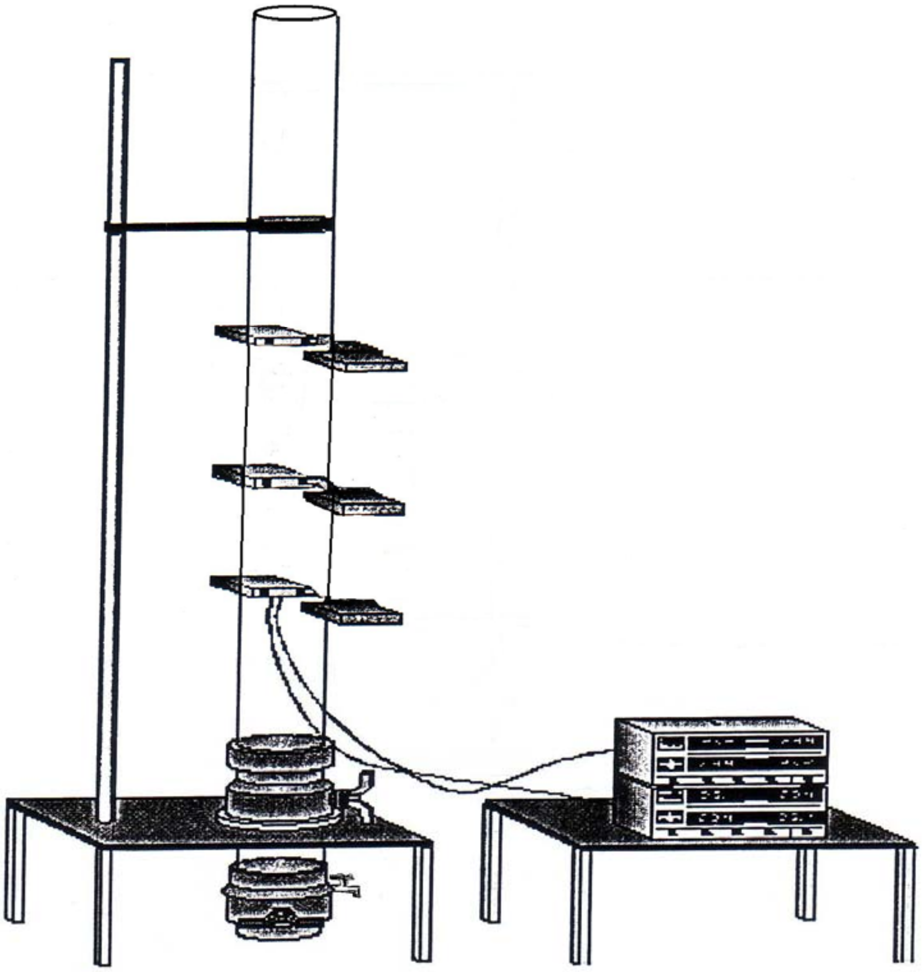

Figure 4-1 Schematic diagram for settling velocity apparatus.

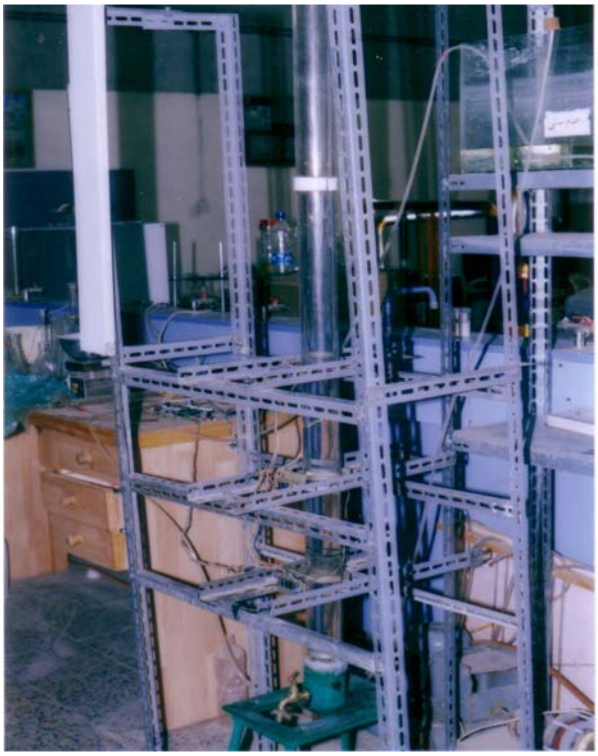

Figure 4-2a Shows the photograph of experimental work.

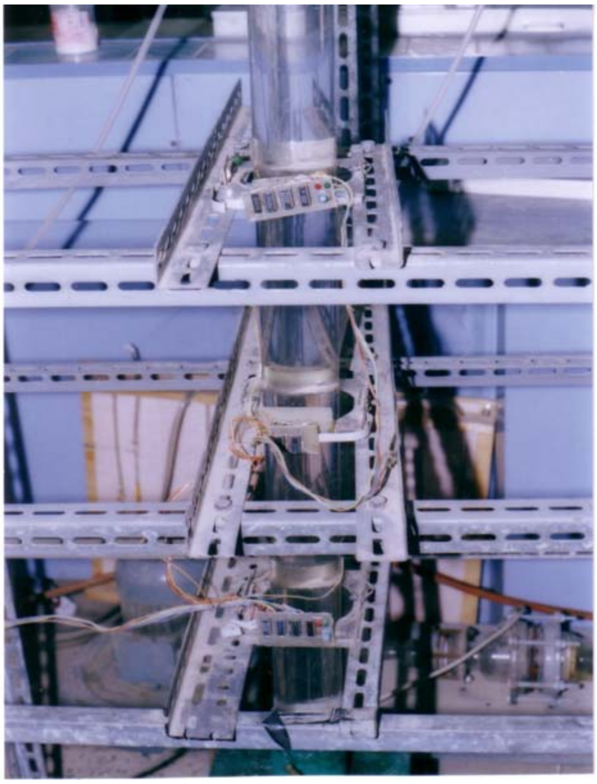

Figure 4-2b Shows the three nets on the pipe's test sections.

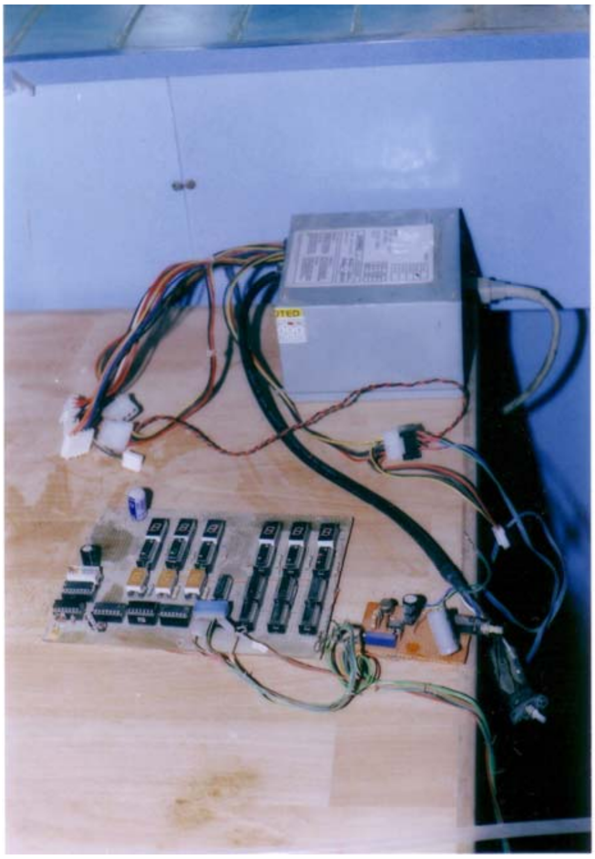

Figure 4-2c Shows the digital board.

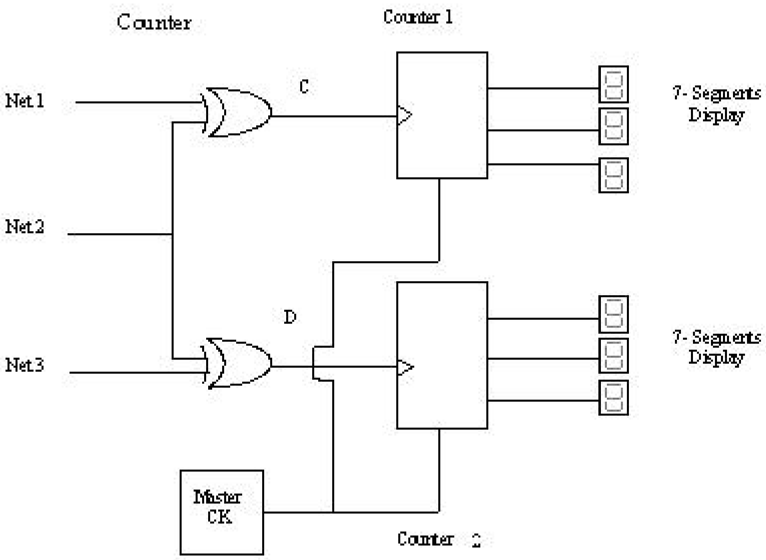

Figure 4-3a The design of counter's circuit.

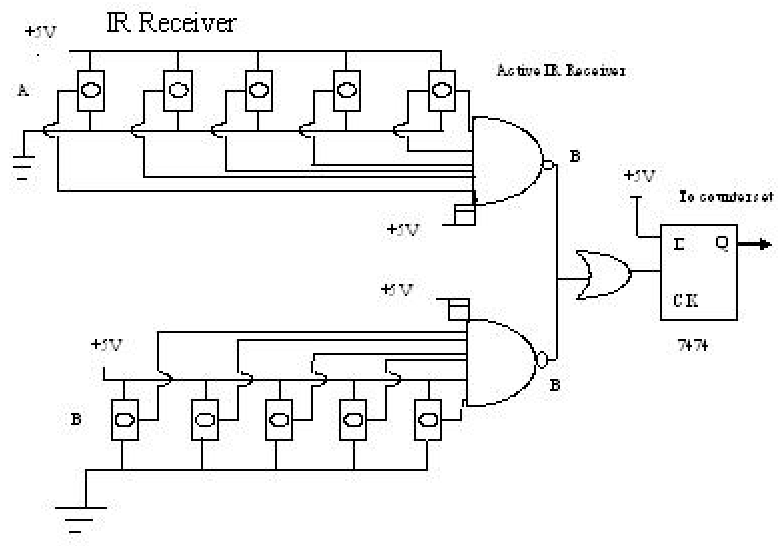

Figure 4-3b The design of the receivers.

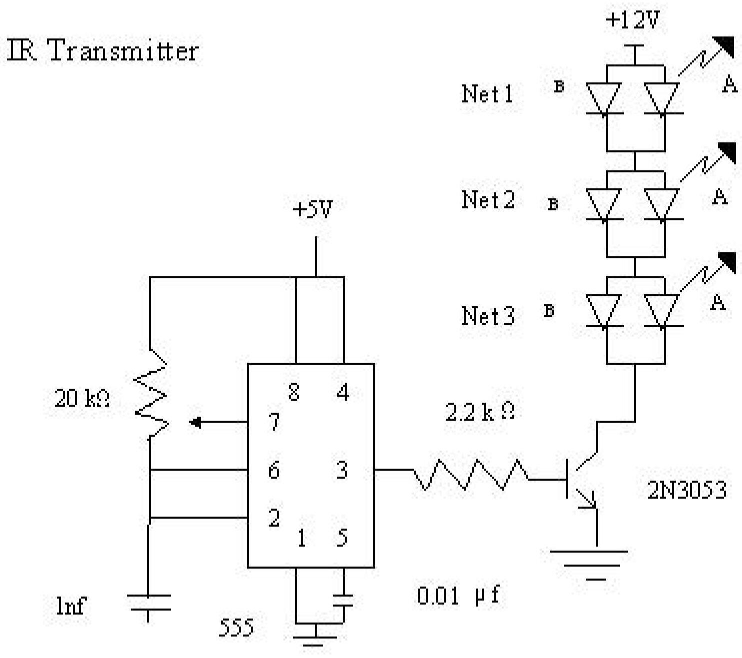

Figure 4-3c The design of the transmitter.

Table 4.1 Concentrations of polymers and Power-Law constants

N0.	Polymer	Concentration, g./l	Power-Law constants
1	CMC	3.71	n=0.73,k=0.015
2	CMC	5	n=0.71,k=0.091
3	CMC	15	n=0.63,k=0.287
4	CMC	17.5	n=0.61,k=0.566
5	Polyacr.	2	n=0.58,k=1.016
6	Polyacr.	4	n=0.51,k=1.135
7	Polyacr.	6	n=0.39,k=3.320

Table 4.2 Physical characteristics of spherical particles

D_s,cm.	Mass, g.	V_p, cm^3	ρ_P, g./cm^3	A_p, cm^2
0.22	0.014	0.0055	2.545	0.038
0.3	0.034	0.0141	2.411	0.071
0.4	0.082	0.033	2.484	0.126
0.6	0.299	0.113	2.646	0.283
0.8	0.675	0.268	2.518	0.503
1	1.338	0.524	2.553	0.785
1.43	3.825	1.531	2.498	1.606
2	10.841	4.189	2.588	3.141

Table 4.3 Physical characteristics of irregular shaped particles

D_s ,cm.	Mass, g.	V_p, cm^3	ρ_P, gr./cm^3	A_p, cm^2
0.984	0.970	0.5	1.940	0.762
1.102	1.554	0.7	2.220	0.954
1.152	1.862	0.8	2.327	1.042
1.198	1.936	0.9	2.151	1.127
1.241	2.735	1	2.735	1.209
1.388	3.042	1.4	2.173	1.513
1.420	2.719	1.5	1.813	1.584
1.563	4.791	2	2.395	1.919
1.789	8.391	3	2.797	2.514
1.823	7.104	3.2	2.220	2.610
1.847	8.358	3.3	2.533	2.679
2.121	10.640	5	2.128	3.536

CHAPTER FIVE
RESULTS AND DISCUSSION

5.1 Introduction

In chapter four, the details are given for measuring the settling velocities of each particle (8 spherical and 12 irregular shaped particles), and the drag coefficient for each of them is calculated in Newtonian (water) and non- Newtonian fluids (CMC and polyacralamide polymers) with different concentrations and flow indices (n) which represented by Power-Law fluid and the results are listed in appendix-A.

This chapter will explain and discuss those results, so new graphs were plotted to show the factors that affect settling velocity and will clearly affect drag coefficient, also this chapter will study the C_d-Re_p Relationship in each fluids for spherical and irregular shaped particles and the effects of rheological properties on this relationship.

5.2 C_d - Re_p Relationships

It is clear from figures 5-1 to 5-8 that the values of drag coefficient are high at low values of Reynolds' number, and as Reynolds' number increased the drag coefficient will decrease, due to fact that the viscous forces are dominated in laminar-slip regime. When this region is ended the transition-slip regime is started, the effect of Reynolds' number on drag coefficient is decreased, until the turbulent-slip regime is started and the drag coefficient will be constant value due to the fact that the inertial forces are dominate in this region and viscous forces will have a small effect. For this reason, the increase in Reynolds' number will not decrease the drag coefficient.

It can be clearly shown from figures 5-1 to 5-8 that the effect of rheological properties on C_d-Re_P Relationship. It is obvious from these figures that as flow behavior index (n) decreased from unity the drag coefficient will increase for the same particle Reynolds' number Re_P, because the particle will settle at lower velocity; and this effect is greatly realized at low values of Reynolds' number especially at Re_P below 10, because at this value the viscous forces is dominated so the flow behavior index (n) have a great influence.

At Re_P above 1000 where the turbulent-slip regime started the influence of (n) is negligible or very little because at this regime the inertial forces dominated which is obvious in figures 5-2 to 5-4.

It is clear from figures 5-5 to 5-7 at particle Reynolds' number $10 < Re_P < 1000$, where the transition slip-regime is presented and the viscous forces will begin to decrease and the inertial forces will started to dominate, the flow behavior index (n) has a little influence on C_d-Re_P relationship than that in laminar-slip regime, also in these figures in addition to figure 5-8 laminar region is started to appear which is at Re_P below 10, the viscous forces will start to dominate and inertial forces will be negligible .

Figure 5-1 shows the C_d-Re_P relationship for Newtonian fluid (water).

It is clear that the C_d-Re_P relationship of water and non-Newtonian fluids of different rheological properties are the same. This due to the modification done on Reynolds' number, since to calculate Reynolds' number the concept of effective viscosity (μ_e) has been used. That means the calculation of μ_e will depend on the type of the fluid, or the relationship between the shear stress and shear rate of the fluid.

The irregular shaped particles are used to compare their drag coefficient with that of spherical particles. It is clear from figures 5-1 to 5-8 that the drag coefficient of irregular shaped particles is greater than that of spherical particles due to the fact that settling velocities of these particles are lower than spherical particles because these particles have different paths during settling. The spheres follow a vertical path while irregular shaped particles rotate, vibrate, oscillate and take spiral paths during settling. So, the drag force on irregular shaped particles will be greater than spheres which have smooth surface.

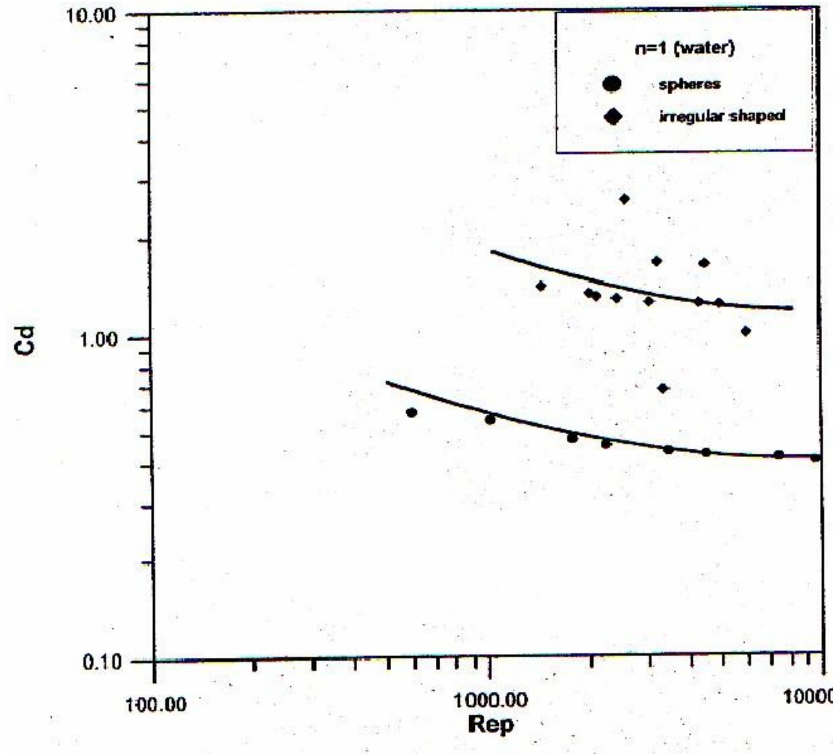

Figure 5-1 C $_d$ -Re $_P$ relationship for n=1

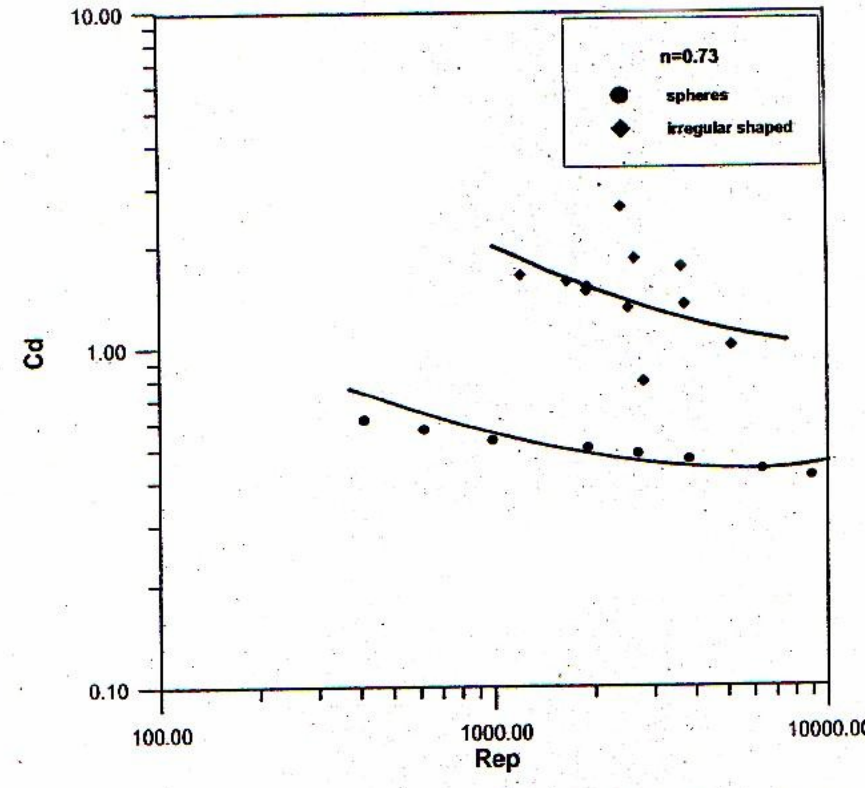

Figure 5-2 C $_d$ -Re $_P$ relationship for n=0.73

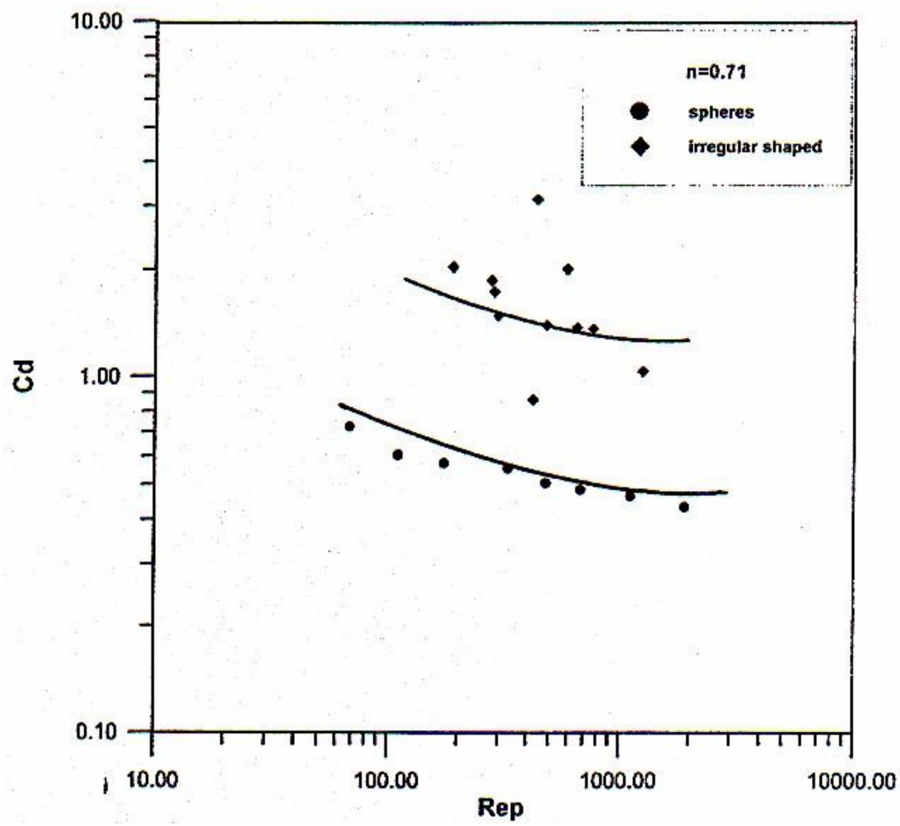

Figure 5-3 C_d -Re_P relationship for n=0.71

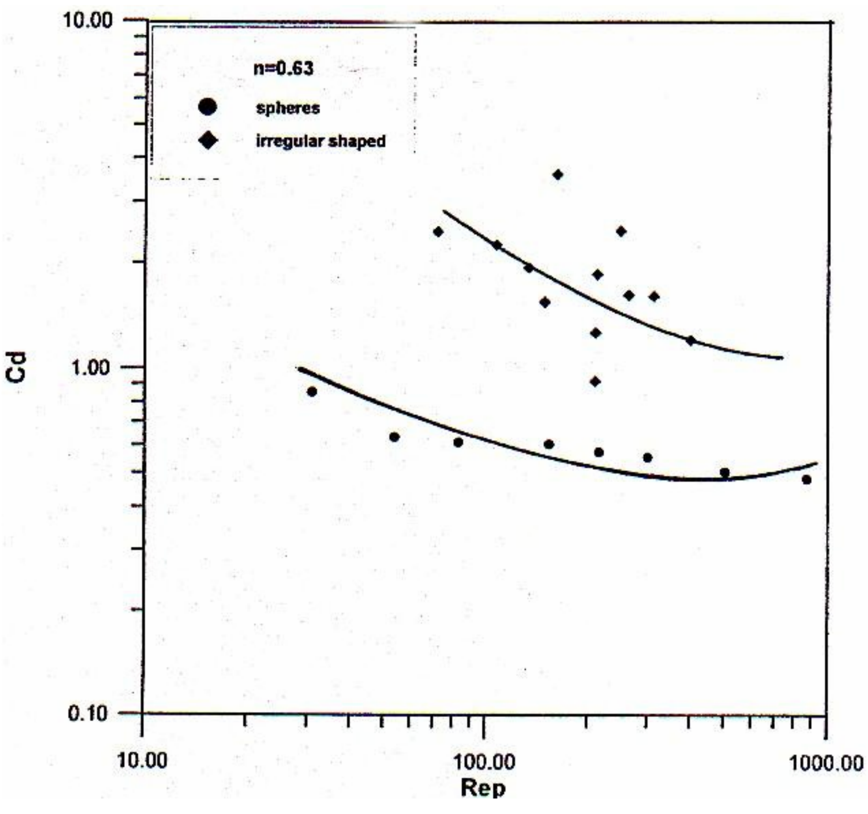

Figure 5-4 C_d -Re_P relationship for n=0.63

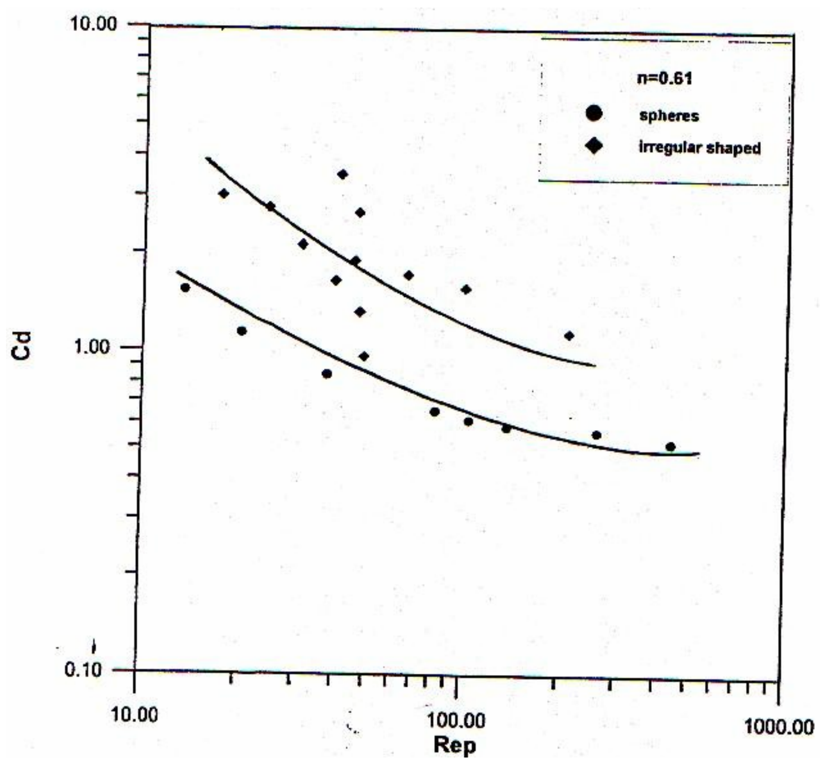

Figure 5-5 C_d -Re_P relationship for n=0.61

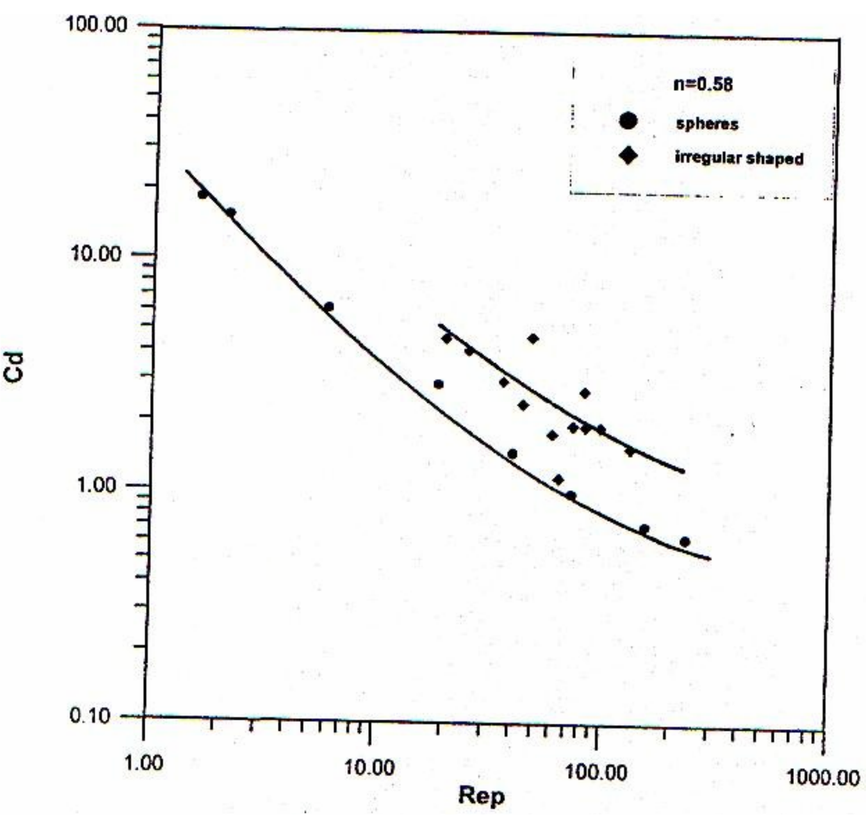

Figure 5-6 C_d -Re_P relationship for n=0.58

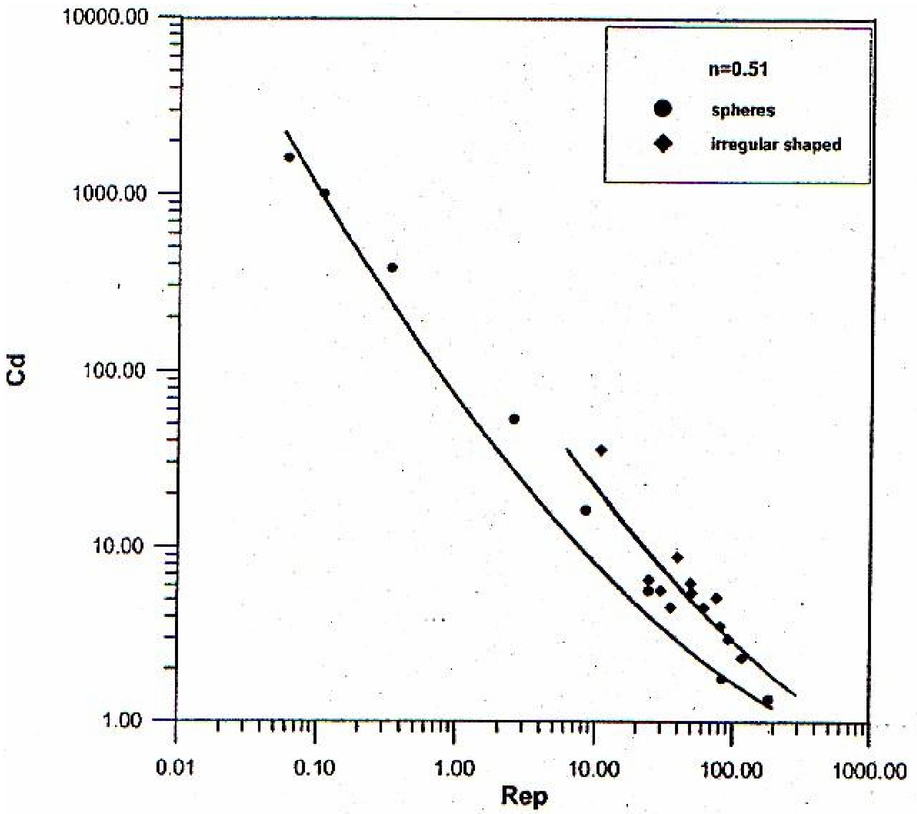

Figure 5-7 C_d-Re_P relationship for n=0.51

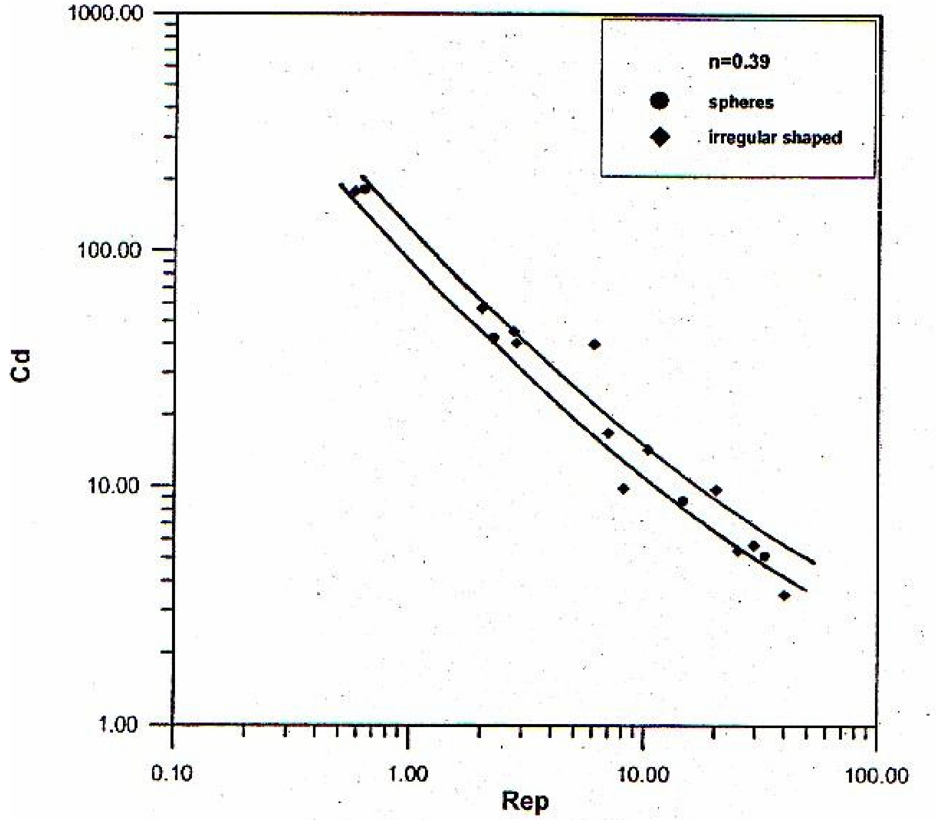

Figure 5-8 C_d-Re_P relationship for n=0.39

5.3 Factors Affect Drag Coefficient

5.3.1 Settling Velocity

The figures 5-9 to 5-15 show the effect of settling velocity of spherical and irregular shaped particles on drag coefficient using fluids with different rheological properties. These plots represent that as the settling velocity of the particles increased the drag coefficient will decrease, because as the velocity increased the drag force exerted by fluid on the particle will be decreased so the drag coefficient will decrease.

A comparison between the drag coefficient of spherical and irregular shaped particles had been done to show the effects of settling velocity on C_d for both of them. It is clear that drag coefficient of irregular shaped is larger than spherical particles, since the settling velocities of these particles are lower than spherical particle due to the fact that they have different orientations during settling as mentioned previously.

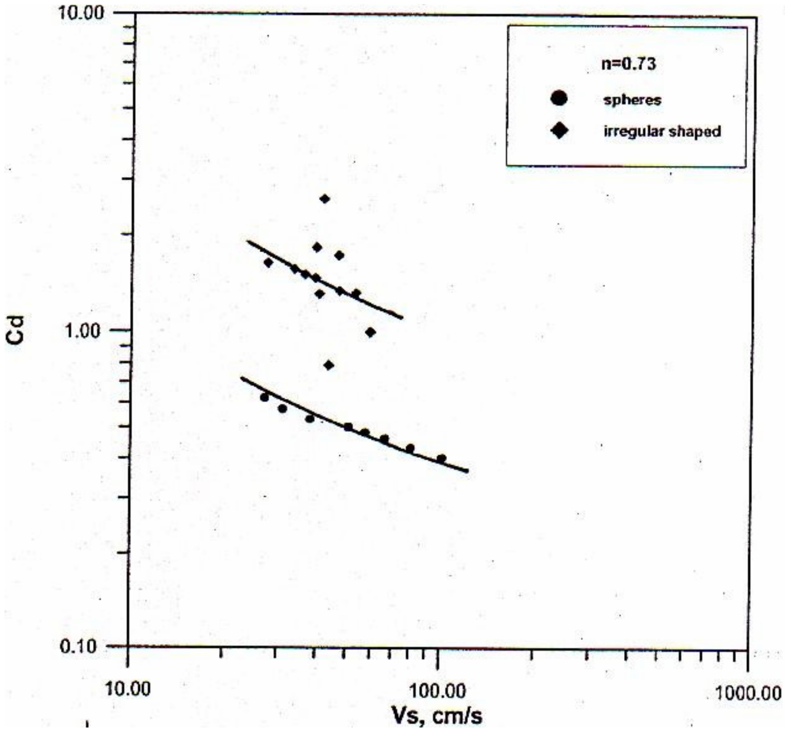

Figure 5-9 The effect of terminal settling velocity on drag coefficient at n=0.73

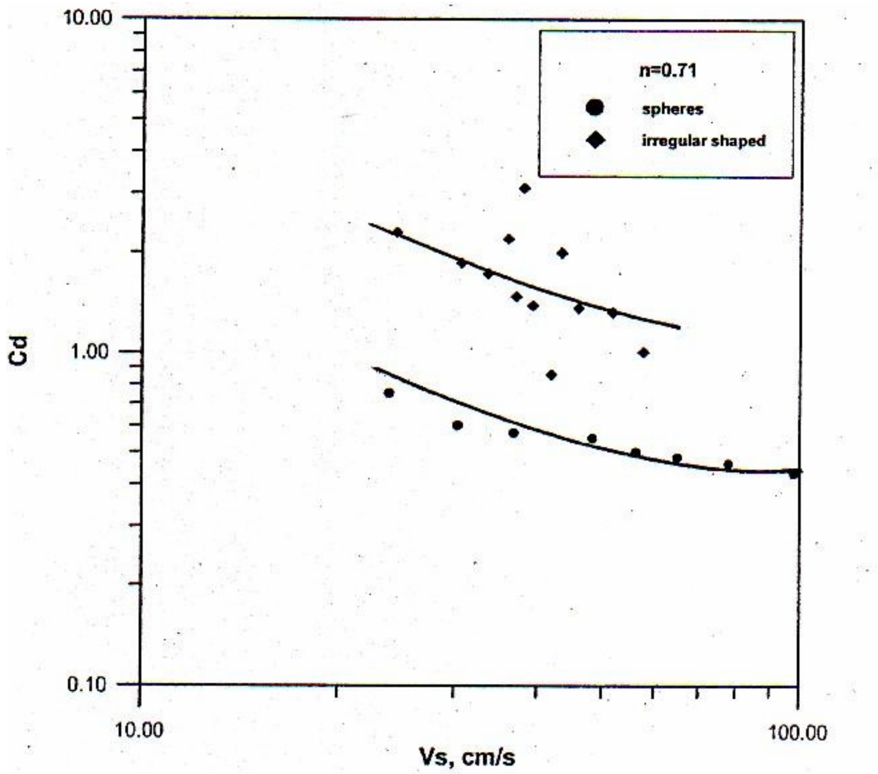

Figure 5-10 The effect of terminal settling velocity on drag coefficient at n=0.71

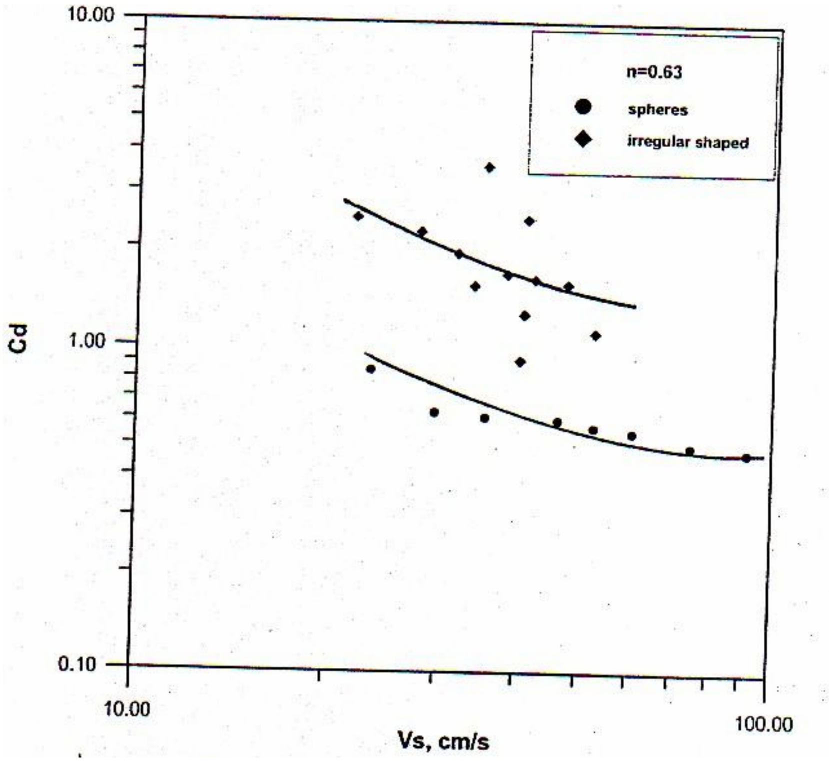

Figure 5-11 The effect of terminal settling velocity on drag coefficient at n=0.63

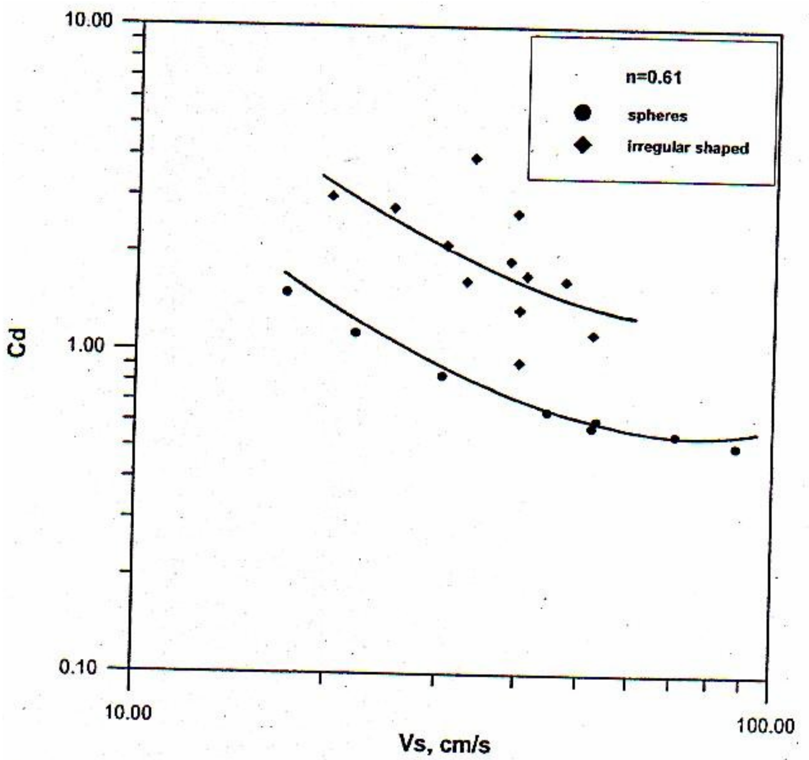

Figure 5-12 The effect of terminal settling velocity on drag coefficient at n=0.61

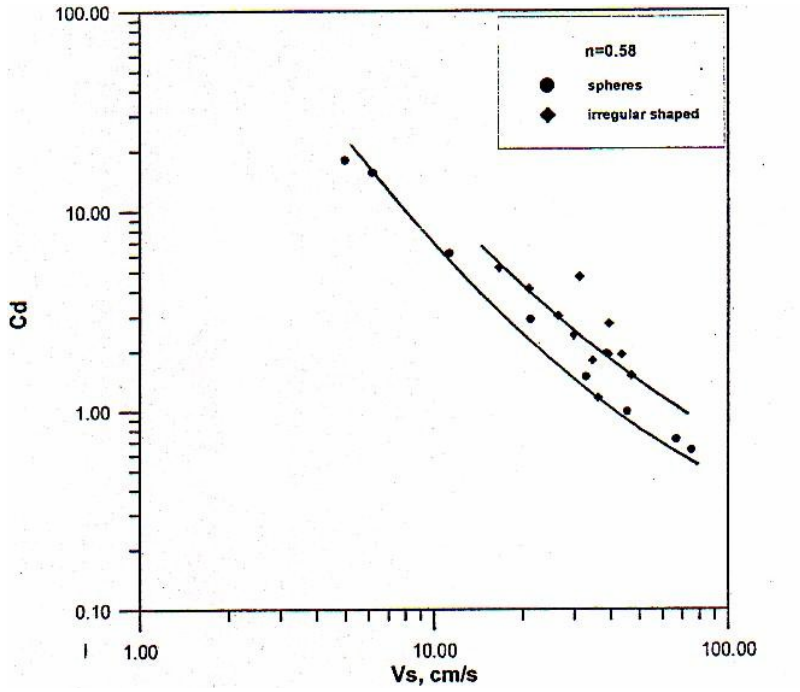

Figure 5-13 The effect of terminal settling velocity on drag coefficient at n=0.58

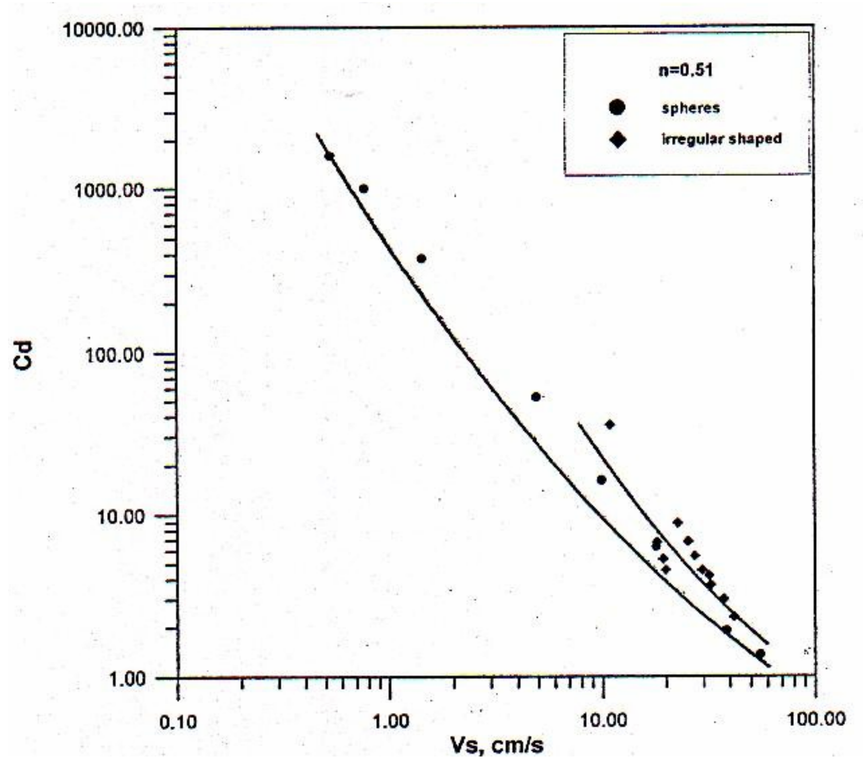

Figure 5-14 The effect of terminal settling velocity on drag coefficient at n=0.51

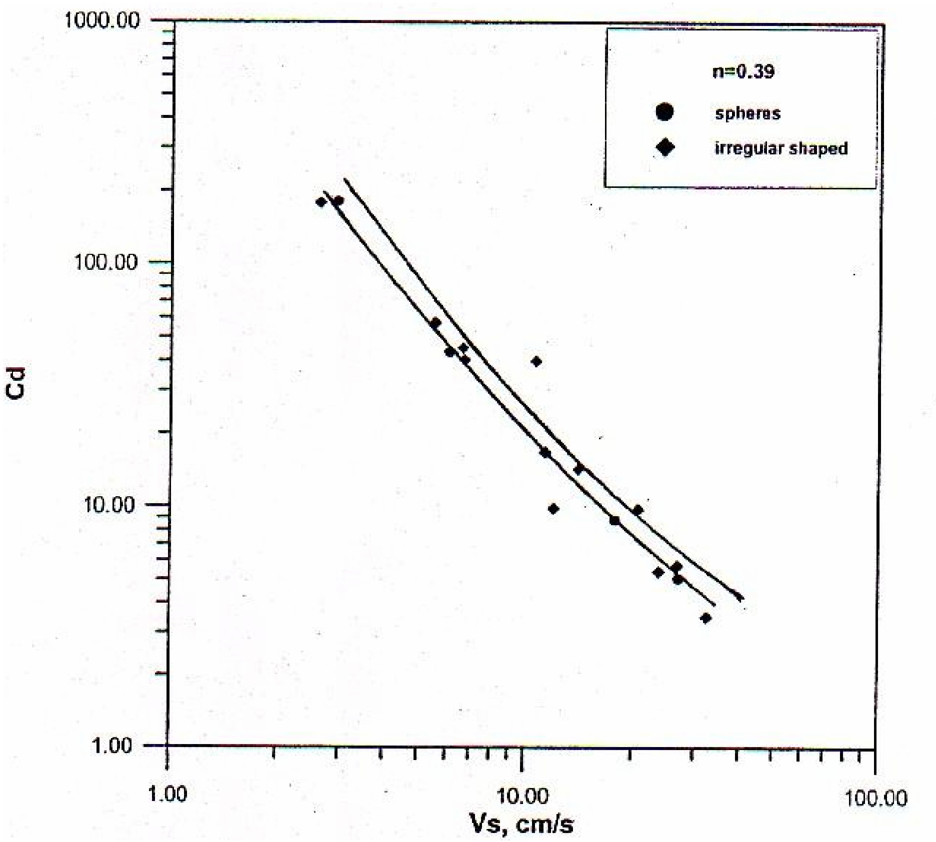

Figure 5-15 The effect of terminal settling velocity on drag coefficient at n=0.39

5.3.2 Particle Diameter

The concept of equivalent sphere diameter has been used to calculate the diameter of irregular shaped particles.

To show the effect of particle diameter on drag coefficient, a plot of particle diameter versus drag coefficient is prepared for each fluid. Figures 5-16 to 5-22 represent that as the particle diameter increased the drag coefficient will be decreased. Due to that as the particle diameter increases the velocity of particle will increase, since the drag force exerted on particle will be decreased, so the drag coefficient decreases.

Also, the comparison between the spheres and irregular shaped particles are done.

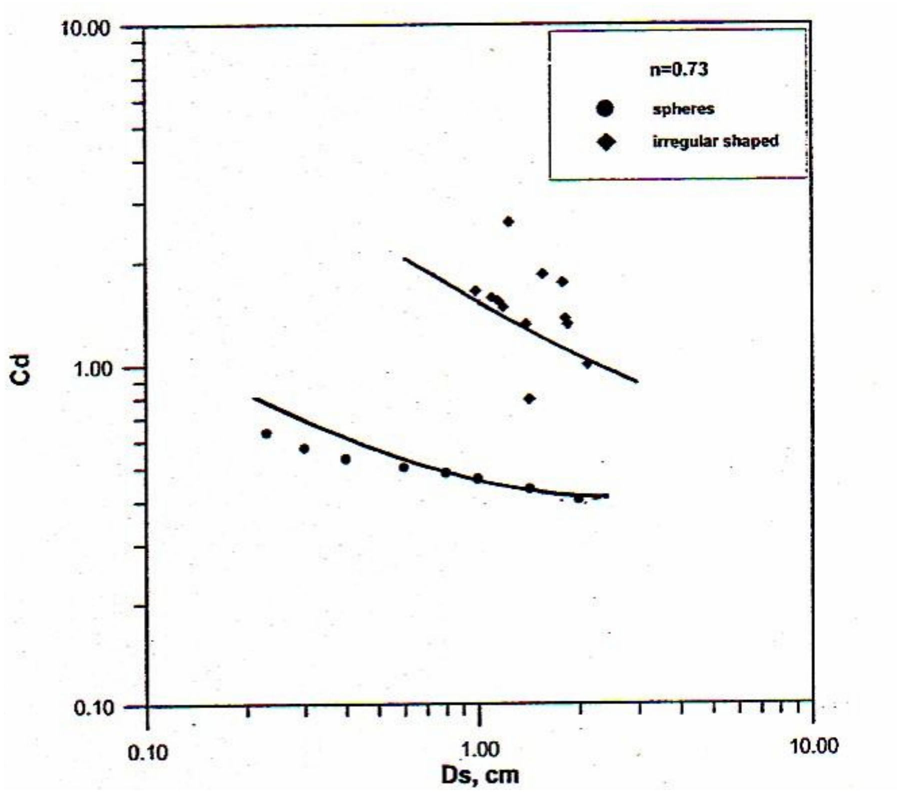

Figure 5-16 The effect of particle diameter on drag coefficient at n=0.73

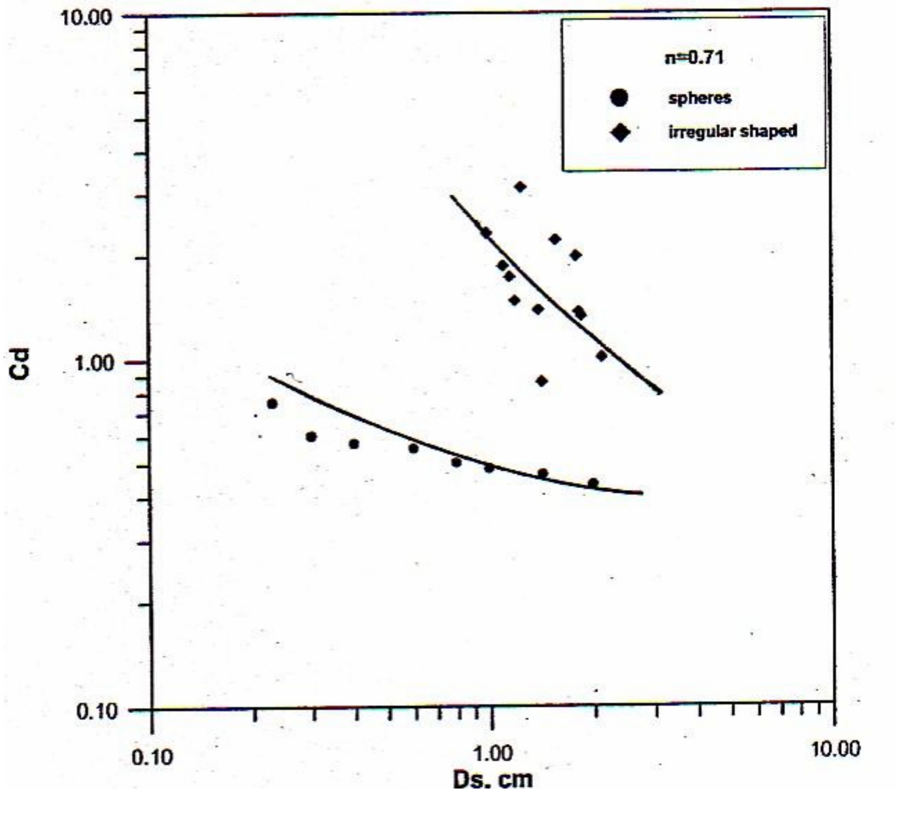

Figure 5-17 The effect of particle diameter on drag coefficiet at n=0.71

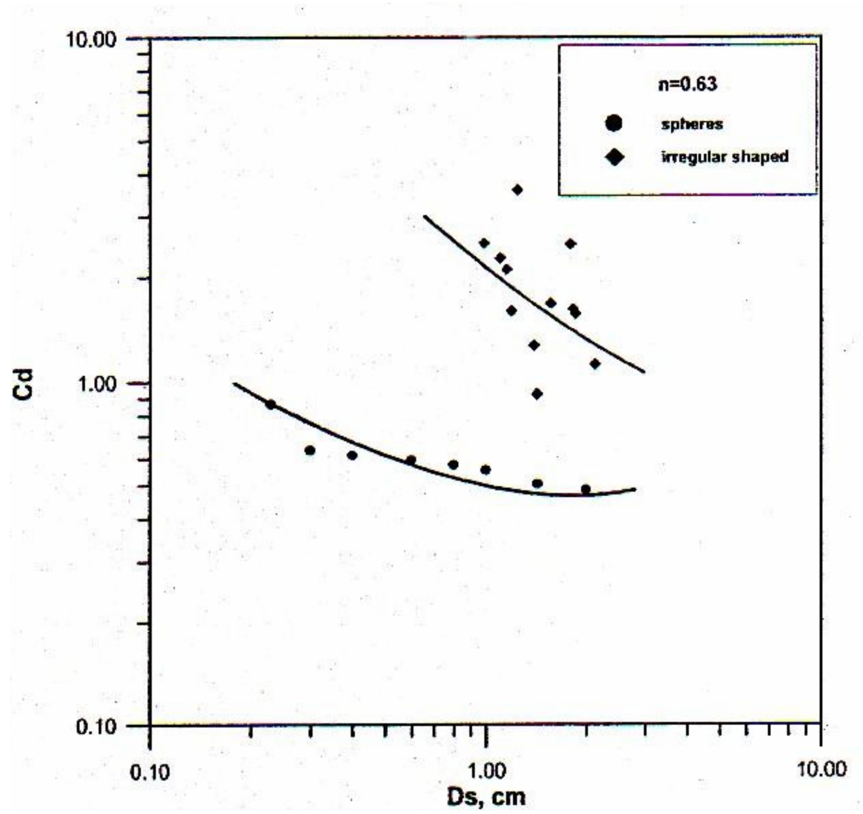

Figure 5-18 The effect of particle diameter on drag coefficient at n=0.63

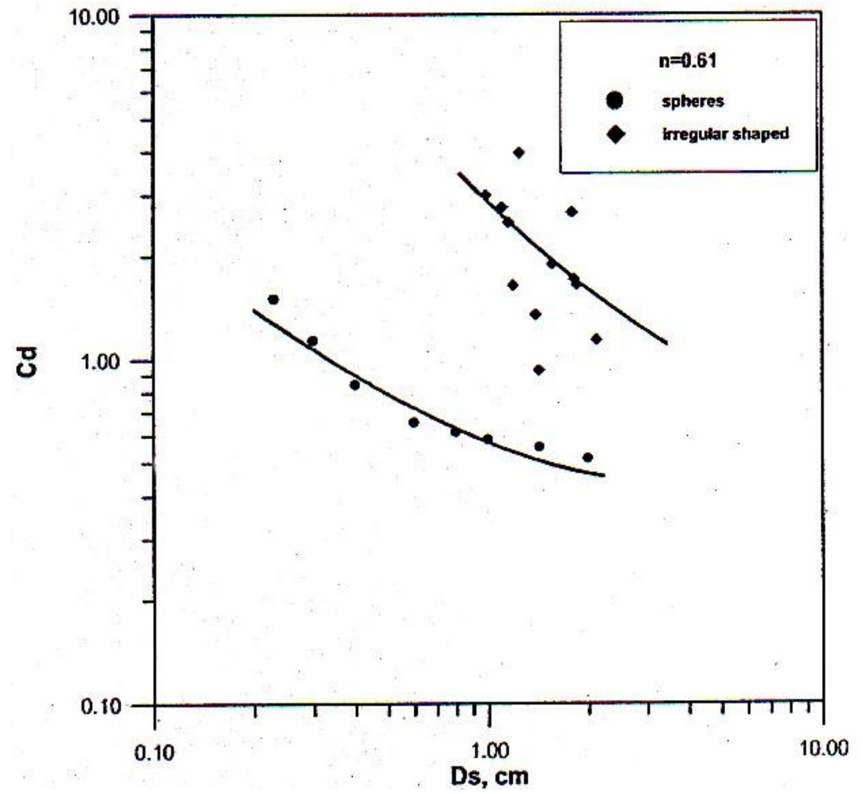

Figure 5-19 The effect of particle diameter on drag coefficient at n=0.61

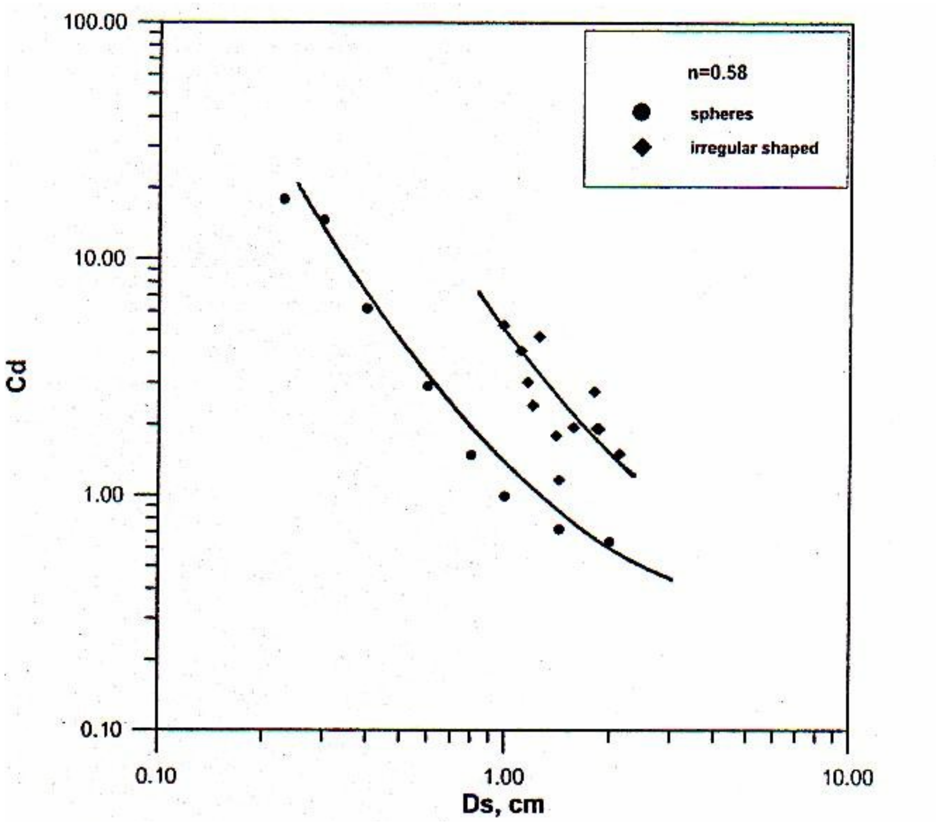

Figure 5-20 The effect of particle diameter on drag coefficient at n=0.58

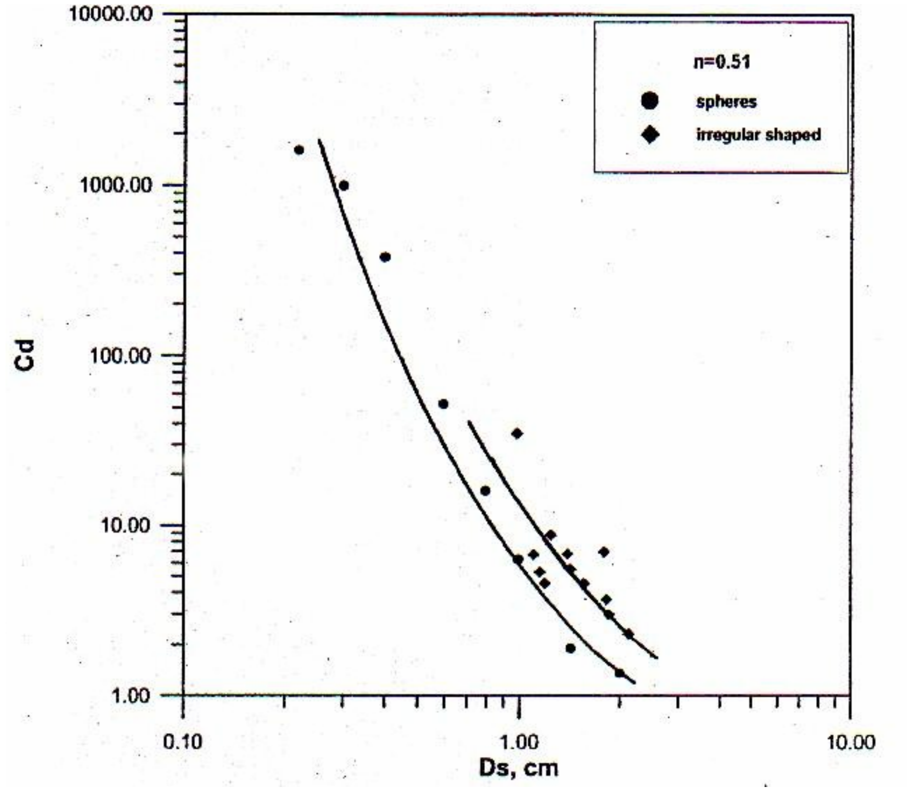

Figure 5-21 The effect of particle diameter on drag coefficient at n=0.51

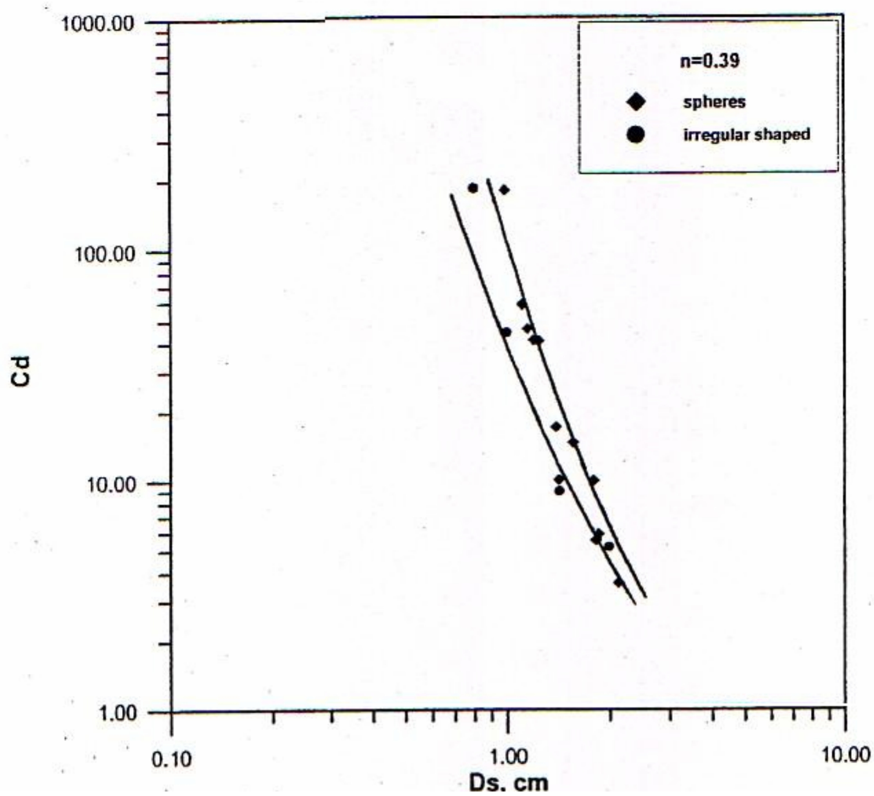

Figure 5-22 The effect of particle diameter on drag coefficient at n=0.39

5.3.3 Difference between Particle and Fluid Densities

Figures from 5-23 to 5-29 for spherical and irregular shaped particles show the effects of the difference between particle and fluid density on C_d, so as the difference between particle and fluid density increased the drag coefficient will increase. The increasing in the fluid density will increase the bouncy force and thus reduces the settling velocity. The fluids which were used in this study had a close densities since they were solutions of polymers, It is obvious from these figures that the spherical particles the difference between particle and fluid density is very close due to that they have close densities so as (n) increased C_d will increased, but for irregular shaped particles this effect is clearly observed. Figures 5-27 to 5-29 C_d of small spherical particles (0.2, 0.3 and 0.4cm) have a very large value than the irregular shaped particles because their settling velocity is very small as shown in appendix A tables A-11, A-13 and A-15, also as the difference between particle and fluid density for irregular shaped particles increase the drag coefficient will increase.

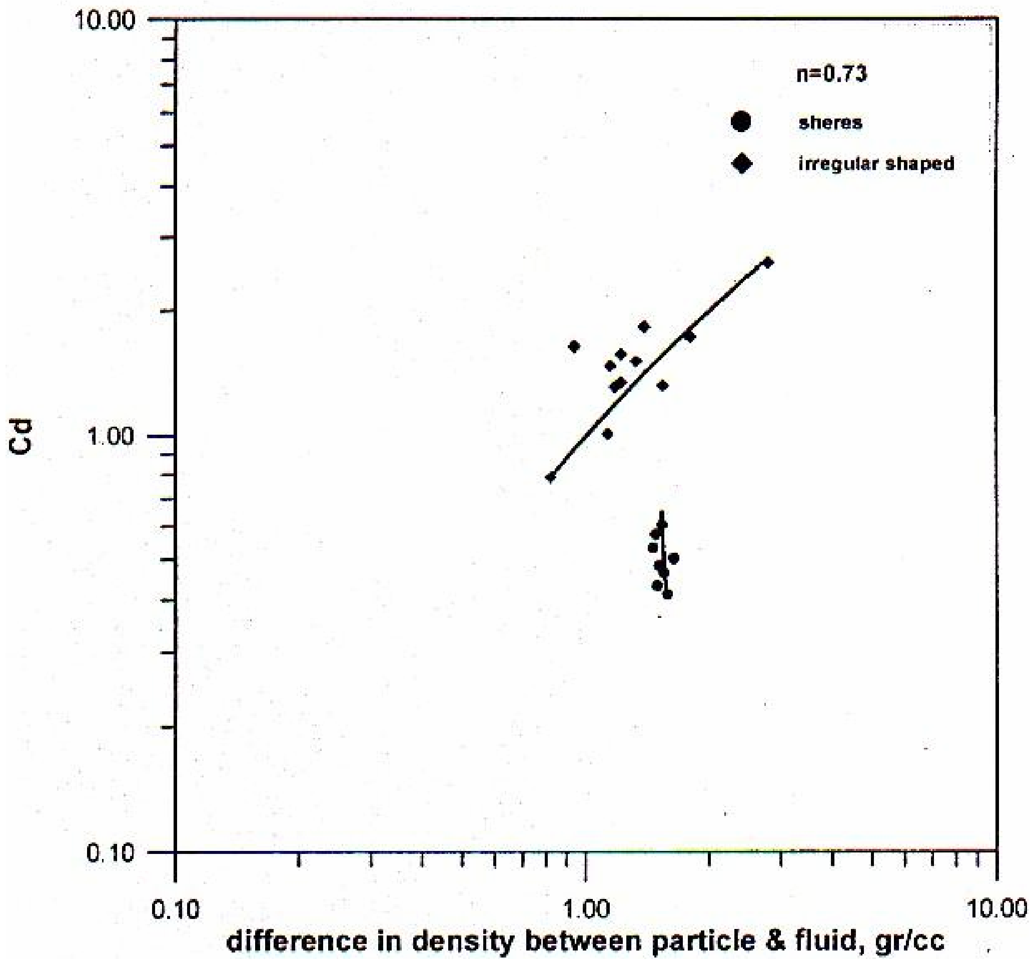

Figure 5-23 The effect of difference in density between the particle and fluid on drag coefficient at n=0.73

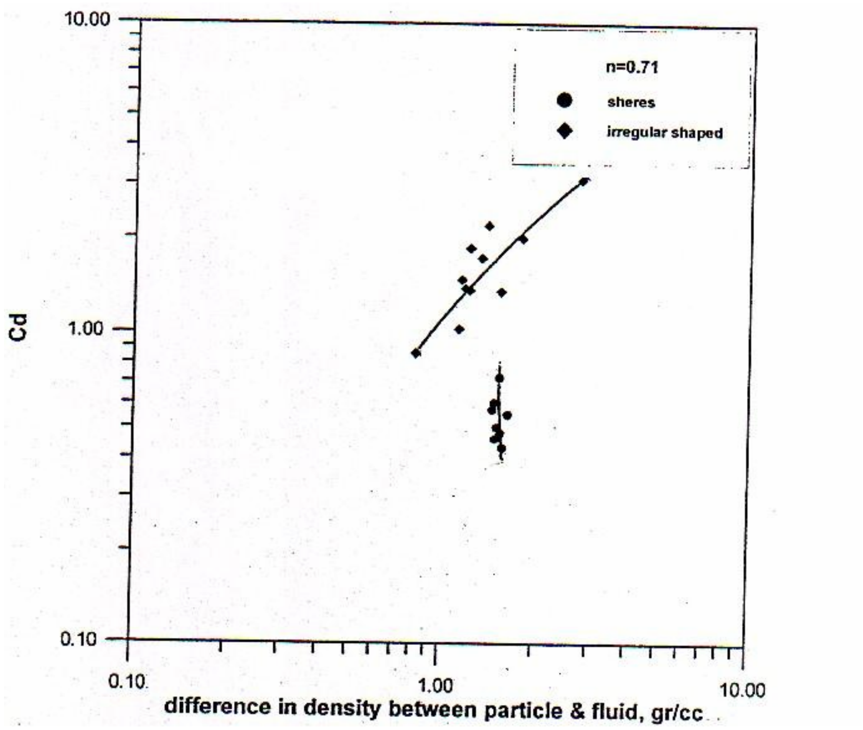

Figure 5-24 The effect of difference in density between the particle and drag coefficient on drag coefficient at n=0.71

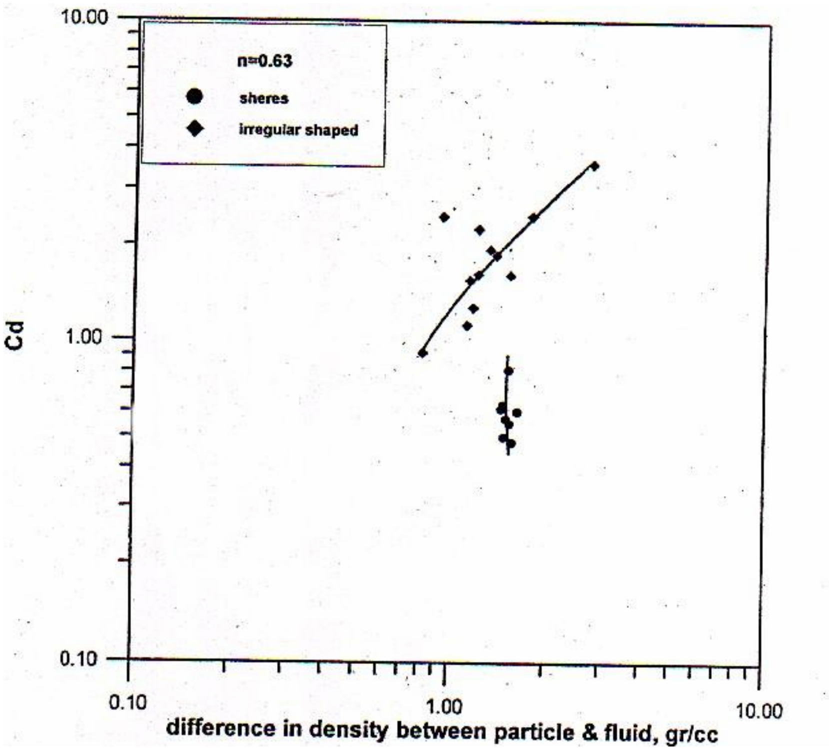

Figure 5-25 The effect of difference in density between the particle and drag coefficient on drag coefficient at n=0.63

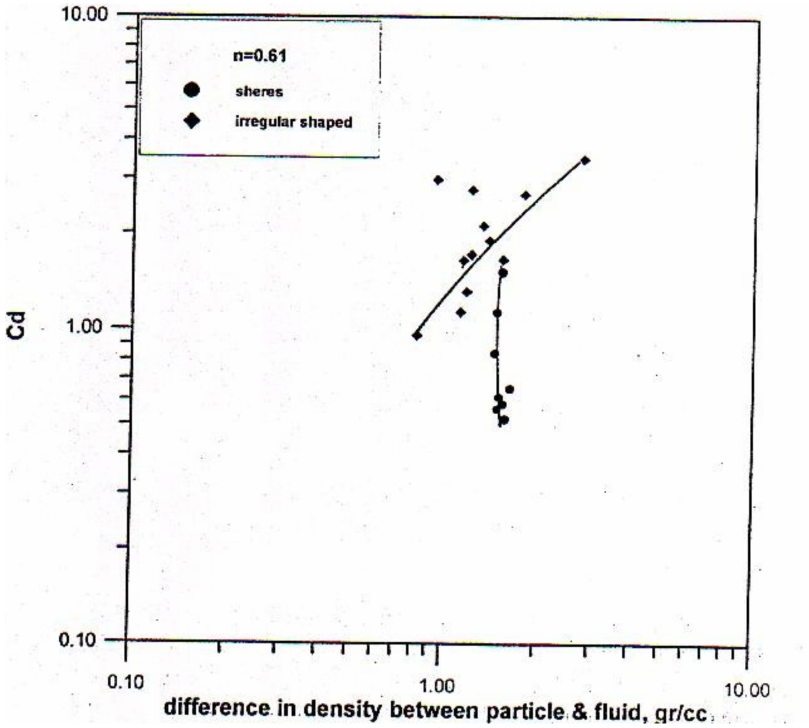

Figure 5-26 The effect of difference in density between the particle and drag coefficient on drag coefficient at n=0.61

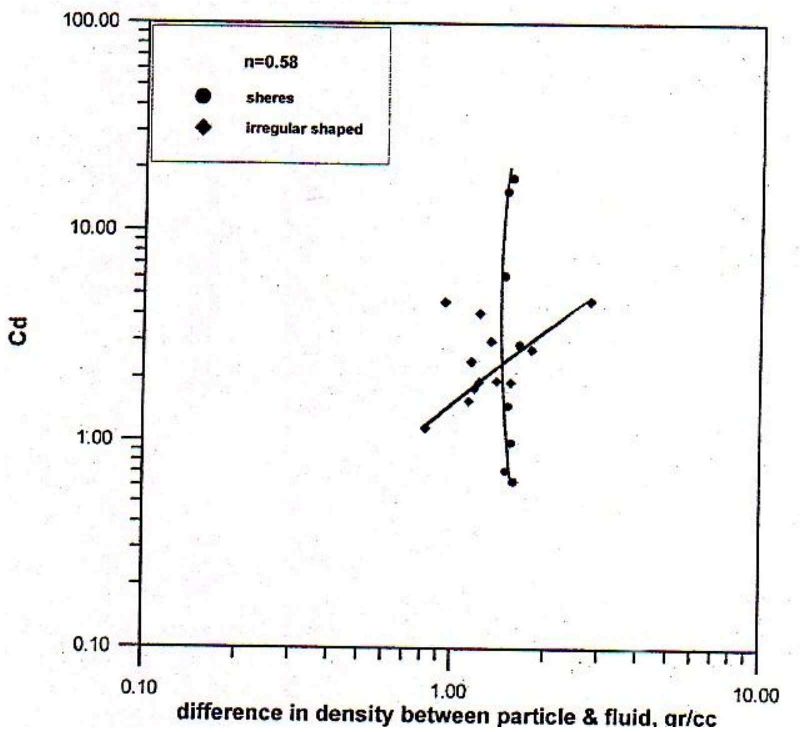

Figure 5-27 The effect of difference in density between the particle and drag coefficient on drag coefficient at n=0.58

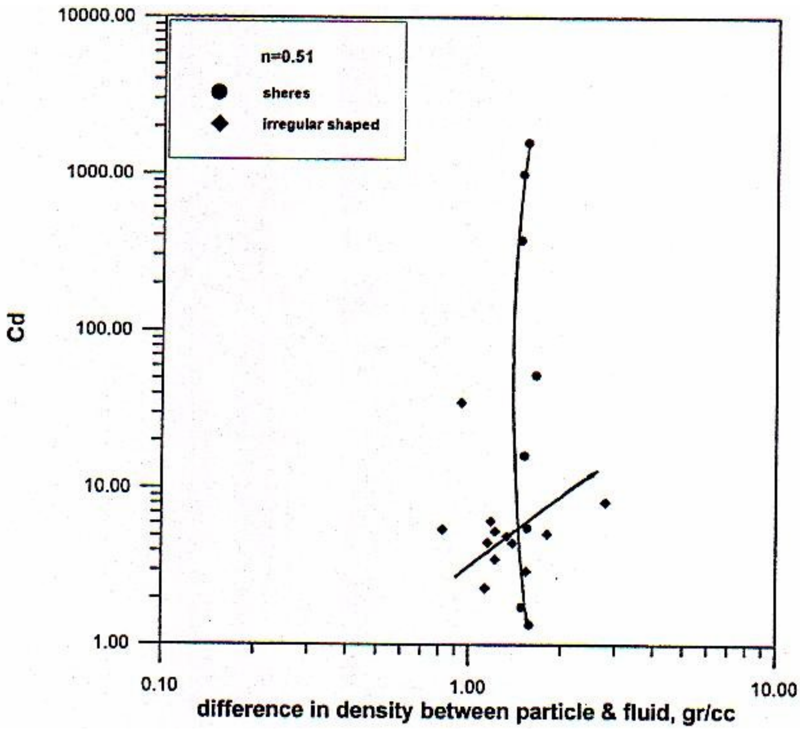

Figure 5-28 The effect of difference in density between the particle and drag coefficient on drag coefficient at n=0.51

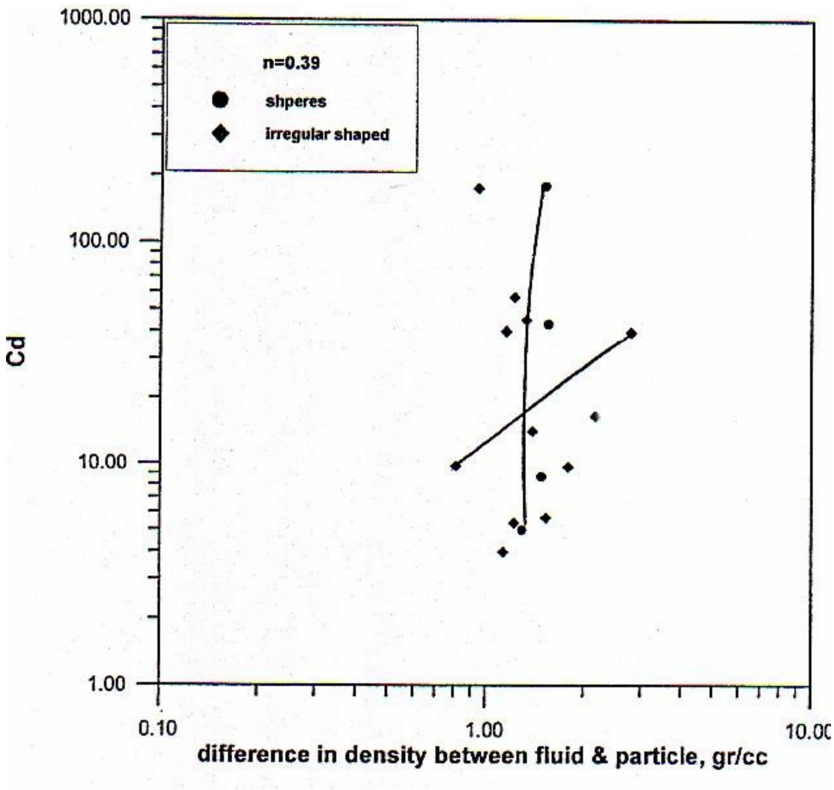

Figure 5-29 The effect of difference in density between the particle and drag coefficient on drag coefficient at n=0.39

5.3.4 Concentration

To show the effect of concentration on drag coefficient, graphs are plotted for particles settling in CMC with concentrations of (3.71, 5, 15, 17.5) g./l and polyacrylamide with concentrations of (2, 4, 6) g./l for spheres and irregular shaped particles to show their behavior in both polymers. It is obvious from the figures 5-30 to 5-37 for spheres in CMC and polyacrylamide that as the concentration increased, the viscosity of fluid will increase and settling velocity will decrease, so the drag coefficient increases with decreasing of the diameter of the particle, that means; the smallest particle diameter i.e. 0.22 cm has the highest C_d, because it has the lowest settling velocity, but the C_d will be increased as the concentration increased. But largest particle diameter i.e. 2 cm has the lowest C_d because it has the highest settling velocity. Similar explanation is applicable for irregular shaped particles as in figures 5-34 to 5-37 in CMC and polyacrylamide. As the concentration increased the C_d increased with decreasing of equivalent diameter. Figure 5-32, have two points only, since the small size spherical particles with diameters of 0.2, 0.3, 0.4, 0.6 cm suspended in concentration with 6g. /l of polyacrylamide because it was so viscous the bouncy force is very large.

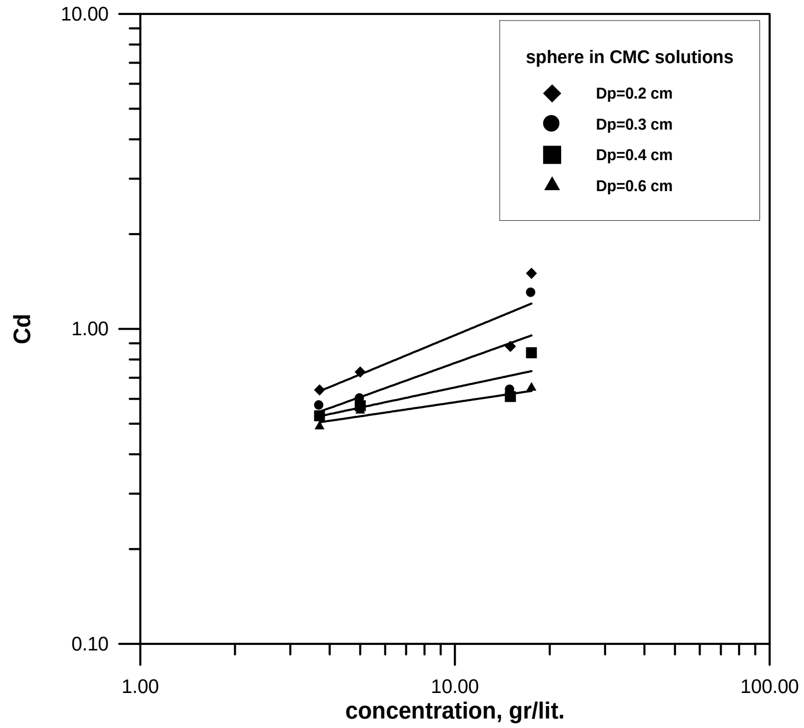

Figure 5-30 The effect of CMCconcentrations on drag coefficient for different diameters of spherical particles

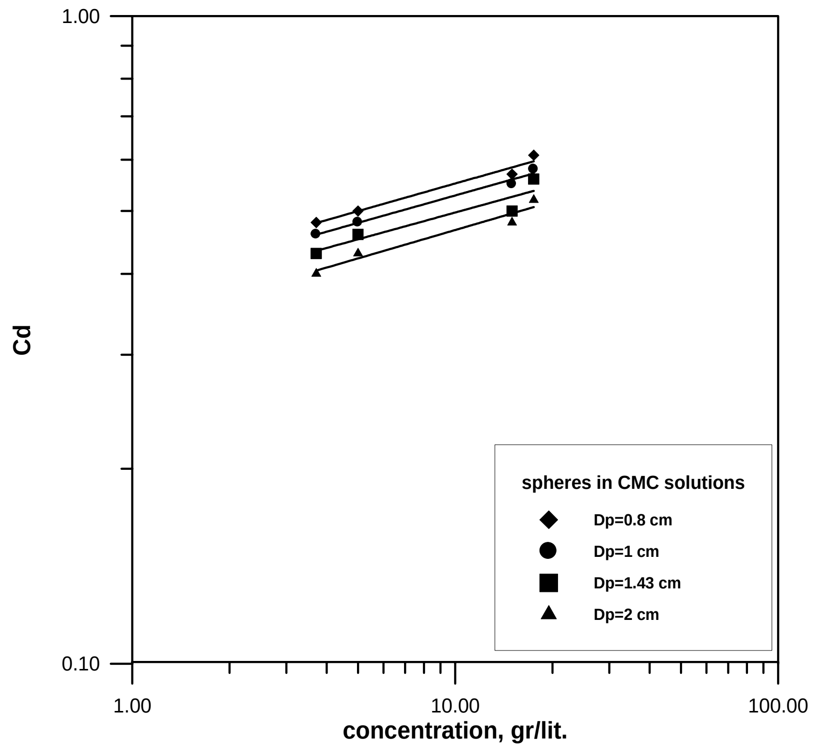

Figure 5-31 The effect of CMC concentrations on drag coefficient for different diameters of spherical particles

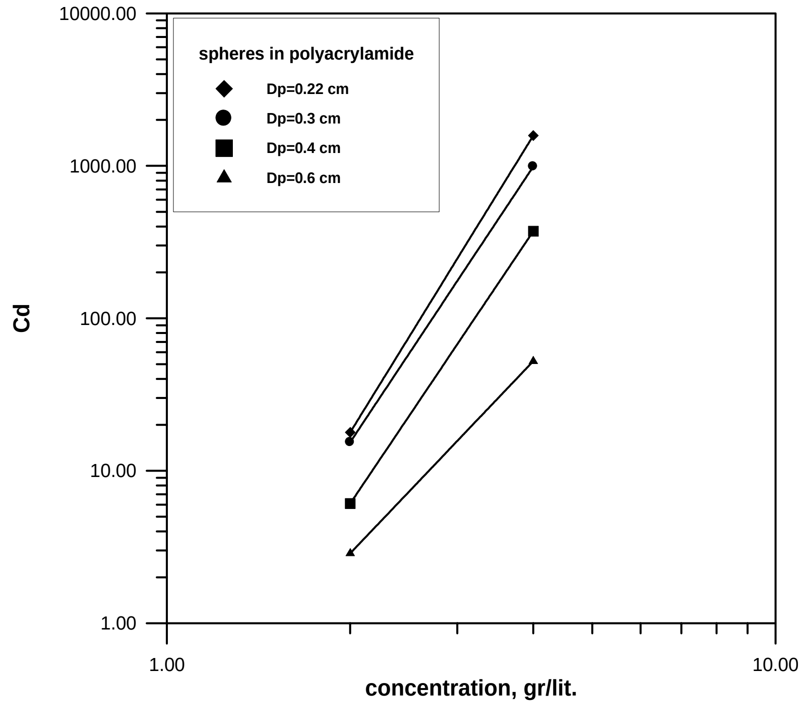

Figure 5-32 The effect of polyacylamide concentrations on drag coefficient for different diameters of spherical particles

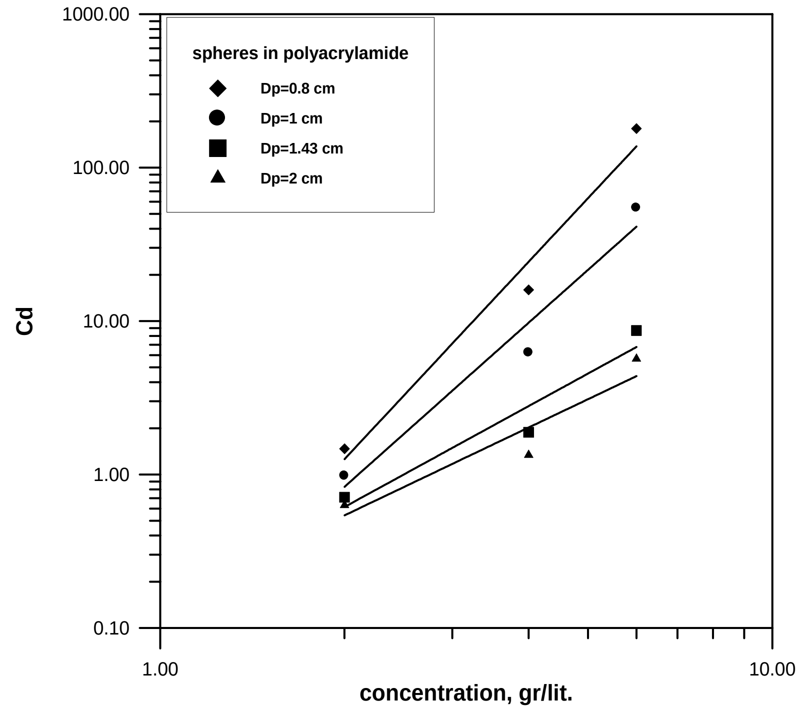

Figure 5-33 The effect of polyacylamide concentrations on drag coefficient for different diameters of spherical particles

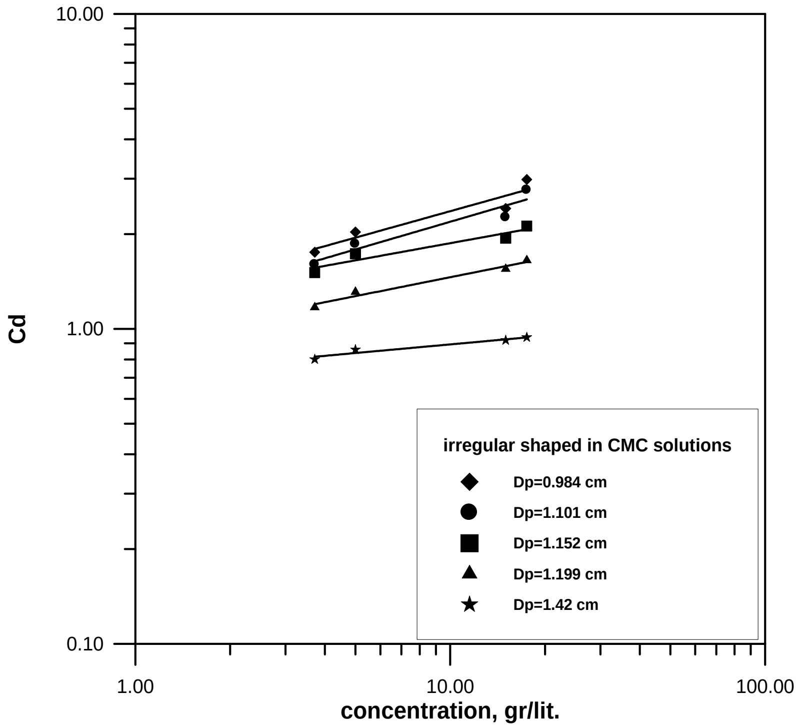

Figure 5-34 The effect of CMC concentrations on drag coefficient for different diameters of irregular shaped particles

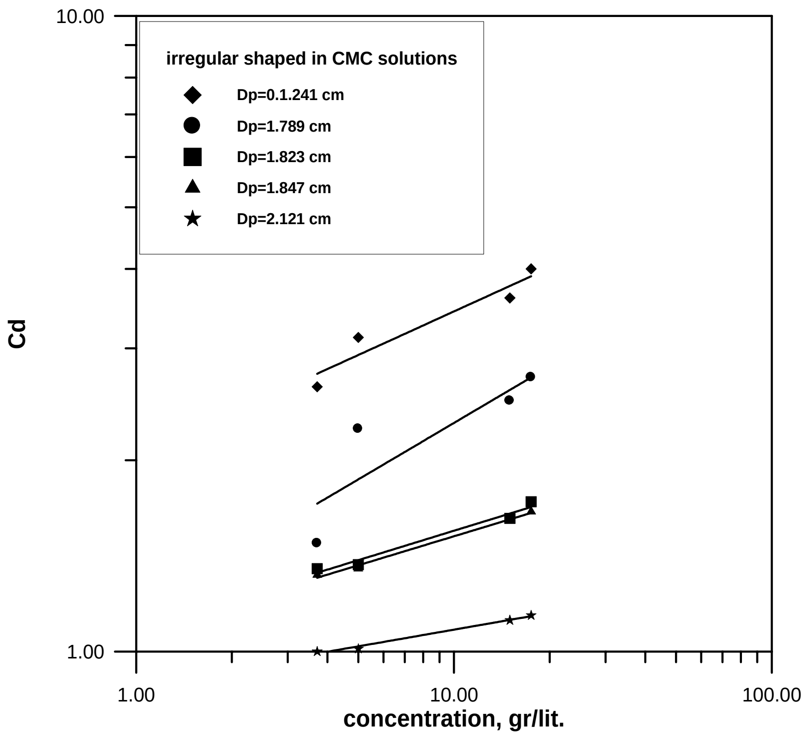

Figure 5-35 The effect of CMC concentrations on drag coefficient for different diameters of irregular shaped particles

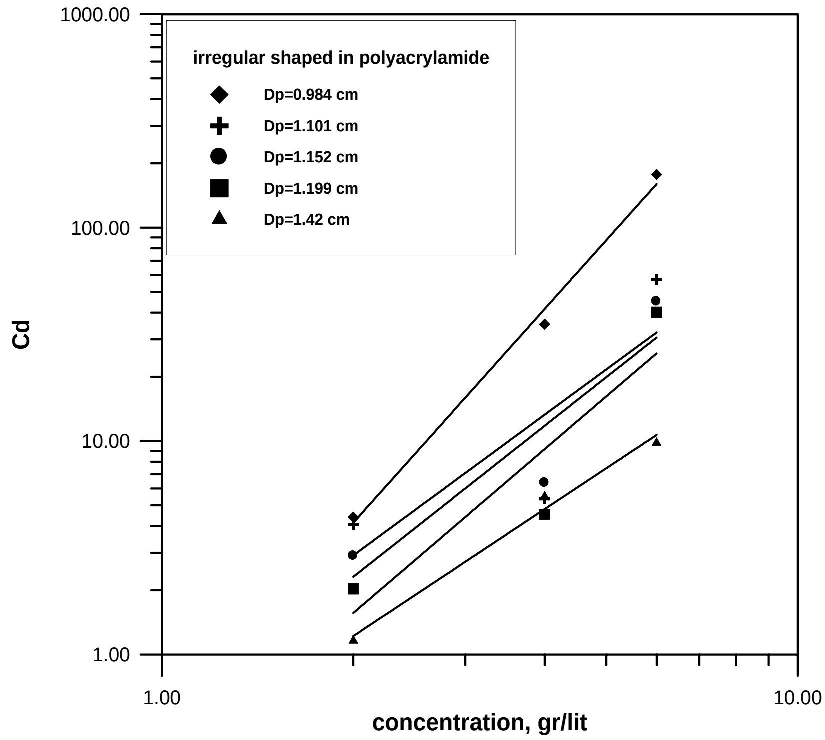

Figure 5-36 The effect of polyacrylamide concentrations on drag coefficient for different diameters of irregular shaped particles

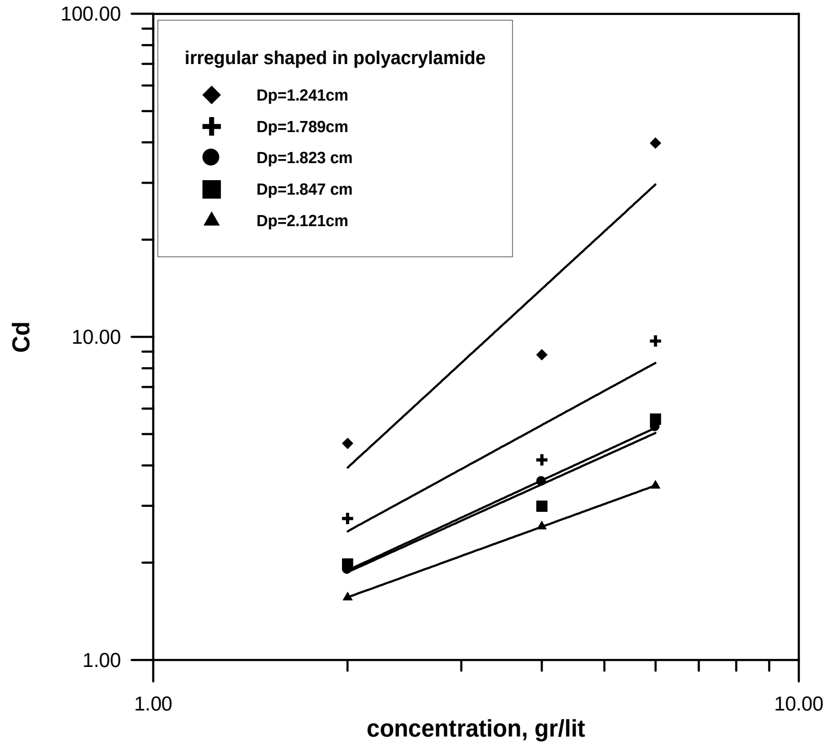

Figure 5-37 The effect of polyacrylamide concentrations on drag coefficient for different diameters of irregular shaped particles

5.3.5 Rheological Properties

To understand the effects of rheological properties, a Power-Law model which depends basically on flow behavior index (n) and consistency index (k) was applied to the non-Newtonian fluids and prepared in this study. Figures 5-38 to 5-41 show the relationships between flow behavior indecies and drag coefficient with particle diameters for both spherical and irregular shaped particles. It is clear that as the flow behavior index increased and approached to unity the drag coefficient decreased with increasing of particle diameters, due to increase the settling velocity with increasing of particle diameters.

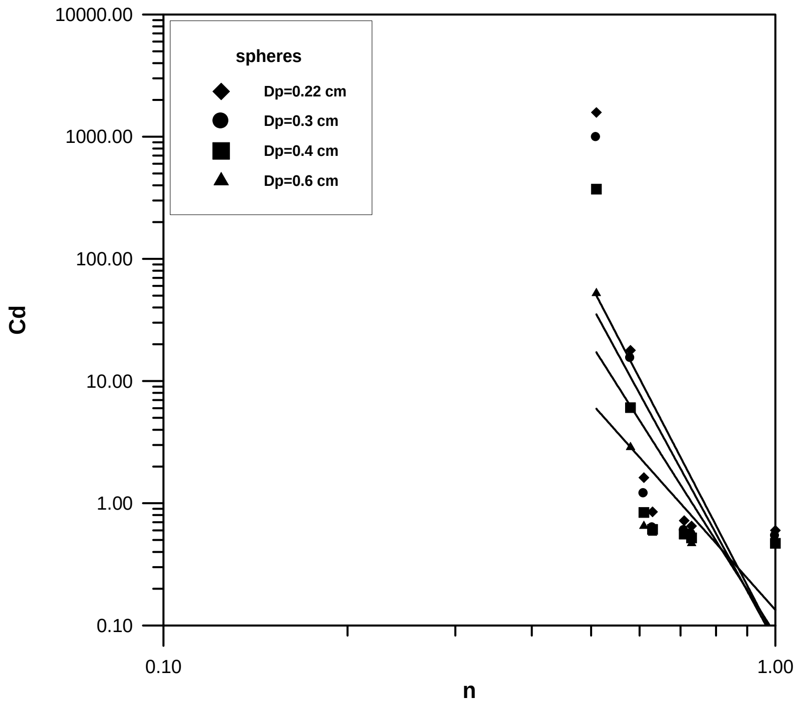

Figure 5-38 The effect of flow index on drag coefficient for different diameters of spherical particles

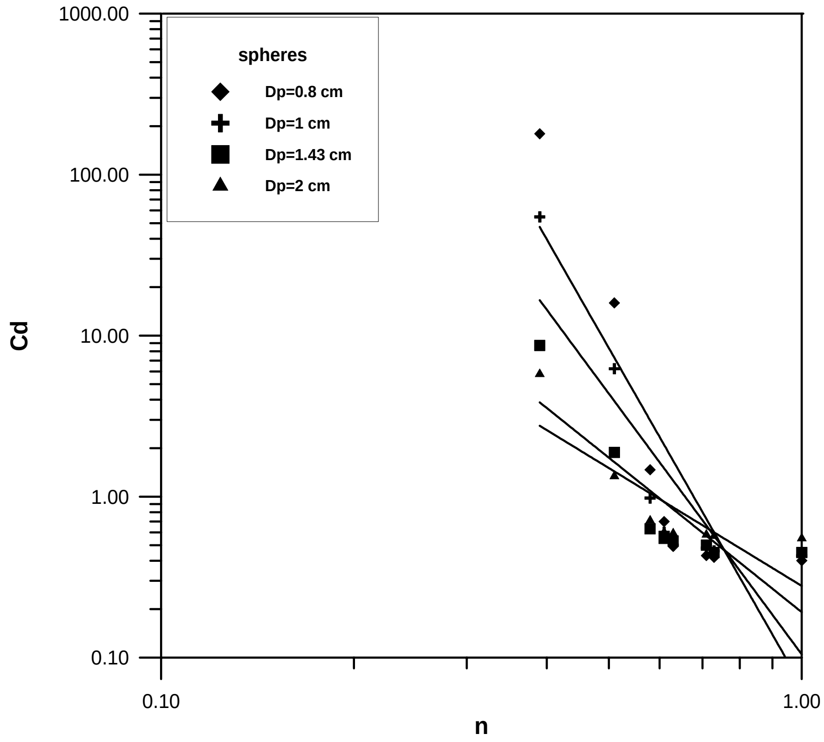

Figure 5-39The effect of flow index on drag coefficient for different diameters of spherical particles

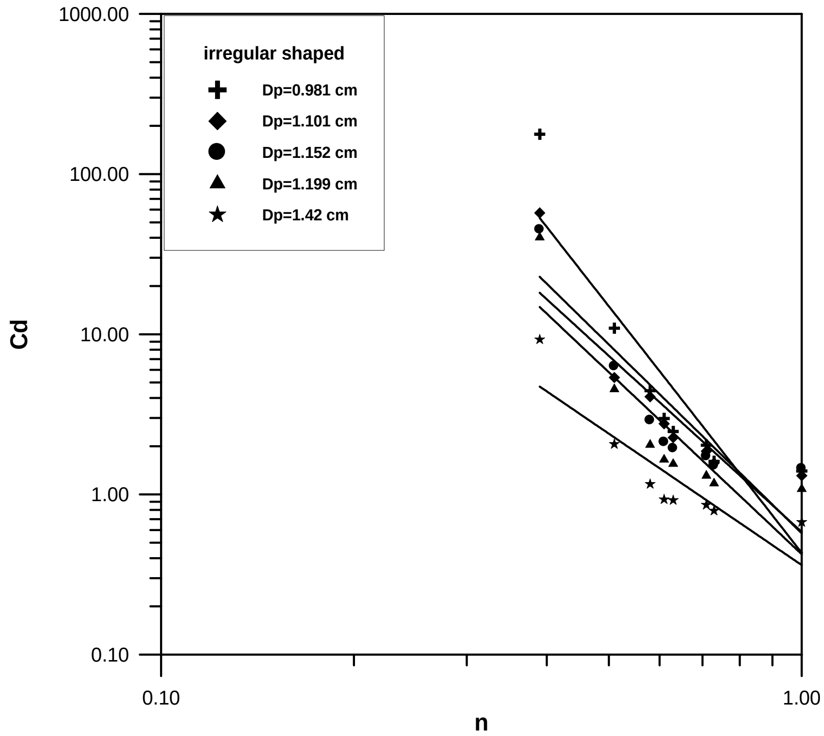

Figure 5-40 The effect of flow index on drag coefficient for different diameters of irregular shaped particles

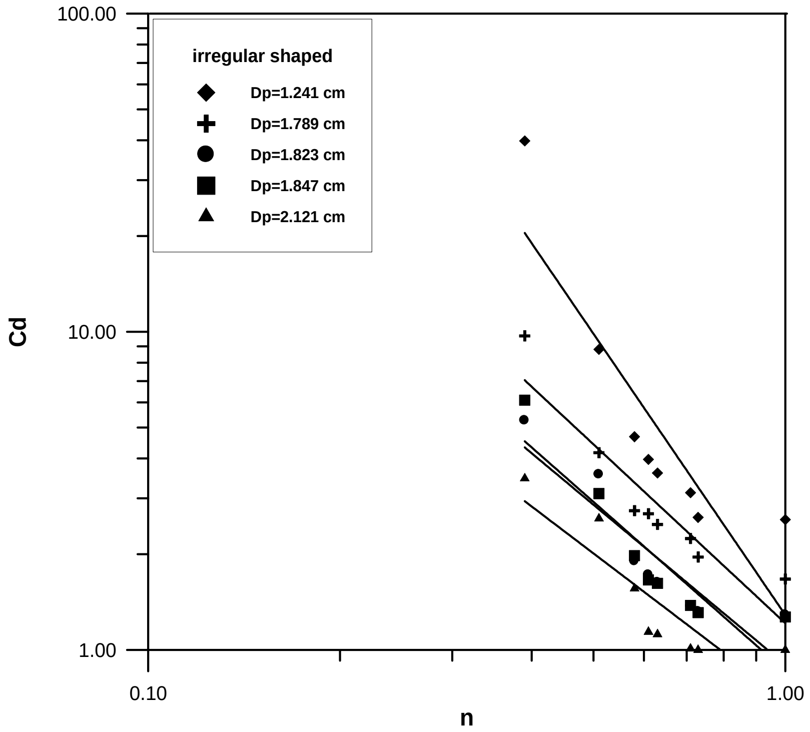

Figure 5-41 The effect of flow index on drag coefficient for different diameters of irregular shaped particles

5.4 Factors Affect Terminal Settling Velocity

5.4.1 Particle Diameter

5.4.1.1 Spherical Particles

To show the relationship between the diameters of spherical particles with terminal settling velocity, a single graph has been plotted for each flow behavior (n). Figures 5-42 to 5-48 show that as the particle diameter D_S increased the settling velocity V_S will be increased. In figure 5-48 it obvious that the small particles (0.2, 0.3 and 0.4 cm.) could not settle at n=0.39 because they have a small size and the bouncy force is very large due to the fact that the concentration and viscosity is very high. Figures 5-49 and

5-50 show the effect of flow behavior index (n) on settling velocity, it is clear that as (n) decreased from unity the settling velocity will be slower, so for particle 0.4 cm at n= 0.73 settling velocity =38.27 cm/s but at n= 0.61 settling velocity V_S =30.39 cm/s, while at n= 0.51 settling velocity =1.44 cm/s.

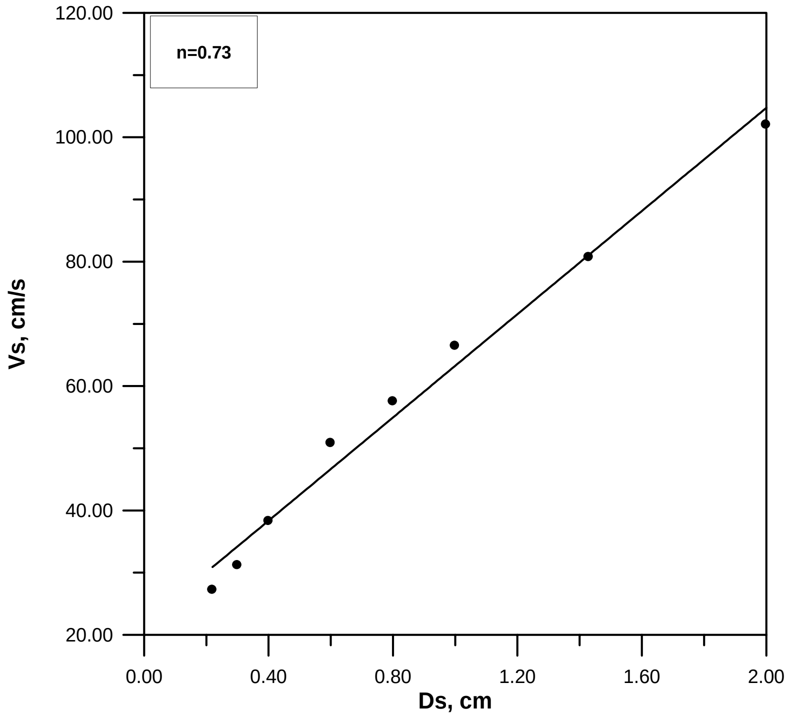

Figure 5-42 The effect of particle diameter on settling velocity at n=0.73

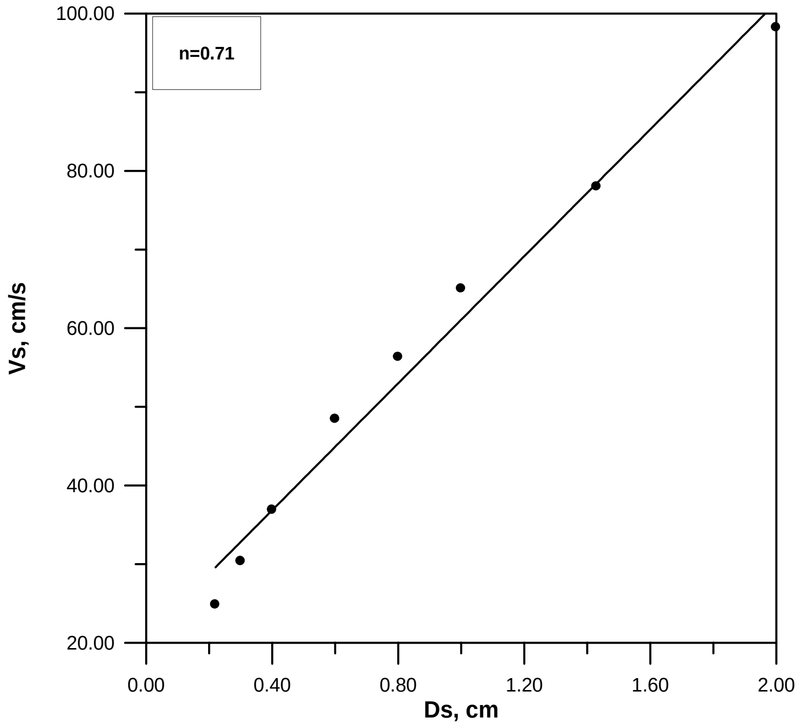

Figure 5-43 The effect of particle diameter on settling velocity at n=0.71

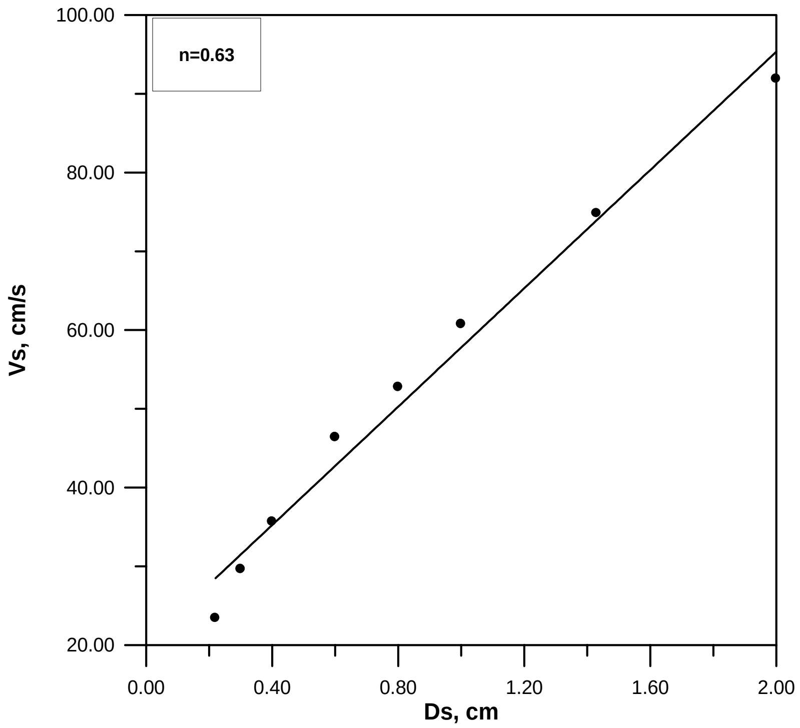

Figure 5-44The effect of particle diameter on settling velocity at n=0.63

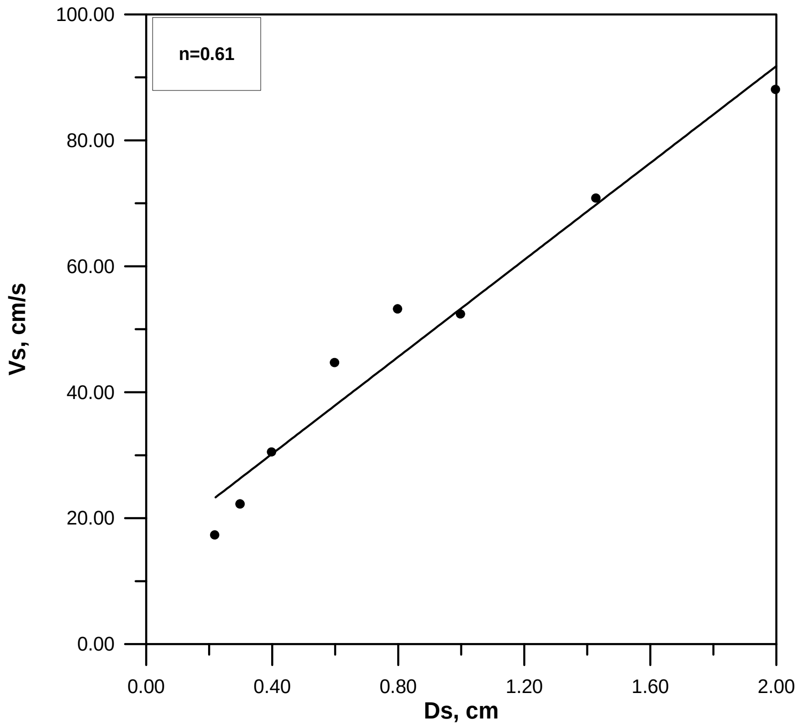

Figure 5-45 The effect of particle diameter on settling velocity at n=0.61

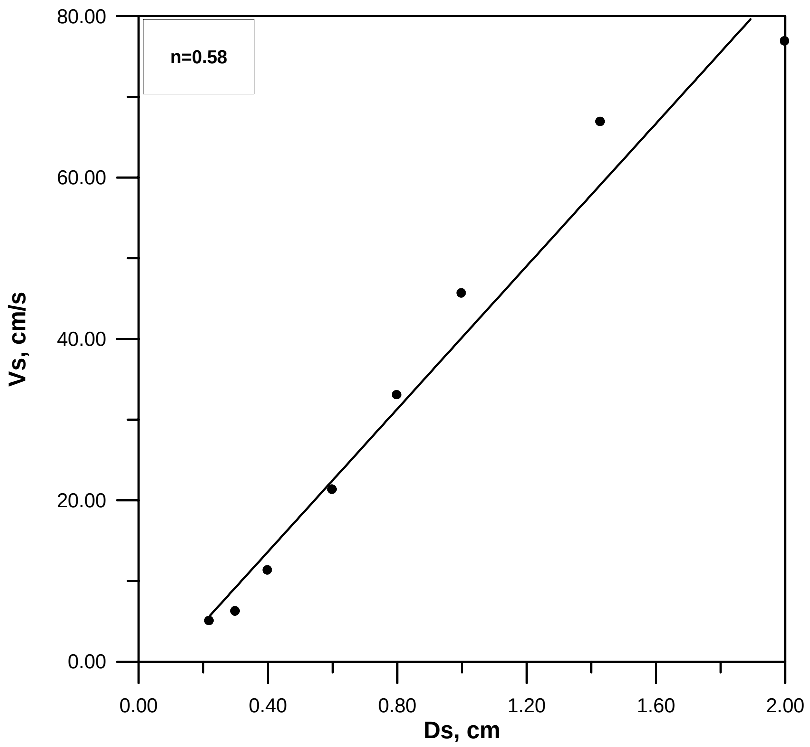

Figure 5-46 The effect of particle diameter on settling velocity at n=0.58

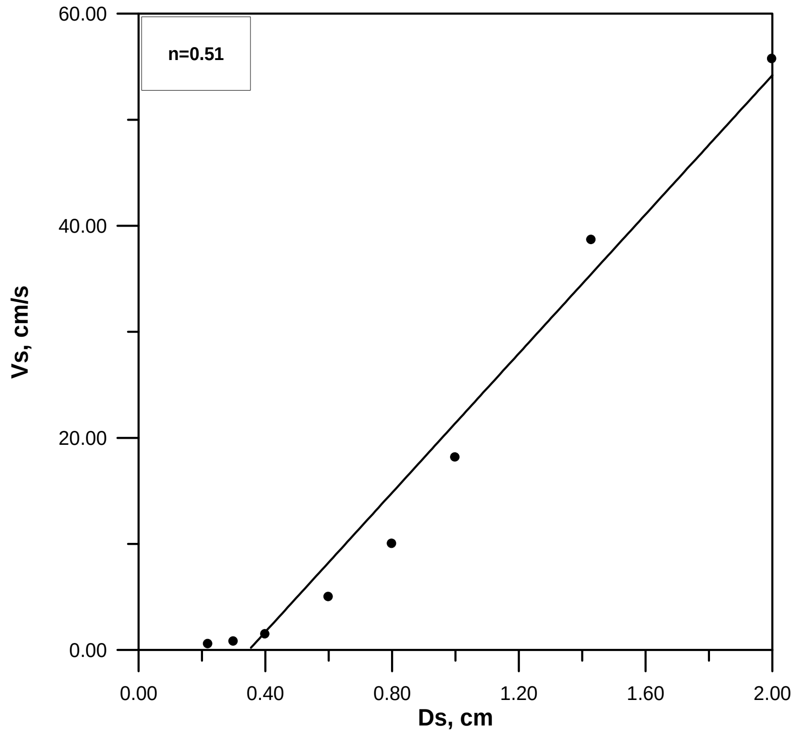

Figure 5-47 The effect of particle diameter on settling velocity at n=0.51

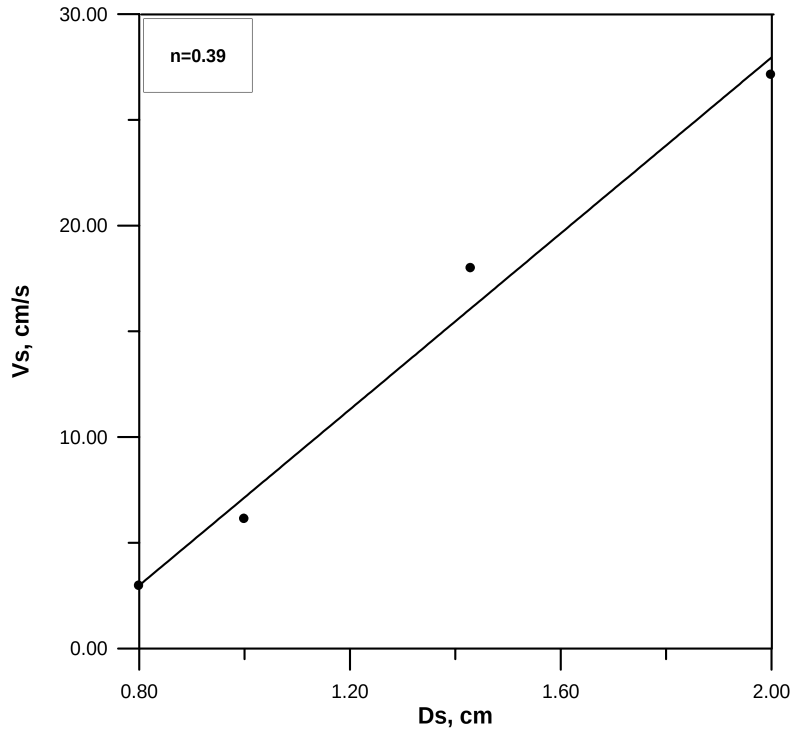

Figure 5-48The effect of particle diameter on settling velocity at n=0.39

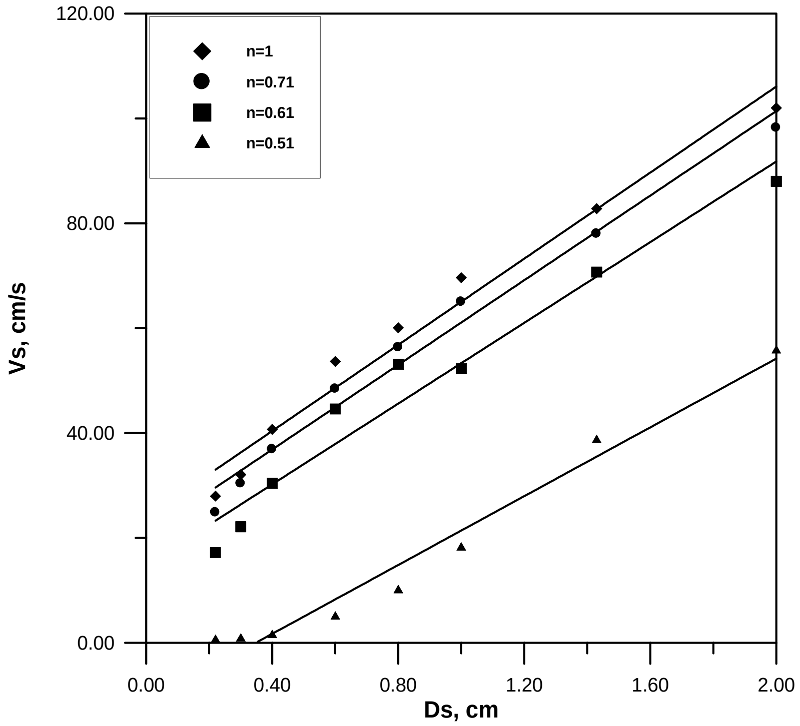

Figure 5-49The effect of particle diameter on settling velocity at n=1, n=0.71, n=0.61 and n=0.51

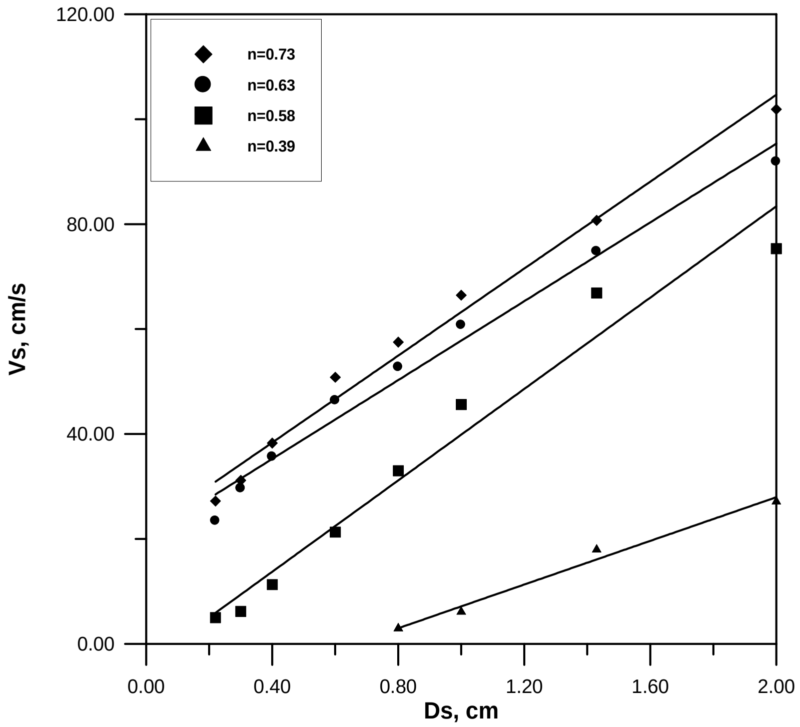

Figure 5-50The effect of particle diameter on settling velocity at n=0.73, n=0.63, n=0.58 and n=0.39

5.4.1.2 Irregular Shaped Particles

For irregular shaped particles, we study the effect of the volumes on their settling velocities. Also, a single graph has been plotted for each flow behavior (n). Figures from 5-51 to 5-57 show as the volume increased the settling velocity will be increased and a comparison in figures 5-58 and 5-59 are done to show the effect of flow behavior index (n) on settling velocity. It is clear from these figures that as (n) decreased the settling velocity will be decreased with increasing of particle volume.

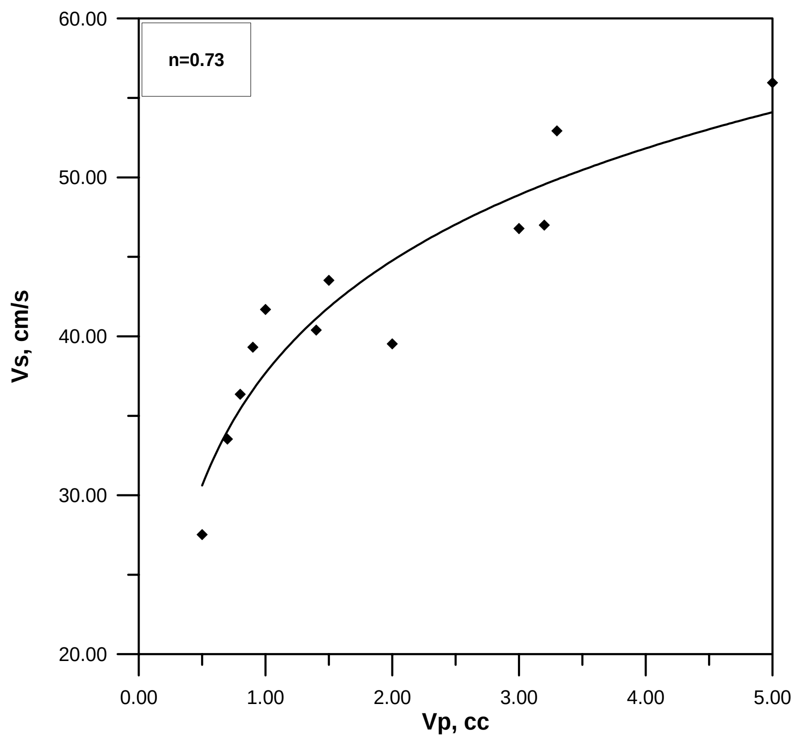

Figure 5-51 The effect of particle volume on settling velocity at n=0.73

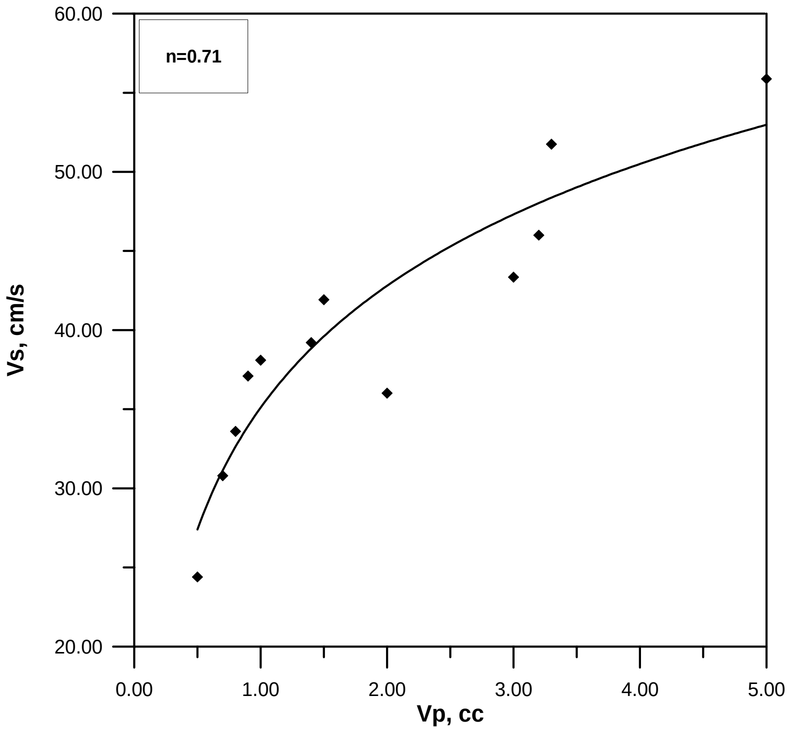

Figure 5-52 The effect of particle volume on settling velocity at n=0.71

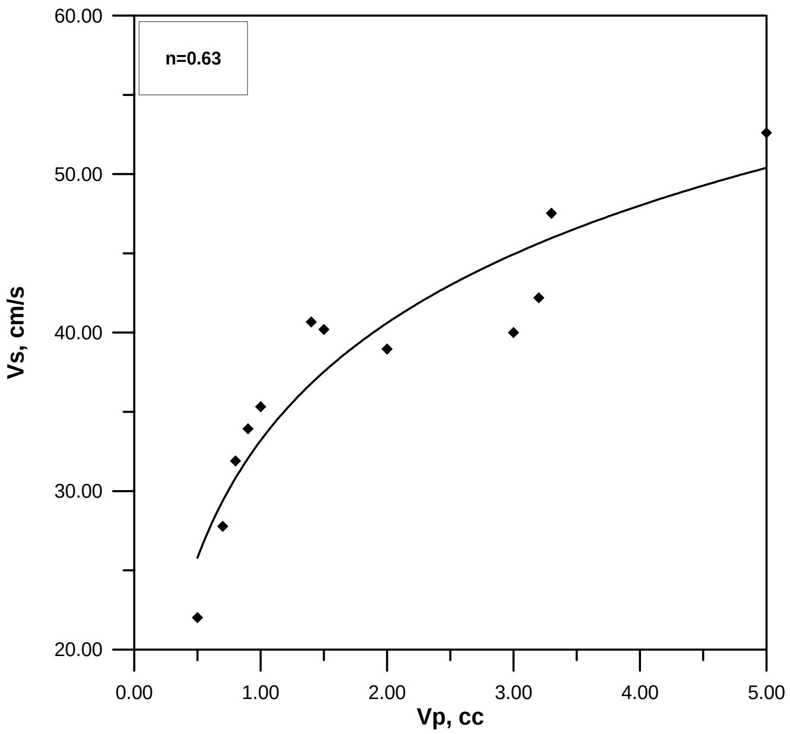

Figure 5-53 The effect of particle volume on settling velocity at n=0.63

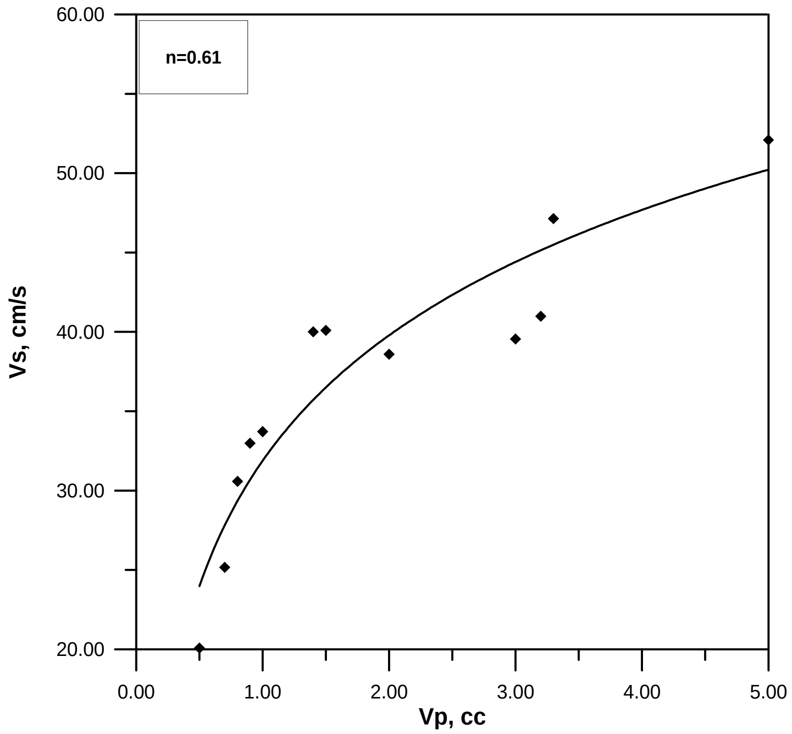

Figure 5-54 The effect of particle volume on settling velocity at n=0.61

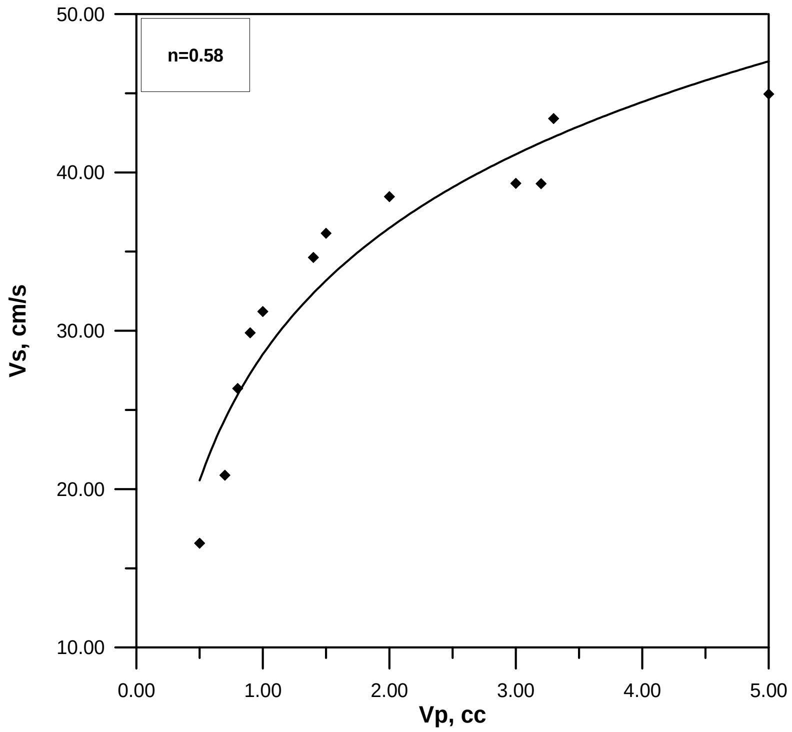

Figure 5-55 The effect of particle volume on settling velocity at n=0.58

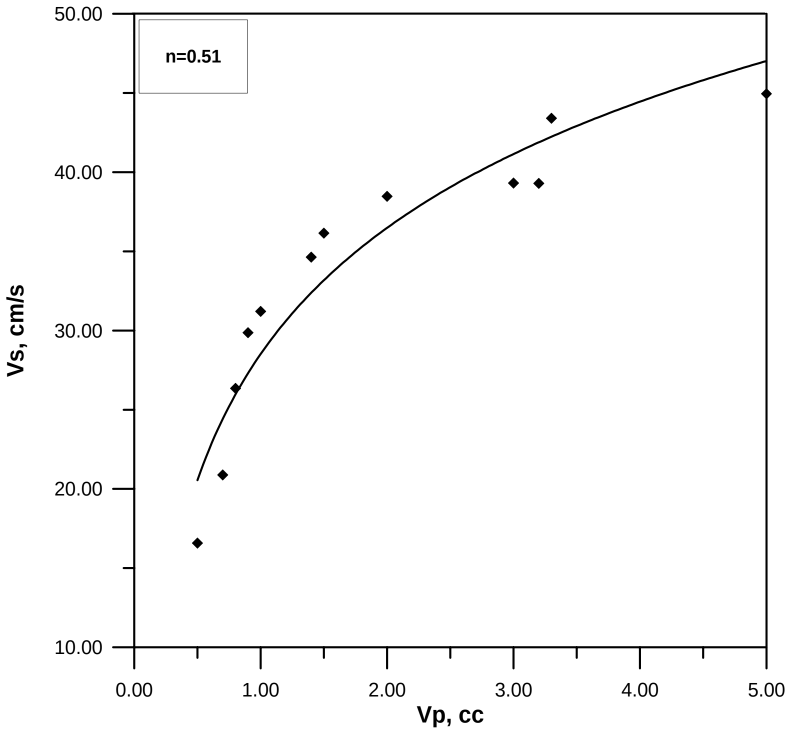

Figure 5-56 The effect of particle volume on settling velocity at n=0.51

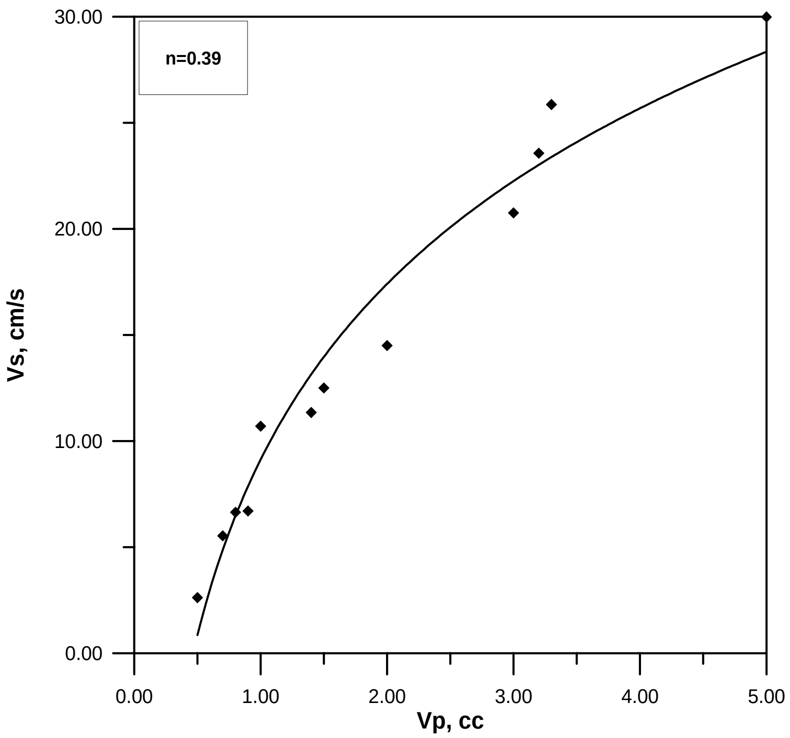

Figure 5-57 The effect of particle volume on settling velocity at n=0.39

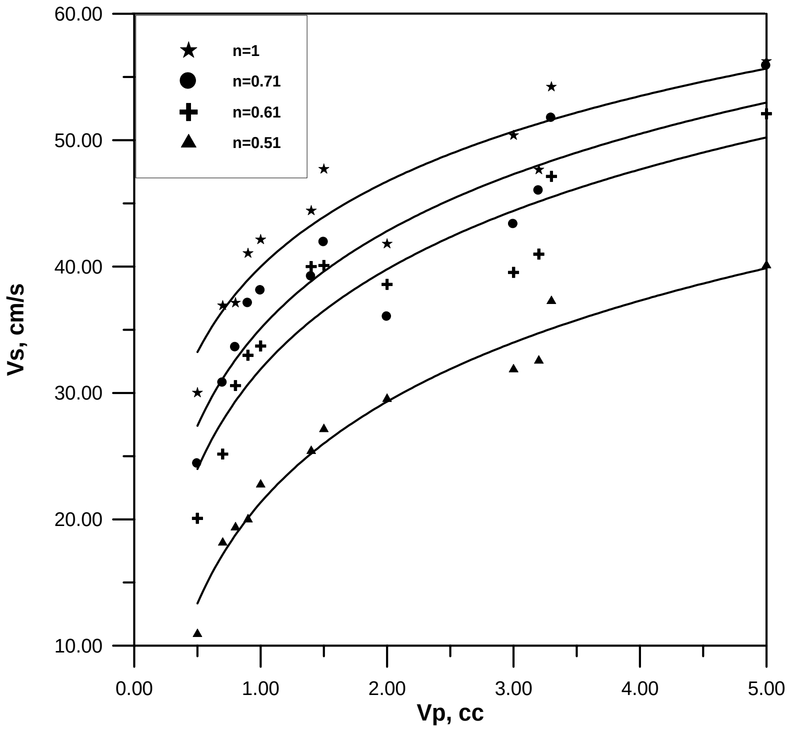

Figure 5-58 The effect of particle volume on settling velocity at n=1, n=0.71, n=0.61 and n=0.51

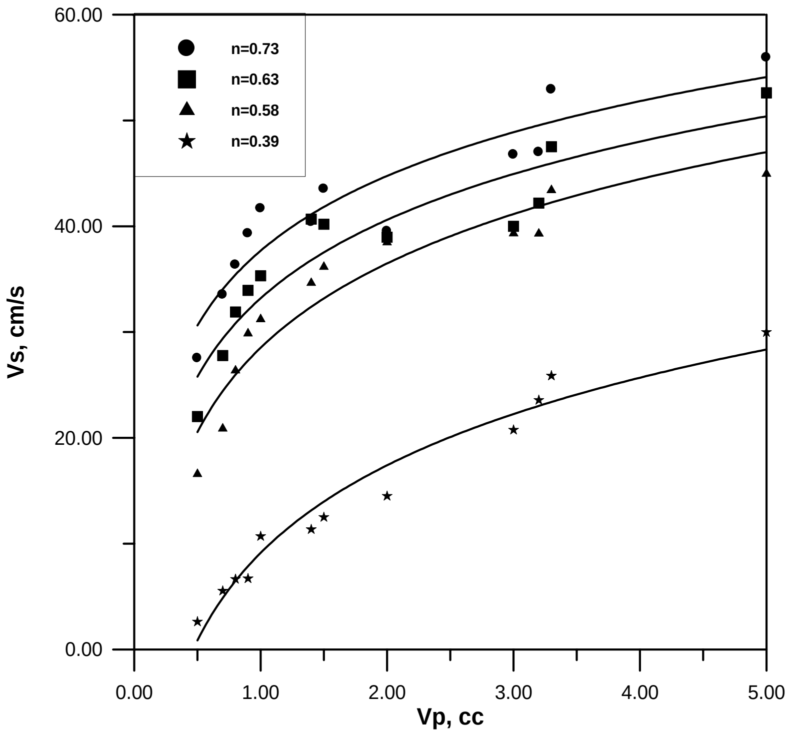

Figure 5-59 The effect of particle volume on settling velocity at n=0.73, n=0.63, n=0.58 and n=0.39

5.4.2 Rheological Properties

Figures 5-60 and 5-61 represent exactly the effect of rheological properties of fluids on settling velocity of spherical particles, it is clear that as the flow behavior (n) increased the settling velocity will be increased with increasing of particle diameter, which means that the sphere of 0.22 cm has a lower settling velocity but its settling velocity increases as the flow behavior (n) approaches to unity. This analysis is applicable for all other particles include irregular shaped particles, thus figures 5-62 and 5-63 show that the smallest irregular shaped particle which has equivalent diameter of 0.984 cm has lower settling velocity than other particles but this velocity increases with increasing of the flow behavior (n).

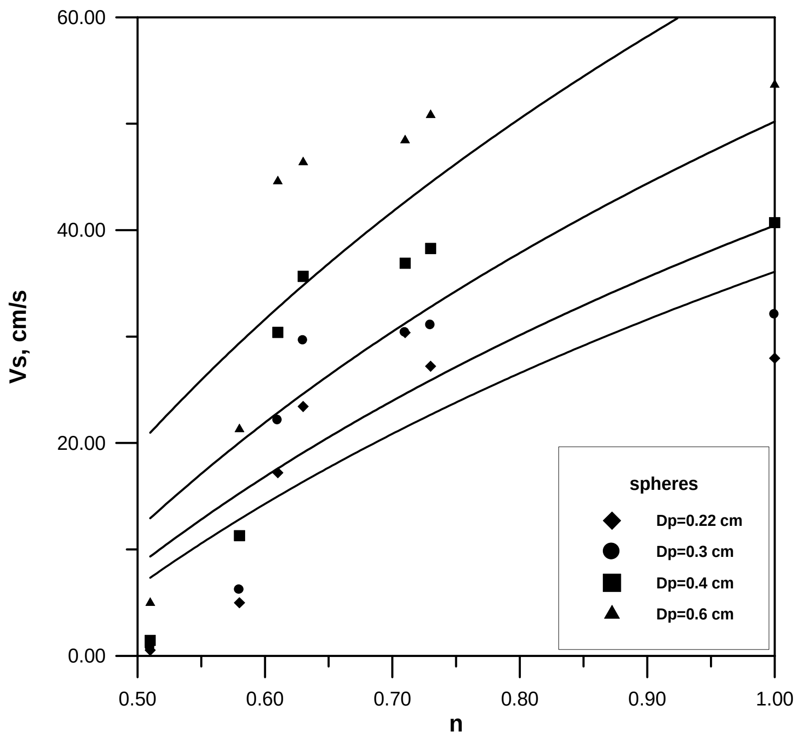

Figure 5-60 The effect of flow behavior index on settling velocity for spherical particles at different diameters

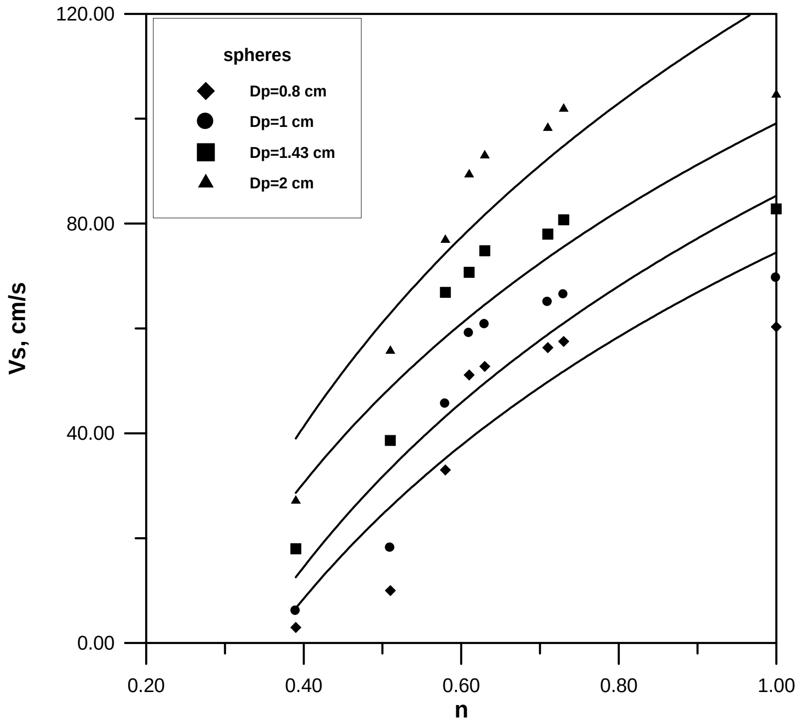

Figure 5-61 The effect of flow behavior index on settling velocity for spherical particles at different diameters

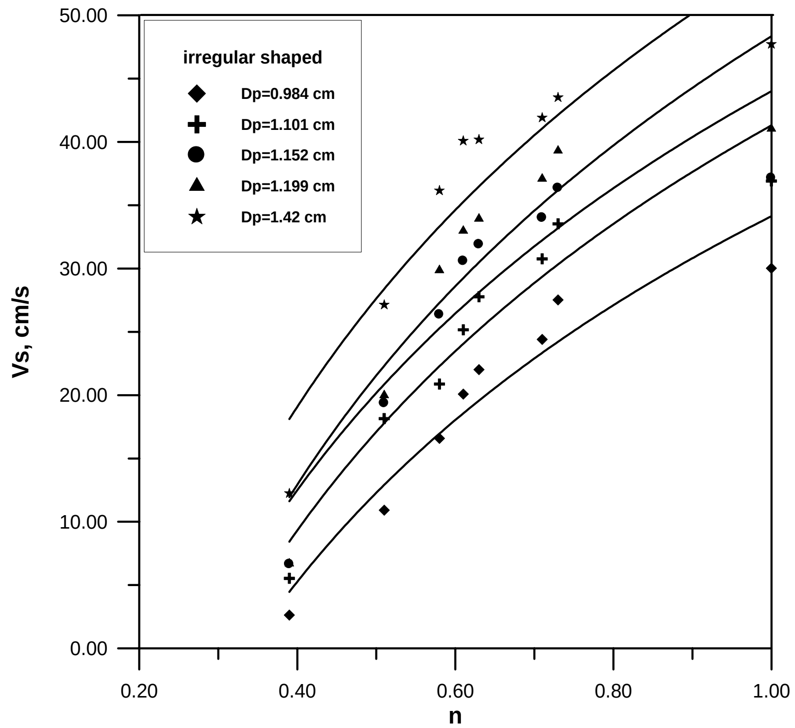

Figure 5-62 The effect of flow behavior index on settling velocity for irregular shaped particles at different diameters

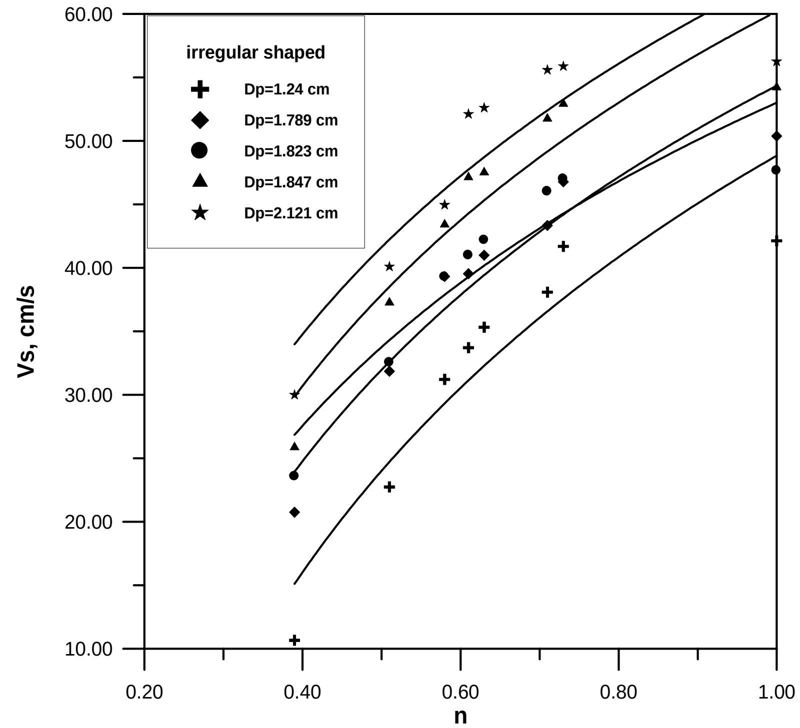

Figure 5-63 The effect of flow behavior index on settling velocity for irregular shaped particles at different diameters

5.4.3 Concentration

The effect of the concentrations of fluids on settling velocity for CMC concentrations (3.75, 5, 15, 17.5) g./l for spherical and irregular shaped particles and also for polyacylamide concentrations (2, 4, 6) gr./lit for spherical and irregular shaped particles is shown in figures 5-64 to 5-71, as the concentration increased the settling velocity will be decreased with increasing particle diameter, which means the particle with the largest diameter has the highest settling velocity but its settling velocity decreases with increasing of concentration of fluids due to increase the drag force on particle so the time required for settling increases thus the settling velocity will be decreased.

Figure 5-66, has two points only, since the small size spherical particles with diameters of 0.2, 0.3, 0.4, 0.6 cm suspended in concentration with 6gr. /lit of polyacrylamide because it was so viscous the bouncy force is very large.

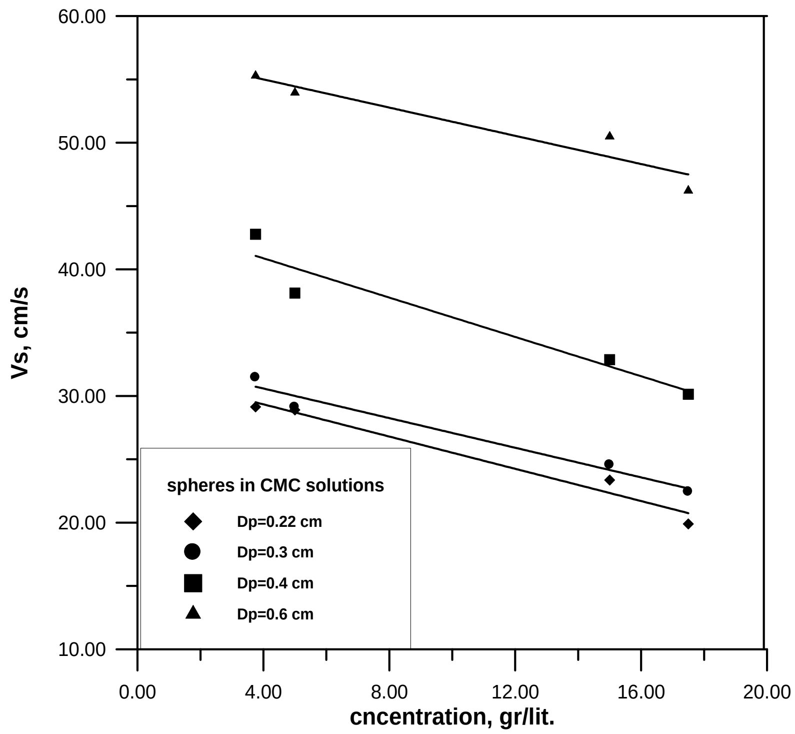

Figure 5-64 The effect of CMC concentration on settling velocity for spherical particles at different diameters

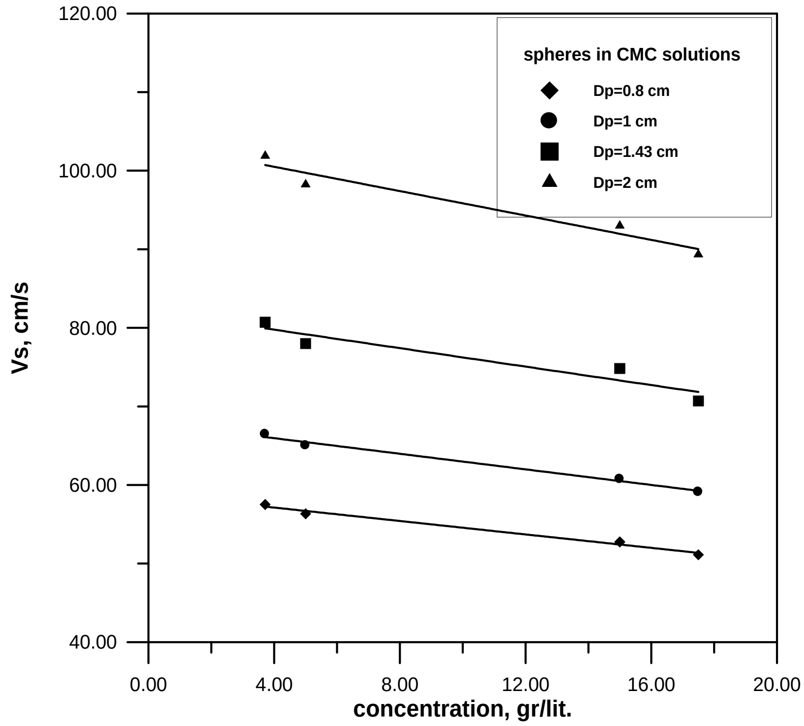

Figure 5-65 The effect of CMC concentration on settling velocity for spherical particles at different diameters

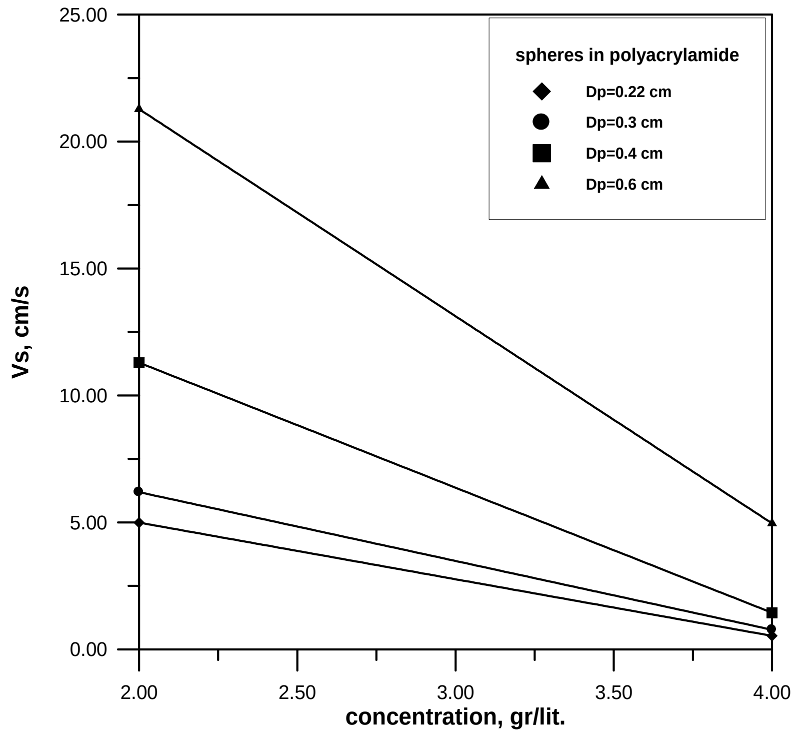

Figure 5-66 The effect of polyacrylamide concentration on settling velocity for spherical particles at different diameters

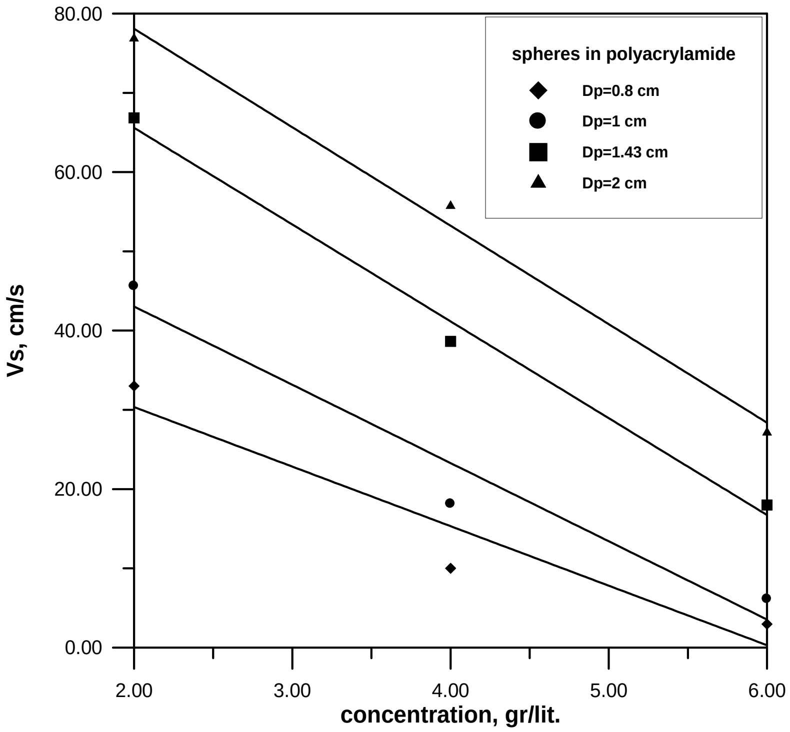

Figure 5-67 The effect of polyacrylamide concentration on settling velocity for spherical particles at different diameters

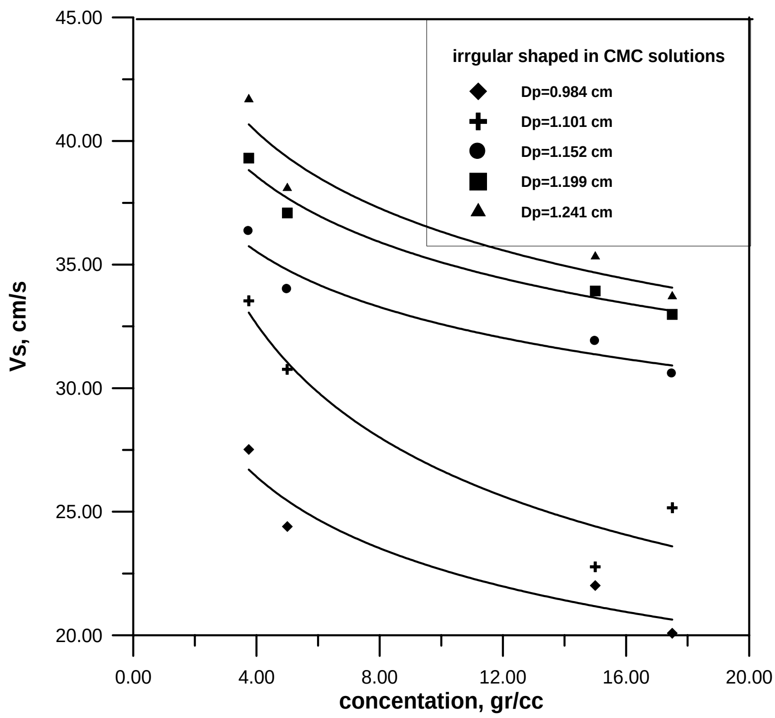

Figure 5-68 The effect of CMC concentration on settling velocity for irregular shaped particles at different diameters

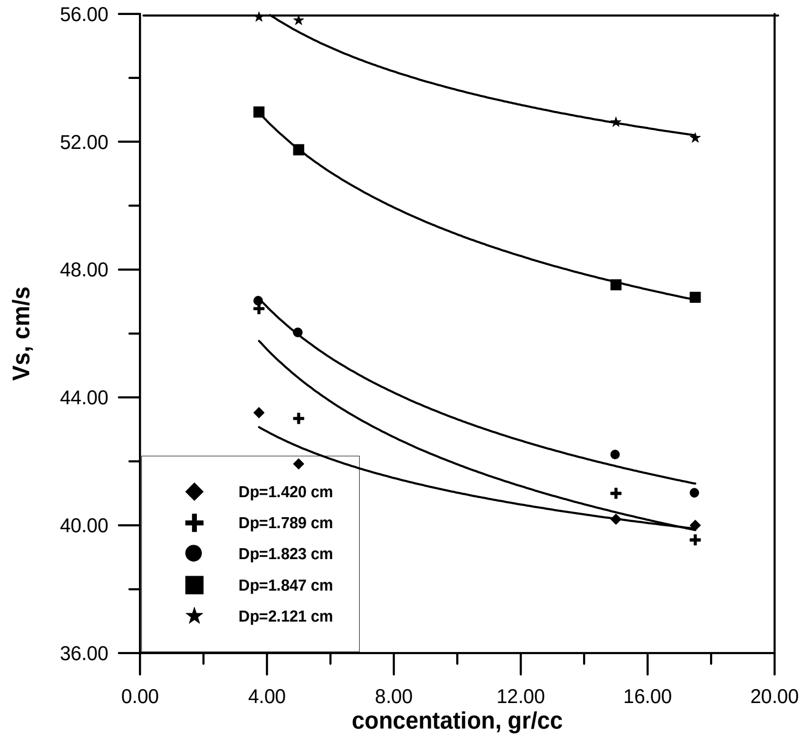

Figure 5-69 The effect of CMC concentration on settling velocity for irregular shaped particles at different diameters

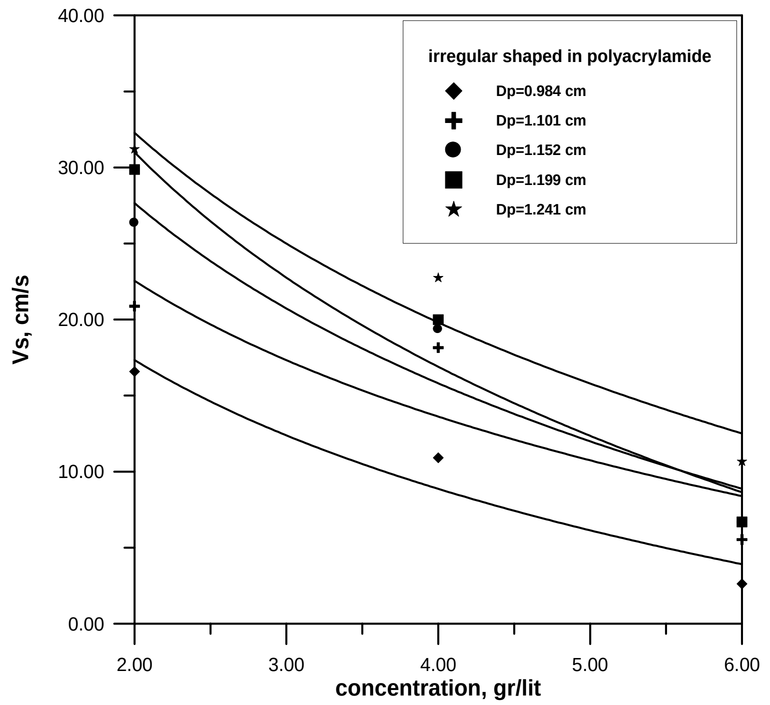

Figure 5-70 The effect of polyacrylamide concentration on settling velocity for irregular shaped particles at different diameters

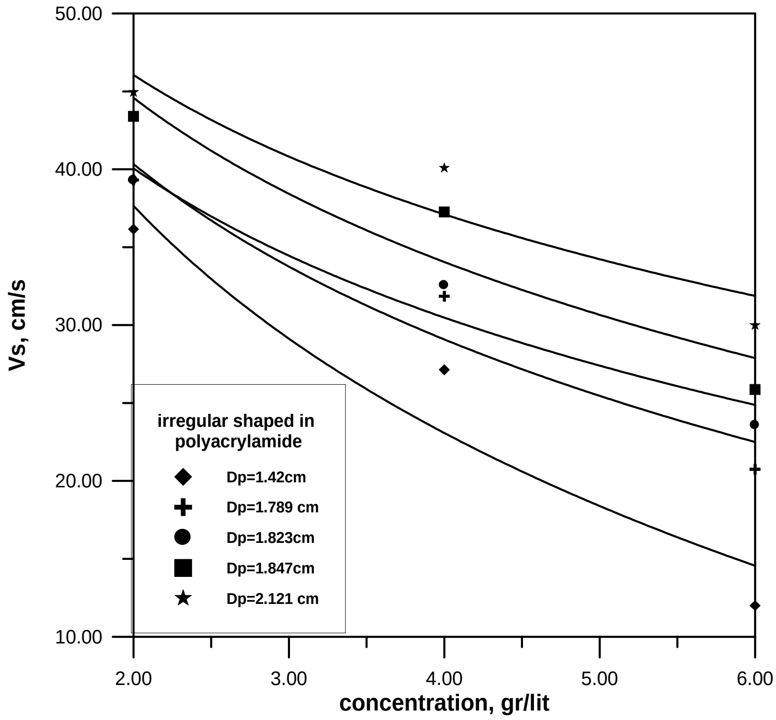

Figure 5-71 The effect of polyacrylamide concentration on settling velocity for irregular shaped

5.5 Empirical Equations

5.5.1 For Drag Coefficient

1. A general formula was obtained for drag coefficient (Y) versus CMC and Polyacrylamide concentrations (X) from our experimental work for spherical particles and irregular shaped particles

$$\text{Log}Y = B \text{ Log } X + A$$

a. For spherical particles

At;	For CMC		For Polyacrylamide	
D_s, (cm.)	B	A	B	A
0.22	0.430	-1.023	6.461	-0.785
0.3	0.305	-1.00	6.006	1.430
0.4	0.213	-0.919	5.933	-2.305
0.6	0.192	-0.920	4.188	-1.848
0.8	0.142	-0.922	4.273	-2.732
1	0.140	-0.961	3.553	-2.648
1.43	0.137	-1.01	2.182	-2.009
2	0.145	-1.096	1.902	-1.932

b. For irregular shaped particles

At;	For CMC		For Polyacrylamide	
D_s (cm.)	B	A	B	A
0.984	0.328	0.096	3.312	-0.869
1.101	0.301	0.085	2.188	-0.447

1.152	0.181	0.208	2.33	-0.791
1.199	0.199	0.083	2.544	-1.311
1.241	0.225	0.710	1.986	-0.806
1.42	0.087	0.318	1.837	0.096
1.789	0.166	0.489	1.092	0.159
1.823	0.162	0.062	0.924	-0.002
1.847	0.148	0.082	1.184	-0.460
2.121	0.105	1.381	0.725	0.057

2. A general formula was obtained for drag coefficient (Y) versus flow behavior index (X) from our experimental work for spherical particles and irregular shaped particles

$$LogY= B \, Log \, X+A$$

a. For spherical particles

At; D_s (cm.)	**B**	**A**
0.22	-9.699	-2.602
0.3	-9.181	-2.603
0.4	-9.181	-2.622
0.6	-7.899	-2.468
0.8	-0.682	-2.589
1	-5.396	-2.259
1.43	-3.322	-1.734
2	-2.850	-1.653

b. For irregular shaped particles

At; **D_s (cm.)**	B	**A**
0.984	-7.862	-2.257
1.101	-5.444	-1.453
1.152	-5.345	-1.535
1.199	-5.511	-1.882
1.241	-4.212	-0.497
1.42	-3.660	-1.128
1.789	-2.460	-0.153
1.823	-2.315	-0.483
1.847	-2.346	0.519
2.121	-2.211	0.765

5.5.2 For Settling Velocity

1. A general formula was obtained for settling velocity(Y) versus CMC and Polyacrylamide concentrations (X) from our experimental work for spherical particles and irregular shaped particles

$$Y=B\,X+A$$

a. For spherical particles

At;	For CMC		For Polyacrylamide	
D_s (cm.)	B	A	B	A
0.22	-0.427	58.827	-2.23	9.45
0.3	-0.497	67.930	-2.71	11.61
0.4	-0.587	82.105	-4.925	21.140
0.6	-0.776	103.607	-8.16	37.600
0.8	-0.811	105.98	-7.512	45.362
1	-0.936	110.98	-9.875	62.773
1.43	-0.951	117.685	-12.22	90.027
2	-1.019	120.521	-12.437	102.613

b. For irregular shaped particles

At;	For CMC		For Polyacrylamide	
D_s	B	A	B	A
0.984	-3.947	31.89	-12.219	25.805
1.101	-4.455	38.749	-12.911	31.520
1.152	-3.024	39.533	-17.086	39.492
1.199	-3.708	43.708	-20.366	45.097
1.241	-2.024	46.286	-18.013	44.767
1.42	-2.024	45.726	-20.99	52.236
1.789	-3.841	50.799	-16.241	51.578
1.823	-3.794	52.013	-13.823	49.623
1.847	-3.799	57.907	-15.200	55.121
2.121	-2.649	59.769	-12.944	55.060

2. A general formula was obtained for settling velocity(Y) versus flow behavior index (X) from our experimental work for spherical particles and irregular shaped particles

$$Y = B\,X + A$$

a. For spherical particles

At; D_s (cm.)	**B**	**A**
0.22	42.699	36.086
0.3	46.194	40.430
0.4	55.361	50.203
0.6	65.565	65.108
0.8	71.850	74.353
1	72.284	85.299
1.43	74.878	99.127
2	86.738	121.434

b. For irregular shaped particles

At; D_s (cm.)	B	**A**
0.984	38.834	38.327
1.101	42.659	45.718
1.152	46.748	51.189
1.199	52.061	56.145

1.241	48.015	55.93
1.42	50.421	61.189
1.789	39.267	58.309
1.823	37.582	58.721
1.847	43.146	66.573
2.121	43.382	70.379

3. A general formula was obtained for settling velocity(Y) versus diameter for spherical particles or volume for irregular shaped particles (X) from our experimental work

$$Y=B\,X+A$$

a. For spherical particles

At; n	B	A
0.73	41.431	27.792
0.71	40.345	20.725
0.63	37.522	20.223
0.61	36.109	16.818
0.58	34.209	14.043
0.51	32.853	13.489
0.39	20.8039	11.659

b. For irregular shaped particles

At; n	B	A
0.73	10.191	37.685
0.71	11.145	35.063
0.63	10.766	33.182
0.61	11.394	31.878
0.58	11.503	31.878
0.51	11.531	21.235
0.39	11.928	9.054

Where A, B are the constants of equation depends on the shape, diameters of particles and flow behavior indeces.

The results of experimental work are given in appendix [A].

CHAPTER SIX
CONCLUSIONS AND RECOMMENDATIONS

6.1 CONCLUSIONS

1. From the experimental work of this research, it has been concluded that the particle diameter having same volume as sphere is a good expression to compare between the irregular shaped particles and spherical particles; it has a major effect on C_d-Re_P relationship.

2. As particle Reynolds number increased the drag coefficient will decrease especially in laminar-slip regime until the drag coefficient reaches a constant value in turbulent-slip regime.

3. Settling velocity of solid particle is greatly affected by a particle path during settling. It has been shown that the spherical particles follow the vertical path during settling, while the irregular shaped particles follow different paths and orientations like springing, circular, oscillating and unstable paths. This orientation will decrease the settling velocity of irregular shaped particles, so the drag coefficient of these particles will increase.

4. The particle size has a great effect on the settling velocity and drag coefficient, as the particle diameter or volume increased the drag coefficient will decrease since the settling velocity will increase. For

example, at n=0.73 a spherical particle of diameter 0.4 cm has a settling velocity of 38.27 cm/s, while a spherical particle of diameter 0.8 cm has a settling velocity of 57.51 cm/s at same flow index n., also for irregular shape the particle of volume 0.5cm^3 has a settling velocity of 27.52 cm/s, while a particle of volume 1cm^3 has a settling velocity of 41.69 cm/s at n= 0.73.

5. The rheological properties of non-Newtonian fluids have a great effect on drag coefficient, because as the fluid became far from Newtonian behavior, (flow index n far from unity), the settling velocity will be decreased and the drag coefficient will be increased. This effect was clearly present in laminar-slip and will decrease or vanished in turbulent and transion-slip regimes.

6. The difference in density between the particle and fluid affect the drag coefficient, as the difference increases the bouncy force will increase and the settling velocity will decrease so the drag coefficient will increase.

7. The C_d-Re_P relationships for Newtonian fluid is the same in non-Newtonian fluids, because the principle of equivalent viscosity is used which represents the ratio of shear stress to shear rate around the surface of particle.

8. The concentrations of polymers fluids have effect on C_d, it shown that as the concentration of fluid increased the drag coefficient will increase to decrease the settling velocity of particles. At concentration 2 g/l (n=.051) of polyacrylamide C_d of spherical diameter of 1 cm is equal to 6.23 while the drag coefficient at concentration of 4 g/l (n=0.39) is equal to 54.62 for same diameter. Also for irregular shaped that have diameter of 1.101 cm at concentration 2 g/l of polyacrylamide C_d=5.37 while at concentration of 4 g/l C_d=57.11 cm for same diameter.

6.2 RECOMMANDATIONS

1. Study the factors which affect drag coefficient using the concept of hindered settling velocity.

2. Study the settling velocity of solid particle in a horizontal pipe and its effects on drag coefficient and on C_d-Re_P relationship.

3. Study the effect of shape of solid particle on drag coefficient and C_d-Re_P relationship by using a shape factor like sphericity or circularity.

REFERENCES

1. Given on internet by Vassilios C. Kelessidis, "Terminal velocity of solid spheres falling in Newtonian and non Newtonian liquids"; (2003), at
   http:// www.mred.tus.gr/puplications/18.pdf
2. Reynolds P.A. and Jones T.E.R., "An experimental study of the settling velocities of single particles in non- Newtonian fluids"; Int. J. of Mineral Processing, 25, (1989).
3. Michell S. J., "Fluid and particle mechanics" p. 288- 301, Pergamon Press LTD., (1970).
4. Pettyjhon E.S. and Cheristiansen E.B. "Effect of particle shape on free settling rates of isometric particles"; Chem. Eng. Progress, 44(1948), 2.
5. Ahchin A.D., Portz M., Deddow J.K. and Vetter A.F."A shape-modified size correction for terminal settling velocity in the intermediate region"; Powder Tech., 48(1986).
6. Brodkey R.S. And Hershey H.C., "Transport phenomena" p. 587-594, John Wiley and Sons, New York 2nd edition (1989).
7. Muhannad A.R. "The effect of particles shape and size and the rheological properties of non-Newtonian fluids on drag coefficient and particle Reynold's number relationship", Ph.D. Thesis, (1998).
8. McCabe W.L., Smith J.C. and Harriott P. "Unit operation of chemical engineering" 5th edition, p.143-163, Mc Graw Hill, New York (1993).
9. Chien S.F., "Settling velocity of irregular shaped particle"; SPE Drilling and Completion, Dec. (1994).

10. Given on internet by Courtney K.Harris, “Sediment transport processes in coastal environments”, (2003), at
http:// www.vims.edu/~ckharris/ms698-03/lecture-2pdf

11. Jamil Malaika “Effect of shape of particles on their settling velocity”, Ph.D. Thesis, (1949).

12. Zeidler H.A. “An experimental analysis of the transport drill particles” SPEJ, Feb. (1972).

13. Concha F. and Barrienotos “Settling velocity of particulate systems, 4. Settling of non spherical isometric particles”, Int. J. of Mineral Processing, 18(1986).

14. Walker R.E. and Mayes T.M. “Design of mud for carrying capacity”, JPT, July (1975).

15. Given on internet by Vassilios C. Kelessidis, “An explicit equation for the terminal velocity of solid spheres falling in Psuedoplasic liquids”; Chem. Eng. Science 59(2004),
http:// www.mred.tus.gr/pulications/17.pdf

16. Becker H.A. “The effects of shape and Reynolds number on drag in the motion of a freely oriented body in an infinite fluid”, The Cand. J. of Chem. Eng., April, (1959).

17. Slattery J.C. and Bird R.B. “Non-Newtonian flow past a sphere”, Chem. Eng. Science vol.16 (1961).

18. Wassermann M.L and Slattery J.C. “Upper and lower bounds on the drag coefficient of a sphere in a Power-model fluid”, AICH J. vol.14, (1964).

19. Valentik L. and Whitmore R.L. “The terminal velocity of spheres in Bingham plastic”, Brit. J. Appl. Phys. vol.16 (1965).

20. Plessis M.P. and Ansely R.W. “Settling parameters in solids pipelining”, J. of Pipeline Division, Proc. Of the Amer. Soc. Of Civil Eng. Vol. 93 No. PL2, July (1967).

21. Issac J. L. and Thodos G. “The free-settling of solid cylindrical particles in the Turbulent regime”, The Cand. J. of Chem. Eng., vol. 45, June (1967).

22. Hottovy J.D. and Sylvester N.D. “Drag coefficient for irregularly shaped particles”, Ind. Eng. Chem. Process Des. Dev., vol. 18, No.3 (1979).

23. Torrest R.S. “Particle settling in viscous non-Newtonian Hydroxyethel Cellulose polymer solutions”, AICH J. vol. 29, No.3, May (1983).

24. Flemmer R.L.C. and Banks C.L “On the drag coefficient of a sphere”, Powder Tech. 48 (1986).

25. Meyer B.R. “Generalized drag coefficient applicable for all flow regimes”, Oil and Gas J., May 26 (1986).

26. Dedegil M.Y. “Drag coefficient and settling velocity of particles in non Newtonian suspensions”, J. of Fluid Eng. Sept., vol. 109 (1987).

27. Given on internet by Ataide C.D., Pereira A.R. and Barrozo M.A.S. “Wall effects on the terminal velocity of spherical particles in Newtonian and non- Newtonian fluids”, Braz. J. Eng. Vol. 16, No.4 Dec.(1999)
http://www.scielo.br/ scielo.php script=sci-arttex & pid=solo4

28. Given on internet by Lesseno C. and EssanoW.J, “PIV Measurements of free-falling irregular particles”, (2002), at
http://www.in3.dem.ist.ut/x aser 2002/papers/paper-13-5.pdf

29. Terence A. “Particle size measurement”, John Wiley and Sons Inc., New York (1975).

30. Given on internet by G.E. Mpndelis and Vassilios C. Kelessidis, "New approach for estimation of terminal velocity of solid spheres falling in Newtonian and non Newtonian fluids"; (2004), at http:// www.mred.tuc.gr/puplication/15.pdf

31. Zdenek K.J. "Particle size analysis", John Wiley and Sons Inc., New York (1970).

32. Irani R.R. and Callis C.F. "Particle size measurement, interpretation, and application", John Wiley and Sons Inc., New York (1963).

33. Hopkin E.A., "Factors affecting cuttings removal during Rotary drilling", J.P.T June, 1967.

34. Fidleris V. and Whitmore R.L. "Experimental determination of the wall effect for spheres falling axially in cylindrical vessels", Brit. J. Appl. Phys. vol.12 (1961).

35. Turian R.M. "An experimental investigation of the flow of aqueous non Newtonian high polymer solutions past a sphere", AICH J. vol.13, No.5 (1967).

36. Bird R.B., Stewart W.E., and E.N. Lightfoot "Transport phenomena", John Wiley and Sons Inc., New York (1960).

37. Chatterji J. and Borchardt J. K., "Applications of water soluble polymers in the oil field", JPT. Nov. (1981).

38. Lauzon R.V. "Water-Soluble polymers for drilling fluids", oil and gas J., April 19 (1982).

APPENDIX [A]

EXPERIMENTAL RESULTS

Table A-1 Results of V_S, Re_P and C_d for spherical particles in Newtonian fluid (water n=1)

D_S, cm	V_S, cm/s	Re_P	C_d	Orientation
0.22	29.97	566.98	0.57	Vertical
0.3	32.07	896.44	0.54	Vertical
0.4	40.70	1801.98	0.47	Vertical
0.6	53.65	2264.19	0.45	Vertical
0.8	60.08	3490.35	0.43	Vertical
1	69.64	4401.92	0.42	Vertical
1.43	82.79	6614.68	0.41	Vertical
2	102.05	9491.73	0.40	Vertical

Table A-2 Results of V_S, Re_P and C_d for irregular shaped particles in Newtonian fluid (water n=1)

D_S, cm	V_S, cm/s	Re_P	C_d	Orientation
0.984	30.01	1468.58	1.38	Flat
1.101	36.91	2020.44	1.33	Flat
1.152	37.13	2124.89	1.32	Flat
1.198	41.05	2443.94	1.28	Springing
1.240	42.13	2197.94	2.57	Oscillating
1.388	44.42	3063.47	1.25	Circular path

1.420	47.72	3367.89	0.67	Circular path
1.56	39.80	2247.49	1.65	Circular path
1.789	45.39	4480.76	1.63	Oscillating
1.823	47.66	4315.68	1.24	Unstable
1.847	54.22	4977.35	1.23	Unstable
2.121	56.25	5930.75	1	Unstable

Table A-3 Results of V_S, Re_P and C_d for spherical particles for CMC, n=0.73

D_S, cm	V_S, cm/s	Re_P	C_d	Orientation
0.22	27.21	376.78	0.6	Vertical
0.3	31.16	592.93	0.57	Vertical
0.4	38.27	1013.34	0.53	Vertical
0.6	50.81	2030.29	0.50	Vertical
0.8	57.51	2699.29	0.48	Vertical
1	66.44	3833.93	0.46	Vertical
1.43	80.71	6392.29	0.43	Vertical
2	101.89	8997.9	0.40	Vertical

Table A-4 Results of V_S, Re_P and C_d for irregular shaped particles for CMC1, n=0.73

D_S, cm	V_S, cm/s	Re_P	C_d	Orientation
0.984	27.52	1201.34	1.64	Flat

1.101	33.53	1657.02	1.57	Flat
1.152	36.35	1897.53	1.51	Flat
1.198	39.31	2162.83	1.47	Circular path
1.240	41.69	2202.08	2.61	Springing
1.388	40.39	2112.91	1.2	Circular path
1.420	43.52	2797.98	0.79	Circular path
1.56	38.51	2637.97	1.83	Springing
1.789	46.78	3613.36	1.93	Unstable
1.823	47	3710.65	1.34	Oscillate
1.847	52.93	4356.19	1.32	Unstable
2.121	55.96	5136.70	1.01	Unstable

Table A-5 Results of V_S, Re_P and C_d for spherical particles for CMC, n=0.71

D_S, cm	V_S, cm/s	Re_P	C_d	Orientation
0.22	24.84	68.66	0.72	Vertical
0.3	30.36	110.94	0.60	Vertical
0.4	36.89	174.96	0.57	Vertical
0.6	48.44	331.56	0.55	Vertical
0.8	56.33	483.09	0.5	Vertical
1	65.02	684.21	0.48	Vertical
1.43	78.77	1118.72	0.46	Vertical
2	98.24	1513.69	0.43	Vertical

Table A-6 Results of V_S, Re_P and C_d for irregular shaped particles for CMC, n=0.71

D_S, cm	V_S, cm/s	Re_P	C_d	Orientation
0.984	24.40	185.71	2.03	Flat
1.101	30.76	267.98	1.86	Unstable
1.152	34.01	284.78	1.73	Flat
1.198	37.09	363.08	1.48	Circular path
1.240	38.08	387.04	3.12	Springing
1.388	39.27	437.38	1.39	Flat
1.420	41.92	481.62	0.86	Circular path
1.56	36.01	421.64	2.24	Springing
1.789	43.34	590.14	1.39	Unstable
1.823	46.01	650.19	1.37	Oscillate
1.847	51.75	763.34	1.36	Unstable
2.121	55.88	923.71	1.03	Unstable

TableA-7 Results of V_S, Re_P and C_d for spherical particles for CMC, n=0.63

D_S, cm	V_S, cm/s	Re_P	C_d	Orientation
0.22	23.42	31.72	0.82	Vertical
0.3	29.63	54.01	0.63	Vertical
0.4	35.66	83.44	0.61	Vertical
0.6	46.38	154.41	0.6	Vertical
0.8	52.76	216.46	0.57	Vertical

1	60.74	301.58	0.55	Vertical
1.43	74.82	507.03	0.41	Vertical
2	92.97	875.60	0.4	Vertical

Table A-8 Results of V_S, Re_P and C_d for irregular shaped particles for CMC, n=0.63

D_S, cm	V_S, cm/s	Re_P	C_d	Orientation
0.984	22.01	73.24	2.47	Flat
1.101	27.77	107.00	2.26	Flat
1.152	31.90	133.06	1.94	Unstable
1.198	33.93	148.75	1.56	Flat
1.240	35.32	161.36	3.60	Circular path
1.388	40.67	210.49	1.27	Flat
1.420	40.17	209.49	0.92	Circular path
1.56	38.93	212.04	1.86	Circular path
1.789	36.01	210.15	2.11	Unstable
1.823	42.19	262.70	1.62	Flat
1.847	47.52	311.67	1.61	Unstable
2.121	52.61	388.57	1.12	Oscillate

Table A-9 Results of V_S, Re_P and C_d for spherical particles for CMC, n=0.61

D_S, cm	V_S, cm/s	Re_P	C_d	Orientation
0.22	17.23	11.82	1.51	Vertical
0.3	22.12	20.38	1.13	Vertical
0.4	30.39	37.78	0.84	Vertical
0.6	44.58	82.41	0.65	Vertical
0.8	51.01	50.59	0.61	Vertical
1	59.10	138.36	0.58	Vertical
1.43	70.82	120.5	0.56	Vertical
2	89.33	447.91	0.52	Vertical

Table A-10 Results of V_S, Re_P and C_d for irregular shaped particles for CMC, n=0.61

D_S, cm	V_S, cm/s	Re_P	C_d	Orientation
0.984	20.08	15.99	2.98	Flat
1.101	25.16	24.20	2.77	Flat
1.152	30.58	30.89	2.12	Flat
1.198	32.97	39.36	1.65	Flat
1.240	33.71	40.55	3.97	Circular path
1.388	40.00	47.01	1.32	Flat
1.420	40.09	48.79	0.93	Springing
1.56	38.49	46.19	1.90	Circular path
1.789	35.94	48.30	2.57	Unstable

1.847	47.13	76.71	1.66	Circular path
2.121	52.12	105.05	1.14	Oscillate

Table A-11 Results of V_S, Re_P and C_d for spherical particles for polyacr., n=0.58

D_S, cm	V_S, cm/s	Re_P	C_d	Orientation
0.22	4.99	1.32	17.84	Vertical
0.3	6.19	2.16	15.38	Vertical
0.4	11.29	6.01	6.09	Vertical
0.6	21.28	18.71	2.87	Vertical
0.8	33.00	40.49	1.47	Vertical
1	45.61	73.26	0.98	Vertical
1.43	66.86	155.41	0.71	Vertical
2	76.86	231.27	0.63	Vertical

Table A-12 Results of V_S, Re_P and C_d for irregular shaped particles for polyacr., n=0.58

D_S, cm	V_S, cm/s	Re_P	C_d	Orientation
0.984	16.58	18.90	4.44	Flat
1.101	20.88	25.15	4.07	Flat
1.152	26.35	35.89	3.01	Flat
1.198	29.86	43.96	2.04	Flat

1.240	31.21	47.95	4.68	Springing
1.388	34.63	59.43	1.79	Flat
1.420	36.15	63.84	1.16	Springing
1.56	38.47	73.28	1.97	Circular path
1.789	35.31	71.89	2.71	Flat
1.823	39.29	83.17	1.94	Circular path
1.847	43.40	96.35	1.92	Springing
2.121	44.95	109.35	1.56	Oscillate

Table A-13 Results of V_S, Re_P and C_d for spherical particles for polyacr., n=0.51

D_S, cm	**V_S, cm/s**	**Re_P**	**C_d**	**Orientation**
0.22	0.53	0.056	1518.12	Vertical
0.3	0.77	0.11	988.77	Vertical
0.4	1.44	0.34	372.18	Vertical
0.6	4.96	2.56	52.31	Vertical
0.8	9.99	8.53	15.97	Vertical
1	18.12	23.15	6.23	Vertical
1.43	38.64	85.38	1.88	Vertical
2	55.71	179.46	1.34	Vertical

Table A-14 Results of V_S, Re_P and C_d for irregular shaped particles for polyacr., n=0.51

D_S, cm	V_S, cm/s	Re_P	C_d	Orientation
0.984	10.12	10.81	35.27	Stable
1.101	18.15	24.39	5.37	Stable
1.152	19.35	29.87	5.36	Stable
1.198	19.99	35.41	4.54	Stable
1.240	22.74	39.24	8.80	Flat
1.388	25.40	46.17	4.32	Flat
1.420	27.13	50.50	2.07	Flat
1.56	29.52	61.50	3.39	Circular path
1.789	31.45	76.18	3.17	Flat
1.823	32.55	81.27	2.76	Flat
1.847	37.26	92.67	2.99	Circular path
2.121	40.09	108.52	2.39	Circular path

Table A-15 Results of V_S, Re_P and C_d for spherical particles for polyacr., n=0.39

D_S, cm	V_S, cm/s	Re_P	C_d	Orientation
0.22	-	-	-	-
0.3	-	-	-	-
0.4	-	-	-	-
0.6	-	-	-	-
0.8	2.95	0.64	179.55	Vertical
1	6.11	2.25	54.62	Vertical

1.43	17.98	14.76	8.68	Vertical
2	27.13	32.74	5.67	Vertical

Table A-16 Results of V_S, Re_P and C_d for irregular shaped particles for polyacr., n=0.39

D_S, cm	V_S, cm/s	Re_P	C_d	Orientation
0.984	2.62	0.58	177.35	Stable
1.101	5.33	1.99	57.11	Stable
1.152	6.64	2.73	45.03	Stable
1.198	6.69	2.81	40.17	Stable
1.240	10.66	6.04	39.84	Stable
1.388	11.34	6.98	16.67	Stable
1.420	12.00	8.14	9.80	Stable
1.56	14.1	10.32	14.24	Stable
1.789	20.75	20.28	9.51	Stable
1.823	23.57	25.17	5.66	Stable
1.847	25.86	29.38	5.56	Stable
2.121	29.99	39.22	3.46	Stable

APPENDIX [B]

SAMPLE OF CALCULATIONS

For spherical particles;

If we take D_S=0.4 cm, the time of falling particle for distance 50 cm. (test section) is=34.72 sec. was calculated from the digital electronic circuit so the settling velocity V_S is;

V_S=1.44 cm/s

$$Re_P = 15.46 \frac{\rho_F V_S D_S}{\mu_{eq}}$$

$$\mu_{eq} = 478.8k\left(0.6\frac{V_S}{D_P}\right)^{n-1}$$

The reheological properties (n, k) of non-Newtonian fluid can be calculated from plotting shear stress τ vs. shear rate γ on log-log paper from readings taken of Fann VG meter

φ, rpm.	θ,deg.	γ,1/sec.	τ lb/100 ft^2
3	2.25	5.11	2.40
6	5.20	10.22	5.55
100	14.06	170.34	15
200	21.99	340.68	23.47
300	24.18	511.02	25.80
600	40	102.04	42.68

where τ and γ can calculated by equations below;

$\gamma = 1.7034\ \varphi$,

$\tau = 1.067\theta$

n can be calculated from the slop and k from the intercept as in figure below.

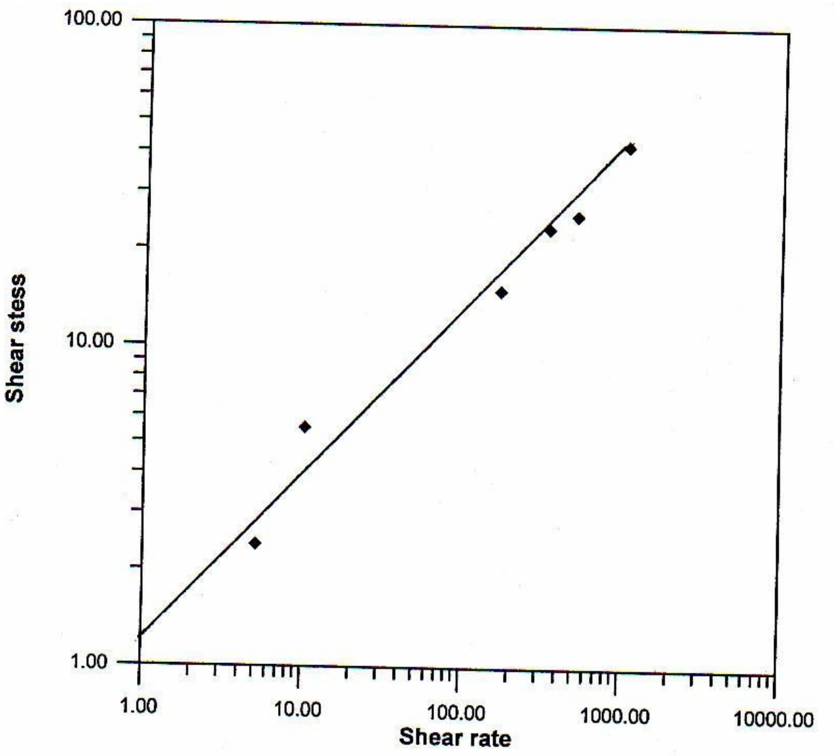

n=0.51, k=1.135 $lb.\sec^{n} / 100\,ft^{2}$

So,

$$\mu_{eq} = 478.8 * 1.135 \left(0.6 \frac{2.83}{0.157}\right)^{0.51-1}$$

$$= 169.23$$

$$\mathrm{Re}_P = 15.46 \frac{8.32 * 2.83 * 0.157}{169.23} = 0.34$$

For irregular particles;

If we take D_S =1.388 cm, the time of falling particle for distance 50 cm. is =1.968 sec. so V_S = 25.40 cm/sec

$$\mu_{eq} = 478.8*1.135\left(0.6\frac{49.99}{0.55}\right)^{0.51-1}$$

$$=76.59$$

$$Re_P = 15.46\frac{8.32*49.99*0.55}{76.59}$$

$$=46.17$$

Where D_S in inches, V_S in ft/min, ρ_P in ppg and μ_{eq} in cp.

الخلاصة

إن هدف هذا البحث هو دراسة العوامل المؤثرة على معامل السحب و سرعة الاستقرار مثل الخواص الريولوجية, تركيز السوائل غيرالنيوتونية, حجم و شكل الجسيمات الصلبة و فرق الكثافة بين الجسيمة الصلبة و السائل, كذلك يهدف هذا البحث إلى دراسة العلاقة بين معامل السحب و عدد رينولدز و تأثير الخواص الريولوجية على هذه العلاقة.

تم تصميم و بناء جهاز مختبري لقياس سرعة استقرار الجسيمات الصلبة يحتوي على أنبوب بيرسبكس ذات أبعاد ٨ سم القطر الخارجي والارتفاع ١٦٠ سم , كذلك تم تصميم دائرة الالكترونية لقياس زمن سقوط الجسيمات في السائل.

تم استخدام نوعان من الجسيمات الصلبة؛ كرات زجاجية ذات أقطار(٠,٢٢ ٠,٣،٠,٤،٠,٦،٠,٨،١،١,٤٣،٢) سم. وصخور غير منتظمة الشكل ذات أقطار (١,١٠٢،٠,٩٨٤، ١,١٥٢، ١,١٩٨ ، ١,٢٤١ ، ١,٣٨٨ ، ١,٤٢٠ ، ١,٥٦٣ ، ١,٧٨٩ ، ١,٨٢٣ ، ١, ٨٤٧ ، ٢,١٢١) سم. وقد تم استخدام نظرية القطر الكروي المكافئ لحساب قطر الجسيمات غير منتظمة الشكل.

تم تطبيق القانون الاسي لتمثيل السوائل غيرالنيوتونية لقياس سرعة استقرار حيث تم استعمال نوعان من البوليمرات هما كاربوكسي مثيل سيليلوز بتراكيز(٣,٧١، ١٥،٥، ١٧,٥)غم/لتر و بولي اكرالامايد بتراكيز (٢ ،٤، ٦) غم/لتر وتم مقارنة النتائج مع نتائج السوائل النيوتينية التي مثلت بالماء.

تم رسم مخططات جديدة لمعرفة العوامل المؤثرة على معامل السحب و سرعة الاستقرار. حيث بينت النتائج إن معامل السحب يقل مع زيادة سرعة الاستقرار و أقطار و أحجام الجسيمات الصلبة. كذلك يزداد معامل السحب كلما زاد ابتعاد السائل عن تصرف السوائل الغيرالنيوتونية, التركيز السوائل و فرق الكثافة بين الجسيمة الصلبة و السائل.

بينت النتائج المختبرية إن هنالك تأثير كبيرللخواص الريولوجية للسوائل غيرالنيوتونية على العلاقة بين معامل السحب و عدد رينولدز في حالة السقوط الصفيحي و يقل التأثير في حالة كل من السقوط الانتقالي و المضطرب.

شكر و تقدير

أود أن اعبر عن خالص شكري و تقديري و امتناني العميق للمشرف الدكتور مهند عبد الرزاق لما قدمه لي من توجيهات قيمة و نصائح سديدة طوال فترة انجاز البحث.

أود أيضا أن اشكر أساتذة و موظفي قسم الهندسة الكيمياوية في جامعة النهرين لإبدائهم المساعدة اللازمة أثناء هذا العمل.وأتقدم بالشكر الجزيل أيضا للمهندس علي مسعود من وزارة العلوم و التكنولوجيا لتصميم و تطوير الدائرة الالكترونية.

و لا أنسى أن أتقدم بالشكر و الامتنان إلى من لازمني طوال فترة البحث و خلال أصعب الظروف إلى اعز من في الوجود إلى أمي و أبي و أخواتي فلهم جزيل الشكر و التقدير.

دينا عادل إيليا

دراسة العوامل المؤثرة على معامل السحب في الترسيب الحر في مائع غير نيوتوني

رسالة

مقدمة الى كلية الهندسة في جامعة النهرين

وهي جزء من متطلبات نيل درجة ماجستير

علوم في الهندسة الكيمياوية

من قبل

دينا عادل إيليا حلاجي

(بكالوريوس علوم في الهندسة الكيمياوية٢٠٠٣)

جمادى الآخرة ١٤٢٧

حزيران ٢٠٠٦